

# LIBRARY Michigan State University

This is to certify that the dissertation entitled

### MODELING DESORPTION KINETIVS IN SOIL COLUMNS

presented by

### **IRFAN ASLAM**

has been accepted towards fulfillment of the requirements for the

Ph.D. degree in Environmental Engineering

Ph.D. degree in Environmental Engineering

Major Professor's Signature

O2/21/06

Date

MSU is an Affirmative Action/Equal Opportunity Institution

PLACE IN RETURN BOX to remove this checkout from your record.

TO AVOID FINES return on or before date due.

MAY BE RECALLED with earlier due date if requested.

DATE DUE	DATE DUE	DATE DUE
DEC 0 4 2007		
A\$ 2 2 9 0 30	3	

2/05 p:/CIRC/DateDue.indd-p.1

# MODELING DESORPTION KINETICS IN SOILS COLUMNS

Ву

Irfan Aslam

### **A DISSERTATION**

Submitted to
Michigan State University
in partial fulfillment of the requirements
for the degree of

# **DOCTOR OF PHILOSOPHY**

Department of Civil and Environmental Engineering

2006

### **ABSTRACT**

### MODELING DESORPTION KINETICS IN SOILS COLUMNS

By

### Irfan Aslam

The influence of desorption resistance on desorption kinetics exhibited by sorbed organic contaminants was investigated due to its importance in remediation.

Experimental and mathematical tools were used to evaluate the effect of partial reversibility of the sorption process. Kinetic parameters in batch and column experiments were compared to assess the relative importance of differential sorption and desorption.

Three natural sandy soils, which included two surface soils and one of an aquifer origin, were selected as natural sorbents. Naphthalene was used as a representative hydrophobic organic compound (HOC) due to its higher solubility and lower hydrophobicity compared to other 16 polycyclic aromatic hydrocarbons (PAHs) included in EPA's list of priority pollutants. A series of batch and column experiments using different techniques were conducted with equilibration time as a primary variable.

This study provides an improved understanding of desorption kinetics in batch and column systems. The results support the hypothesis for the existence of three desorption regimes in columns for a soil-contaminant combination, given that the same observational regimes exist in batch systems. The results also indicate that packing the aggregate material in soil columns limits desorption as a result of an increase in diffusion path lengths, which causes a greater fraction of the soil matrix to behave in a rate-limited mode.

The experimental evidence also suggests that a small fraction of contaminant becomes desorption resistant immediately on contact with the solid phase. An increase in the soil-contaminant contact time results in a significant shift of contaminant from the rate-limited domain to the desorption-resistant domain. However, the effect of contact time on desorption rate coefficients, which describe desorption from the rate-limited domain, is not significant.

Application of mathematical models to describe desorption in batch and column systems confirmed the importance of representing observational regimes with a compatible mathematical description for improved predictions and highlights the need for models based on time-independent parameters. This study also reveals that an increase in the number of fitting parameters other than the minimum required to represent the observational regimes is not justified.

**DEDICATION** 

To my family

### **ACKNOWLEDGEMENTS**

I want to convey my thanks to my advisors Dr. Thomas C. Voice and Dr. Mantha S. Phanikumar for the guidance and support they provided throughout my research. I also convey my gratitude to my committee members Dr. Roger Wallace and Dr. David Long.

I am also grateful to National University of Science and Technology (NUST)

Pakistan for creating a joint programme with MSU for graduate studies, which enabled me to achieve my goal of graduate education in the United States.

I feel obliged to mention here about my friend Shaukat Alvi and his family. We have enjoyed their love and company since our first day at MSU. I personally have always drawn inspiration form Shaukat in difficult times during my research.

It is also fair to mention the name of my colleagues Chris Saffron, Shawn McElmurry, with whom I could discuss my research problems and get a meaningful critique and ideas to work on.

# **TABLE OF CONTENTS**

LIST OF TABLES	viii
LIST OF FIGURES	x
LIST OF APPENDICES	xiii
CHAPTER 1. INTRODUCTION AND OBJECTIVES	1
Introduction	3
CHAPTER 2. LITERATURE REVIEW	6
Review of sorption process	6
Sorption mechanisms	
Effect of dissolved organic matter (DOM) on sorption	9
Modeling sorption kinetics in batch systems	10
Modeling desorption kinetics in batch systems	10
Chemical site models	
Kinetic models	12
Distributed-rate models	13
Pore diffusion models	14
Sorption/desorption in contaminant transport models	
Equilibrium transport in porous media	
Non- equilibrium transport in porous media	
Transport-related nonequilibrium	
A diffusion based interpretation of physical nonequilibrium	
Sorption-related nonequilibrium	
Comparison of equilibrium and nonequilibrium approaches	
Comparison of physical and chemical nonequilibrium approaches	
Multiple-process induced non-equilibrium	
Irreversible sorption in transport models	
Statistical models	
Temporal and spatial moments	
Statistical models used in chromatography	
Focus of studies in contaminant transport.	
Retardation.	
Dispersion	
Mass transfer.	
Effect of nonlinear sorption	
Review of experimental techniques	

Summary	.36
References	.37
CHAPTER 3. DESORPTION KINETICS OF NAPHTHALENE IN BATCH AND	
COLUMN EXPERIMENTS	44
Abstract	.44
Introduction	.45
Material and methods	.48
Analysis	.54
Results and discussion	.61
Conclusions	.79
References	.81
CHAPTER 4. EFFECTS OF AGING ON DESORPTION KINETICS IN SOIL	
COLUMNS	.84
Abstract	.84
Introduction	.85
Material and methods	.88
Analysis.	.90
Results and discussion	
Conclusions.	
References	117
CHAPTER 5. EFFECTS OF PORE-WATER VELOCITY ON SORPTION	
NONEQUILIBRIUM1	19
Abstract1	19
Introduction1	21
Material and methods	124
Analysis	128
Results and discussion	134
Conclusions	62
References1	64
CHAPTER 6. DISSERTATION SUMMARY AND CONCLUSIONS1	67
Dissertation summary1	67
Recommendations 1	

# LIST OF TABLES

Table 3-1	Characteristics of soils and packed columns
Table 3-2	Fractions of equilibrium, rate-limited and non-desorption sites and the desorption rate coefficients for batch desorption of naphthalene estimated by fitting the three-site model
Table 3-3	Retardation factors and dispersion coefficients estimated using the equilibrium model
Table 3-4	Desorbable, water-extractable and solvent-extractable naphthalene mass for each soil in column desorption experiments69
Table 3-5	Comparison of batch and column sorption distribution coefficients70
Table 3-6	Parameters for the two-site and the three-site models in column desorption experiments
Table 4-1	Details of the soil mass and the liquid-phase volumes used for the isotherm and series-dilution desorption experiments89
Table 4-2	Summary of column conditions and the calculated column distribution coefficients at 3 days, 2 months and 5 months aging time102
Table 4-3	Parameters of the two-site and the three-site models for Kalkaska-A in column desorption experiments
Table 4-4	Parameters of the two-site and the three-site models for SPCF in column desorption experiments
Table 4-5	Parameters of the two-site and the three-site models for Plume-A sand in column desorption experiments113
Table 5-1	Properties of packed soil columns
Table 5-2	Dimensionless parameters for the two-site and the three-site models133
Table 5-3	Retardation factors and the dispersion coefficients with 95% confidence intervals

Table 5-4	Column Peclet numbers and mass fractions for the three soils at different velocities
Table 5-5	Estimated parameters for Kalkaska-A using the two-site and the three-site models
Table 5-6	Estimated parameters for SPCF using the two-site and the three-site models
Table 5-7	Estimated parameters for Plume-A sand using the two-site and the three-site models

# **LIST OF FIGURES**

Figure 3-1	Experimental setup for column desorption52
Figure 3-2	Three-day sorption isotherms of naphthalene61
Figure 3-3	Best fits of the three-site model to the observed naphthalene desorption data in batch experiments
Figure 3-4	Best fits of the equilibrium model to tritiated water BTCs at 0.1 mL/min
Figure 3-5	Naphthalene desorption from soil columns in three soils68
Figure 3-6	Model best fits for the two-site and the three-site models to the observed naphthalene desorption data in soil columns
Figure 3-7	Model best fits of the two-site and the three-site models to the observed naphthalene desorption data in soil columns showing the cumulative mass desorbed
Figure 3-8	Schematic showing an increase in diffusion path lengths as a result of packing in soil columns
Figure 3-9	Comparison of batch and column parameters obtained by nonlinear regression using the three-site model
Figure 4-1	Sorption isotherms for the three soils. Squares, circles and diamonds represent 3-day, 2-month and 5-month equilibration period respectively
Figure 4-2	Series-dilution desorption in Kalkaska-A for different equilibration periods. The solid lines represent the sorption phase and the dashed lines represent the desorption isotherms96
Figure 4-3	Series-dilution desorption in SPCF for different equilibration periods. The solid lines represent the sorption phase while the dashed lines represent the desorption isotherms
Figure 4-4	Series-dilution desorption in Plume-A sand for different equilibration periods. The solid lines represent the sorption phase while the dashed lines represent the desorption isotherms

Figure 4-5	Change in the non-desorbable concentration $(S_{nd})$ and the fraction of non-desorption sites $(f_{nd})$ with an increase in aging period99
Figure 4-6	Cumulative naphthalene desorption from the soil columns at an aging time of 3 days, 2 months and 5 months. A summary of desorbable, water-extractable and solvent-extractable naphthalene mass from each column desorption experiment is also shown
Figure 4-7	Best fits of the two-site and the three-site models for Kalkaska-A107
Figure 4-8	Best fits of the two-site and the three-site models for SPCF108
Figure 4-9	Best fits of the two-site and the three-site models for Plume-A sand109
Figure 4-10	Changes in the fractions of equilibrium, rate-limited and non-desorption sites and the desorption rate coefficients with aging115
Figure 5-1	Experimental setup for pulse-type experiments with naphthalene and tritiated water
Figure 5-2	Box model representations of four variations of the three-site model
Figure 5-3	Three-day sorption isotherms for naphthalene134
Figure 5-4	Tritiated water BTCs for Kalkaska-A. Circles represent the experimental data and solid lines are simulations using the equilibrium model
Figure 5-5	Tritiated water BTCs for SPCF. Circles represent the experimental data and solid lines are simulations using the equilibrium model
Figure 5-6	Tritiated water BTCs for Plume-A sand. Circles represent the experimental data and solid lines are simulations using the equilibrium model
Figure 5-7	Best fits of the two-site and the three-site models to the observed naphthalene breakthrough data for Kalkaska-A

Figure 5-8	Best fits of the two-site and the three-site models to the observed naphthalene breakthrough data for SPCF	151
Figure 5-9	Best fits of the two-site and the three-site models to the observed naphthalene breakthrough data for Plume-A sand	152
Figure 5-10	The effect of SOM on transport of naphthalene	156
Figure 5-11	The effect of pore-water velocity on transport of naphthalene	161

# LIST OF APPENDICES

Table A-1	Details of the independently measured and estimated parameters for the
	two-site and the three-site models in column desorption
	experiments

# CHAPTER 1 INTRODUCTION AND OBJECTIVES

#### 1.1 Introduction

A variety of anthropogenic activities worldwide are responsible for the leaching of organic chemicals into the soil, which are cause for concern and are the focus of remediation efforts. In the past, the fate and transport of these chemicals in the subsurface environment has been extensively researched. These studies range in scope from analyzing the behavior of chemicals in simple lab-scale batch systems to field-scale remediation designs employing state-of-the-art technologies.

Contaminants are typically retarded relative to water during subsurface transport.

A continuous sampling of contaminants often shows skewed breakthrough curves (BTCs) with pronounced tailing. This non-ideal behavior is attributed to the presence of nonequilibrium that may be sorption-related or transport-related. Batch and column studies are normally conducted either concurrently or in isolation to develop an understanding of processes governing the fate and transport of contaminants. The knowledge gained through these studies is useful for protection of ground water resources or in designing remediation strategies for contaminated sites.

Traditionally, the soil matrix to which the contaminants sorb, is believed to be comprised of two different domains i.e., an equilibrium domain and a kinetic/rate-limited domain. Sorption and desorption behavior of organic contaminants in soils has been characterized based on this dual domain conceptualization for a wide range of soil-contaminant combinations. The soils include low organic-carbon aquifer materials as well as high organic-carbon surface soils while the contaminants include organic as well

as inorganic chemicals. Recent research, however, provides evidence for the existence of a third domain, commonly referred to as the non-desorption or desorption-resistant domain (Connaughten et al., 1993; Park, 2000; Park et al., 2003; Park et al., 2001). It is generally believed that the fraction of the contaminant sorbed to non-desorption domain either does not desorb at all or desorbs at a very slow rate, which is insignificant compared to the time scales of most lab studies. These batch studies have focused on quantifying the desorption-resistant fraction of the soil matrix and desorption rates.

Desorption resistance, however, has not received due attention in saturated column studies, which represent an environment closer to subsurface flow in the saturated zone. In fact, there are only a limited number of studies that have systematically tried to address this aspect. A comprehensive understanding of desorption-resistance in transport studies is important from a remediation perspective. The focus of remediation efforts is also shifting towards in-situ bio-remediation, which is believed to be a cost effective method with a potential to completely mineralize organic chemicals.

Traditionally, bioremediation efforts have been based on the assumption that a contaminant can be degraded biologically in the liquid-phase only. Recently, evidence of sorbed-phase biodegradation has been obtained in some studies (Guerin and Boyd, 1992) and further research in this area is underway. It is therefore essential to explore desorption-resistance in flow-through systems.

### 1.2 Research Objectives

The overall objective of this research was to study the effect of irreversible sorption on contaminant transport under saturated conditions in natural soils. In order to do a systematic evaluation, we set forth three main objectives. Experiments were specifically designed to address each of these objectives. A brief description is provided in the following paragraphs. The details of the experimental design and methods of analysis to address each objective have been documented in a separate chapter in this dissertation.

The first specific objective (Chapter 3) was to verify, experimentally, the existence of three desorption regimes i.e., an instantaneous regime, a rate-limited regime and a very slow regime (irreversible relative to the experimental time scale) in the column experiments. This was achieved by designing rate studies in batch and column systems coupled with solvent extractions at the end of desorption to quantify the non-desorbable contaminant mass. Based on the experimental observations in batch and column systems, the existing dual-domain mathematical model for contaminant transport (Van Genuchten and Wagenet, 1989) was modified to account for irreversible sorption by incorporating a non-desorption domain. Naphthalene desorption from soil columns was analyzed using the existing two-site model and the proposed three-site model.

Conclusions about difference in batch and column systems could also be drawn based on the comparison of desorption in batch and column systems and using a three-regime model for both systems.

The second objective (Chapter 4) was to evaluate the effects of soil-contaminant contact time, commonly referred to as "aging", on desorption in batch and column

systems. The experiments were conducted employing differentially-aged soils and to evaluate the effect of soil-contaminant contact time on desorption in batch and column systems.

The third objective (chapter 5) was to study the effects of column residence time on sorption nonequilibrium because of its analogy to soil-contaminant contact time i.e., aging. In this study, column experiments were conducted over a range of pore-water velocities resulting in different soil-contaminant contact time. For data analysis, a variety of mathematical formulations were employed to model the observed breakthrough curves. This evaluation made it possible to ascertain the best mathematical approach to describe the combined sorption/desorption behavior in soil columns for organic contaminants, which are likely to exhibit significant desorption resistance. The developed model can prove to be an effective tool in evaluating the effect of irreversible sorption on natural attenuation of organic contaminants with a prior knowledge of kinetic parameters.

Chapter 6 is a summary of the complete work with important conclusions and recommendations for future research pertaining to desorption in soil columns.

# 1.3 References

- Connaughten, D.F., Stedinger, J.R., Lion, L.W. and Schuler, M.L., 1993. Description of time-varying desorption kinetics: Release of naphthalene from contaminated soils. Environmental Science & Technology, 27(12): 2397-2403.
- Guerin, W.F. and Boyd, S.A., 1992. Differential bioavailability of soil-sorbed naphthalene to 2 bacterial species. Applied and Environmental Microbiology, 58(4): 1142-1152.
- Park, J.H., 2000. Bioavailability of sorbed organic contaminants. Ph.D. Thesis, Michigan State University, East Lansing, 155 pp.
- Park, J.H., Feng, Y.C., Ji, P.S., Voice, T.C. and Boyd, S.A., 2003. Assessment of bioavailability of soil-sorbed atrazine. Applied and Environmental Microbiology, 69(6): 3288-3298.
- Park, J.H., Zhao, X.D. and Voice, T.C., 2001. Biodegradation of non-desorbable naphthalene in soils. Environmental Science & Technology, 35(13): 2734-2740.
- Van Genuchten, M.T. and Wagenet, R.J., 1989. Two-site/two-region models for pesticide transport and degradation: Theoretical development and analytical solutions. Soil Science Society of America Journal, 53(5): 1303-1310.

# CHAPTER 2 LITERATURE REVIEW

# 2.1 Review of sorption process

The word sorption carries the meaning of a chemical's association with the solid phase and encompasses both adsorption onto a two-dimensional surface or absorption into a three-dimensional matrix (Schawarzenbach et al., 1993). The sorption distribution coefficient  $K_d$  is usually measured by developing sorption isotherms, which involve mixing a certain amount of soil with an aqueous solution containing the target compound. The isotherms are typically linear at low aqueous concentrations, but have been reported to exhibit nonlinearity at high concentrations (Means et al., 1980; Schawarzenbach and Westall, 1981). The linearity of partitioning coefficients in hydrophobic organic compounds (HOCs) at low concentrations is assumed to be due to constant activity coefficients in sufficiently dilute systems, which have been proposed as  $< 10^{-5} \, \mathrm{M}$ (Karichoff et al., 1983) and equal to  $10^{-3}$  M (Chiou et al., 1979). Other than aqueous concentrations, the factors that are known to affect partitioning include soil-to-water ratio and mixing conditions. Decrease in  $K_d$  with an increase in soil-to-water ratio has also been reported. Voice et al. (1983) reported that rapid mixing in batch results in substantial soil abrasion and can create active sorption sites, while Maraqa et al. (1998) argued that mixing conditions do not influence the ultimate sorptive capacity of the soil.

The Freundlich and the Langmuir models are normally used to describe nonlinearity in sorption isotherms. The Freundlich model is based on the assumption that

6

the number of sorption sites is large relative to the number of contaminant molecules and is mathematically described by:

$$S = K_F C^n \tag{2-1}$$

where S is the solid-phase concentration ( $\mu g/Kg$ ), C is the aqueous concentration ( $\mu g/L$ ),  $K_F$  is the Freundlich coefficient (mL/g) and n is the exponent that describes nonlinearity. In the Langmuir model, sorption increases linearly with increasing aqueous concentration at lower concentrations; however, the sorbed-phase concentration approaches a constant value at higher concentrations due to a limited number of sorption sites in the soil matrix. The mathematical form of the Langmuir model is:

$$S = \frac{K_L bC}{1 + K_I C} \tag{2-2}$$

where  $K_L$  is the Langmuir coefficient (mL/g) and b is the maximum sorbed-phase concentration ( $\mu$ g/Kg).

### 2.1.1 Sorption mechanisms

Two distinct mechanisms are widely accepted to explain sorption i.e., adsorption onto a two-dimensional mineral surface or hydrophobic partitioning to soil organic matter (SOM) (Mingelgrin and Gerstl, 1983). Predominance of either of these mechanisms is believed to depend on the conditions existing in the system. Sorption to the mineral surfaces is typically considered to be a surface phenomenon, which is nonlinear and competitive in nature (Chiou et al., 1979). It is also considered as a charge-driven phenomenon that depends on the charge of the mineral surface, which can be either positively or negatively charged depending on the solution composition and pH. The surface charge affects the sorption of polar and ionic organic chemicals (Laird and Fleming, 1999).

In natural soils, the main sorbent for nonionic organic chemicals is the naturally occurring organic matter, which is conceptualized as a mesh of macromolecules with physico-chemical properties similar to that of a polymer (Altfelder, 2000). Sorption of chemicals to SOM is known to follow a partitioning that is linear and non-competitive (Chiou et al., 1979). The organic-rich domains provide a thermodynamically favorable environment for non-polar organic compounds compared to water, such that in the presence of an organic matrix, the organic solutes will be driven from the aqueous phase and concentrate in the organic phase (Chiou et al., 1979; Chiou and Schmedding, 1983). The driving force for sorption is the hydrophobic effect resulting in a free energy gain during diffusion from water to the sorbent. Weber and Huang (1996) proposed two domains within SOM with different physico-chemical properties i.e., an outer "rubbery" domain, which exhibits linear sorption, and an inner "glassy" domain with a nonlinear sorption. Two distinct stages of sorption due to SOM heterogeneity have also been postulated (Pignatello, 1998; Pignatello and Xing, 1996) i.e., a fast stage with an equilibration time of hours and a slow stage extending to weeks, months or years. For a dominant organic partitioning, the sorption distribution coefficient is usually normalized by the fraction of organic carbon.

$$K_d = f_{oc} K_{oc} \tag{2-3}$$

where  $K_{oc}$  is the organic carbon partitioning coefficient and  $f_{oc}$  is the mass fraction of the organic carbon.  $K_{oc}$  has been successfully correlated with other solute properties, most notably with octanol-water partitioning coefficient  $(K_{ow})$ , which is a quantitative measure for the degree of hydrophobicity of the solute in question. The correlation of  $K_{oc}$  and  $K_{ow}$  is given by:

$$Log(K_{oc}) = ALog(K_{ow}) + B (2-4)$$

where A and B are the empirical regression coefficients. A compilation of these regressions from relevant literature has been reported by Ball (1989).  $K_{oc}$  values are sometimes normalized by the fraction of organic carbon in SOM using the relation:

$$K_{om} = K_{oc} f_{oc/om} \tag{2-5}$$

where  $K_{om}$  is the organic matter partitioning coefficient and  $f_{oc/om}$  is the fraction of organic carbon in SOM. Chiou (1989) proposed the following relation to estimate the contaminant solubility in SOM  $(S_{om})$  if  $K_{om}$  and water solubility  $(S_w)$  are known:

$$S_{om} = K_{om} S_w \tag{2-6}$$

# 2.1.2 Effect of dissolved organic matter (DOM) on sorption

Dissolved organic matter is present in most surface waters and contains up to 90% of the humic substances. A change in DQM concentration is likely to cause reorganization in the macromolecular structure of dissolved humic substances, which is probably responsible for the alteration of their association capacity with HOCs (Akkanen and Kukkonen, 2003). The quality and variations of DOM can affect desorption and subsequently biodegradation. Plaehn et al. (1999) studied the impact of DOM on desorption and mineralization rates of naphthalene using DOM extracted from high organic soils as well as prepared from commercially available fulvic acid reference standards. The authors found that neither the partitioning of naphthalene nor the desorption rate was affected by the presence of DOM. They caution however, that although not apparent in their data, the effects of DOM on the mechanisms of desorption and biodegradation may be important for other contaminant-soil-organism combinations.

# 2.2 Modeling sorption kinetics in batch systems

Sorption has been typically modeled as biphasic. In a dual-domain conceptualization, the sorbent is assumed to consist of two separate domains i.e., an equilibrium domain and a rate-limited domain. In the equilibrium domain, the sorption is fast compared to the duration of experiment. Therefore the assumption of equilibrium is considered valid. The mass transfer between the aqueous phase and the rate-limited domain is driven by the concentration gradient. Mathematically, the solid-phase concentration in the two domains is represented by:

$$S_{eq} = f_{eq} K_d C (2-7)$$

$$\frac{\partial S_{neq}}{\partial t} = \alpha [(1 - f_{eq})K_dC - S_{neq}]$$
 (2.8)

where C is the concentration in the liquid-phase ( $\mu g/L$ ),  $S_{eq}$  and  $S_{neq}$  are the sorbed-phase concentrations ( $\mu g/Kg$ ) in the equilibrium domain and rate-limited domains respectively,  $f_{eq}$  is the fraction of sorption sites that undergo instantaneous sorption and  $\alpha$  is the sorption rate coefficient (hour -1). Replacing the equilibrium distribution coefficient  $K_d$  with a Freundlich distribution coefficient  $K_F$  or the Langmuir coefficient  $K_L$  with necessary mathematical adjustments accounts for the effects of nonlinear sorption.

# 2.3 Modeling desorption kinetics in batch systems

Desorption is kinetically controlled by either release from surface sorption sites or by diffusion through the sorbent to water (Van Noort et al., 2003). A variety of mathematical models have been proposed to describe desorption based on different conceptualizations of the desorption process. These models include chemical site models i.e., the two-site model (Rao et al., 1979; Van Genuchten and Wagenet, 1989) and the

10

three-site model (Park, 2000; Park et al., 2001; Park et al., 2002), two and three-parameter pore diffusion models (Johnson et al., 2001), three-parameter kinetic model (Cornelissen et al., 1998a; Cornelissen et al., 1998b), five-parameter kinetic model (Cornelissen et al., 1998a; Cornelissen et al., 1997), gamma-distribution model (Connaughten et al., 1993) and hybrid gamma model (Ahn et al., 1999). Each of these models is briefly described in the following paragraphs.

# 2.3.1 Chemical site models

A two-site desorption model for the batch systems assumes that soil matrix has two types of desorption sites i.e., equilibrium and nonequilibrium/rate-limited sites. Equations 2-7 and 2-8 describe desorption based on a two-site conceptualization. In a three-site desorption model (Park, 2000), the soil matrix has three types of desorption sites i.e., equilibrium, nonequilibrium/rate-limited and nondesorption sites. The equilibrium and nondesorption partitioning in the model are described by:

$$S_{eq} = f_{eq} K_d C_{des} (2-9)$$

$$S_{nd} = f_{nd} K_d C_{e(sorp)} (2-10)$$

while the release from the rate-limited sites follows the first-order expression:

$$\frac{dS_{neq}}{dt} = \alpha \left[ f_{neq} K_d C_{des} - S_{neq} \right]$$
 (2-11)

where  $S_{eq}$ ,  $S_{neq}$  and  $S_{nd}$  are the sorbed-phase concentrations in equilibrium, rate-limited and nondesorption sites respectively,  $C_{des}$  is the liquid-phase concentration in the desorption assay,  $C_{e(sorp)}$  is the liquid-phase concentration at sorption equilibrium,  $f_{eq}$ ,  $f_{neq}$  and  $f_{nd}$  are the equilibrium, rate-limited/kinetic and nondesorption site fractions and  $\alpha$  is the first order desorption rate coefficient for the rate-limited sites. In the two- and

the three-site models, the solute exchange between the aqueous and solid phases is described by a driving force formulation based on the linear distribution coefficient  $K_d$ .

# 2.3.2 Kinetic models

The kinetic models viz., three- and five-parameter kinetic models use only kinetic rate coefficients to describe desorption from each domain. A three-parameter kinetic model assumes that the soil matrix is divided into two domains i.e., a rapid desorption domain that exhibits rapid desorption and a slow desorption domain, for which, the desorption occurs at slower rates compared to the rapid domain. The mathematical formulation of the three-parameter kinetic model is as follows:

$$\frac{dS_r}{dt} = -\alpha_r S_r \tag{2-12}$$

$$\frac{dS_s}{dt} = -\alpha_s S_s \tag{2-13}$$

$$S_T = S_r + S_s \tag{2-14}$$

$$f_r + f_s = 1 (2-15)$$

A five-parameter kinetic model accounts for very slow desorption and is based on following set of equations:

$$\frac{dS_r}{dt} = -\alpha_r S_r \tag{2-16}$$

$$\frac{dS_s}{dt} = -\alpha_s S_s \tag{2-17}$$

$$\frac{dS_{vs}}{dt} = -\alpha_{vs}S_{vs} \tag{2-18}$$

$$S_T = S_r + S_s + S_{vs} (2-19)$$

$$f_r + f_s + f_{vs} = 1 (2-20)$$

In the kinetic models, S is the sorbed-phase concentration ( $\mu g/Kg$ ),  $\alpha$  is a desorption rate coefficient (hour<sup>-1</sup>) and f represents the domain size. The subscripts r, s and vs denote rapid, slow and very slow desorption.

### 2.3.3 Distributed-rate models

A gamma-distribution model assumes the entire soil matrix divided into a series of compartments. Associated with each compartment is a different desorption rate coefficient that follows the gamma distribution. The time rate of change in sorbed-phase concentration is described by:

$$\frac{dS_T}{dt} = \int_0^\infty -k_i (S_i - K_d C) \frac{k_i^{\alpha - 1} \beta^{\alpha} e^{-\beta k_i}}{\Gamma(\alpha)} dk_i$$
 (2-21)

where k is the desorption rate coefficient for the i th compartment,  $\alpha$  and  $\beta$  are the two parameters the for gamma distribution and  $\Gamma$  is the gamma function. Similar to the chemical two-site model, the hybrid gamma-distribution model assumes the soil matrix is comprised of two domains, i.e., an equilibrium domain and a rate-limited domain. The rate-limited domain is modeled in the same manner as the gamma-distribution model while the equilibrium domain is treated similar to that of the chemical two-site model. The following set of equations is used to represent desorption in a hybrid gamma-distribution model:

$$S_{eq} = f_{eq} K_d C (2-22)$$

$$\frac{dS_{neq}}{dt} = \int_{0}^{\infty} -k_i (S_i - K_d C) \frac{k_i^{\alpha - 1} \beta^{\alpha} e^{-\beta k_i}}{\Gamma(\alpha)} dk_i$$
 (2-23)

$$S_T = S_{eq} + S_{neq} \tag{2-24}$$

### 2.3.4 Pore diffusion models

One, two and three-parameter pore diffusion models are also based on a conceptualization of one, two and three domains respectively. However, the desorption from the rate-limited domain is described by using a formulation based on Fick's law which accounts for a specific geometry of the porous medium. For spherical geometry, the equations for the three-parameter pore diffusion model are:

$$\frac{\partial S_{neq}}{\partial t} = D \left[ \frac{\partial^2 S_{neq}}{\partial r^2} + \frac{2}{r} \frac{\partial S_{neq}}{\partial r} \right]$$
 (2-25)

$$S_T = S_{eq} + S_{neq} + S_{nd} \tag{2-26}$$

where D is the pore diffusion coefficient (cm $^2$ /hour) and r is the radial distance (cm).

Some of these models (i.e., the chemical three-site model, the three-parameter pore diffusion model and the five-parameter kinetic model) explicitly account for the non-desorbable fraction. There are advantages and disadvantages to each of these models and it is difficult to designate any model as the best. Ahn et al. (1999) applied the two-site/two-region model and the gamma-distribution model to describe naphthalene desorption and found that the two-site model failed to capture the slow desorption while the gamma- distribution model was unable to describe the initial rapid release. Similarly, Culver et al. (1997) pointed out that the performance of the two-site model was very sensitive to the value of  $K_d$ , while the performance of distributed-rate models was robust over a wide range of partitioning coefficients. Saffron (2005) applied nine different models to previously reported naphthalene and atrazine desorption data and concluded that overall the three-regime models better describe the desorption of the two

contaminants than the two-regime models do. Johnson et al. (2001) also reached a similar conclusion while testing six models to describe phenanthrene desorption.

# 2.4 Sorption/desorption in contaminant transport models

Flow through porous media has been investigated by conducting column studies, which have been useful in characterizing the processes affecting the fate and transport of contaminants. These processes include dispersion, diffusion, sorption, ion-exchange etc. Many conceptualizations of the porous media and the corresponding mathematical formulations exist e.g., the capillary tube model, the cell model and statistical models. However it has always been simplified in a manner so as to treat all these processes at a macroscopic scale rather than microscopic due to computational limitations and mathematical complexities.

### 2.4.1 Equilibrium transport in porous media

An example of the simplifications mentioned above is the convection-dispersion equation (CDE). For flow through a non-aggregated homogeneous porous medium under saturated conditions, the transport of a solute is described by:

$$\frac{\partial C}{\partial t} + \frac{\rho}{\theta} \frac{\partial S}{\partial t} = D \frac{\partial^2 C}{\partial x^2} - v \frac{\partial C}{\partial x}$$
 (2-27)

where C is the solute concentration in liquid phase ( $\mu g/L$ ), S is the concentration in sorbed phase ( $\mu g/Kg$ ), D is the hydrodynamic dispersion coefficient ( $cm^2/hr$ ),  $\rho$  is the soil density ( $g/cm^3$ ),  $\theta$  is the saturated porosity ( $cm^3/cm^3$ ),  $\nu$  is the average pore-water velocity (cm/hr), x is distance along the direction of flow (cm), and t is time (hr). The CDE is referred to as the equilibrium model if the condition of local equilibrium is

15

assumed between the two phases. In that case, the governing equation for the solute transport becomes:

$$R\frac{\partial C}{\partial t} = D\frac{\partial^2 C}{\partial x^2} - v\frac{\partial C}{\partial x}$$
 (2-28)

where  $R = 1 + \frac{\rho K_d}{\theta}$ . The equilibrium model is based on the local equilibrium assumption (LEA), which considers the sorption rates to be faster compared to other processes such as advection and dispersion. The equation representing the solute transport is simplified with this assumption, as only the mobile pore water needs to be explicitly considered and the sorbed-phase concentration can be defined in terms of the aqueous concentration at each spatial location in the porous medium (Ball, 1989). If the LEA is valid, the breakthrough curves for column experiments employing the nonionic organic contaminants, which are hydrophobic, should exhibit symmetrical BTCs. On the contrary, the observed BTCs in most lab and field studies exhibit asymmetry and tailing. This provided a motivation for the researchers to hypothesize and test alternative mechanisms responsible for asymmetrical behavior and to lay down the criteria for the validity of the LEA.

A measure of the relative importance of kinetic to equilibrium processes is the Damköhler number, which is defined as the ratio of the transport and reaction time scales. The Damköhler number has traditionally been used to assess the validity of the LEA. It has been shown that LEA is generally valid when the Damköhler number is greater than 100 (Valocchi, 1985) and is considered to be a fair approximation when its value is greater than 10 (Brusseau and Rao, 1989a). In most cases however, the condition is not met, which warrants the use of a nonequilibrium model rather than relying on the LEA-

based equilibrium model. Brusseau et al. (1991b) found via sensitivity analysis of a bicontinum model that the leftward shift of the BTC is minimal when the Damköhler number is in the range of approximately 4 or greater, and hence the nonequilibrium should have a minimal effect on the determination of the retardation factor (R) when these conditions are met. In a separate study by Maraqa et al. (1999) the LEA was found to be invalid at a very low pore-water velocity of 0.7 cm/hr.

# 2.4.2 Nonequilibrium transport in porous media

Nonequilibrium in contaminant transport through a porous medium is viewed to exist due to processes that are either sorption-related or transport-related. Transport-related nonequilibrium (also referred to as physical nonequilibrium) is assumed to exist due to entrapment of a fraction of the mobile phase in the pores that are isolated from the main flow, while sorption-related nonequilibrium is due to sorptive interactions of the solute with a dual-property matrix, in which the sorption is instantaneous for one fraction while it is rate-limited for the other.

### 2.4.2.1 Transport-related nonequilibrium

Transport-related nonequilibrium results from slow solute diffusion into and out of relatively stagnant water regions, which might be created by the nature of the porous matrix e.g., a higher degree of aggregation or a level of saturation that is less than fully saturated. Under these conditions, the total water content is assumed to be distributed between two regions i.e., a mobile region and an immobile region (Coats and Smith, 1964; Van Genuchten and Wierenga, 1976). The solute transfer between the mobile water region (instantaneous sorption domain) and the immobile water region (rate-limited sorption domain) can be described by Fick's law if the geometry of the porous medium

can be specified. But as the models based on geometry are difficult to apply in the field, the solute transfer between the mobile and immobile water regions have been mostly described using first order rate expressions. The model based on this conceptualization of a transport-related nonequilibrium is also referred to as the two-region nonequilibrium model or mobile-immobile model (MIM). The mathematical formulation of the MIM (Van Genuchten and Wierenga, 1976) is given as:

$$(\theta_m + f \rho K_d) \frac{\partial C_m}{\partial t} = \theta_m D_m \frac{\partial^2 C_m}{\partial x^2} - J_w \frac{\partial C_m}{\partial x} - \alpha (C_m - C_{im})$$
 (2-29)

$$\left[\theta_{im} + (1 - f)\rho K_d\right] \frac{\partial C_{im}}{\partial t} = \alpha (C_m - C_{im})$$
(2-30)

where the subscripts m and im refer to the mobile and immobile liquid regions respectively,  $J_w = v\theta = v_m\theta_m$  is the volumetric flux density (cm/hr), f represents the fraction of sorption sites that equilibrate with the liquid phase in the mobile region and  $\alpha$  is the first order mass transfer coefficient (hr<sup>-1</sup>) governing the rate of solute exchange between the mobile and immobile liquid regions. Here  $\theta = \theta_m + \theta_{im}$ . Normalized equations for the two-region nonequilibrium model for a linear sorption case are:

$$\beta R \frac{\partial C_1}{\partial T} = \frac{1}{P} \frac{\partial^2 C_1}{\partial Z^2} - \frac{\partial C_1}{\partial Z} - \omega (C_1 - C_2)$$
 (2-31)

$$(1-\beta)R\frac{\partial C_2}{\partial T} = \omega(C_1 - C_2) \tag{2.32}$$

where

$$C_1 = \frac{C_m}{C_o}, \quad C_2 = \frac{C_{im}}{C_o}, \quad Z = \frac{x}{L}, \quad T = \frac{vt}{L}, \quad P = \frac{v_m L}{D_m} = \frac{vL}{D}$$

$$R = 1 + \frac{\rho K_d}{\theta}$$
,  $\beta = \frac{\theta_m + f \rho K_d}{\theta + \rho K_d}$  and  $\omega = \frac{\alpha L}{\nu \theta}$ 

where  $C_1$  and  $C_2$  are the normalized average relative concentrations in the mobile and immobile water regions respectively. P is the Peclet number for the mobile zone,  $D_m$  is the dispersion coefficient in the mobile zone and  $\omega$  is the dimensionless mass transfer coefficient between the mobile and immobile water regions. The models based on the concept of physical nonequilibrium are sometimes referred to as diffusive mass transfer models as they describe the rate-limiting sorption process as a physical rather than a chemical process (Maraga, 1995).

Three different mathematical treatments of the solute transfer between the mobile and immobile regions in the porous medium exist (Brusseau, 1989) i.e., (1) by using Fick's law (2) by use of first order mass transfer expression and (3) by using a lumped dispersion coefficient that includes the hydrodynamic dispersion as well as axial diffusion. Physical nonequilibrium is believed to affect the transport of both sorptive as well as non-sorptive solutes. In most of the current transport-related nonequilibrium models, sorption kinetics have been simulated using a formulation that assumes a constant mass-transfer coefficient, one that is independent of pore-water velocity (Maraqa et al., 1999).

# 2.4.2.2 A diffusion based interpretation of physical nonequilibrium

Two diffusive mass transfer models are the intra-particle diffusion model (Ball and Roberts, 1991) and the intra-organic matter diffusion model. Retarded intra-particle diffusion involves diffusion of solutes through pores contained in micro porous particles, with retardation occurring by instantaneous sorption to the walls. Intra-organic matter diffusion involves diffusion within the matrix of the organic carbon components of the solid phase (Brusseau et al., 1991a).

Diffusion of the solute from the mobile region to the immobile region takes place in a series of steps, which include diffusion from the bulk solution to the boundary-layer. film diffusion and intra-aggregate diffusion (any of which could be rate-limiting). Intraaggregate diffusion may occur either by pore diffusion or surface diffusion or both. As these two processes act in parallel, the faster of the two will be the predominant transport mechanism and therefore will control the transfer rate (Brusseau, 1989). Although the dominance of surface diffusion has been found in activated carbon (Fettig and Sontheimer, 1987), the same is not believed to hold for soil/aquifer systems due to less tortuosity as compared to the activated carbon. The choice of the model incorporating surface diffusion or pore diffusion is only important for nonlinear isotherms, as identical BTCs are expected in both cases for linear isotherms (Weber and Chakravorti, 1974). The relative importance of each of these processes is often quantified through the Biot number, which is the ratio of the film transfer rate to the intra-aggregate transfer rate. Generally, the intra-aggregate diffusion is considered as the rate-limiting step during sorption (Brusseau and Rao, 1989b).

Spherical geometry is commonly applied for describing the immobile phase and is applicable when the flow surrounds the spherical aggregates or sorbents containing immobile water. For spherical geometries, the average aqueous concentration in the immobile phase is described by:

$$C_{im}(x,t) = \frac{3}{a^3} \int_0^a r^2 C(r,x,t) dr$$
 (2-33)

where a is the radius of the immobile zone, r is the radial distance from the center of the immobile region and C is the aqueous concentration of solute within the pore at position r, time t and distance x.

# 2.4.2.3 Sorption-related nonequilibrium

Sorption-related nonequilibrium is caused by slow solute interaction with all or some specific sorption sites of the solid matrix. Sorption nonequilibrium models assume that the sorption reaction is the rate-limiting process (Cameron and Klute, 1977). In a two-site nonequilibrium model, the adsorption sites are sub-divided into two categories i.e., equilibrium sites and rate-limited sites (Van Genuchten and Wagenet, 1989). For steady flow in a homogeneous soil, the transport of a linearly- adsorbed solute is given by:

$$\left(1 + \frac{f_{eq}\rho K_d}{\theta}\right)\frac{\partial C}{\partial t} = D\frac{\partial^2 C}{\partial x^2} - v\frac{\partial C}{\partial x} - \frac{\alpha\rho}{\theta}\left[\left(1 - f_{eq}\right)K_dC - S_{neq}\right]$$
(2-34)

$$\frac{\partial S_{neq}}{\partial t} = \alpha \left[ \left( 1 - f_{eq} \right) K_d C - S_{neq} \right]$$
 (2-35)

where  $\alpha$  is the first-order kinetic rate coefficient (hr<sup>-1</sup>),  $f_{eq}$  is the fraction of exchange sites that are always at equilibrium, the subscripts eq and neq refer to the equilibrium and rate-limited/kinetic sorption sites respectively. Employing the dimensionless parameters, the two-site model reduces to the following dimensionless form:

$$\beta R \frac{\partial C_1}{\partial T} = \frac{1}{P} \frac{\partial^2 C_1}{\partial Z^2} - \frac{\partial C_1}{\partial Z} - \omega (C_1 - C_2)$$
 (2-36)

$$(1-\beta)R\frac{\partial C_2}{\partial T} = \omega(C_1 - C_2) \tag{2-37}$$

where:

$$C_1 = \frac{C}{C_0}$$
,  $C_2 = \frac{S_{neq}}{(1 - f_{eq})K_dC_0}$ ,  $Z = \frac{x}{L}$ ,  $T = \frac{vt}{L}$ , and  $R = 1 + \frac{\rho K_d}{\theta}$ 

$$P = \frac{vL}{D}$$
,  $\beta = \frac{\theta + f_{eq}\rho K_d}{\theta + \rho K_d}$  and  $\omega = \frac{\alpha(1-\beta)RL}{v}$ 

Subscripts 1 and 2 refer to the equilibrium sites and rate-limited sites respectively,  $\beta$  is the dimensionless partitioning coefficient and  $\omega$  is the dimensionless mass transfer coefficient.

### 2.4.3 Comparison of equilibrium and nonequilibrium approaches

In most studies involving transport in soil columns, the focus has been to prove either the existence of transport-related or sorption related nonequilibrium. Each of these cases has arguments to support their respective cases. In general, the nonequilibrium models describe the transport of reactive solutes better than the equilibrium models. This limits the reliability of the LEA approach except for the ideal transport cases involving conservative solutes. For example, Maraqa et al. (1999) used two non-ionic organic compounds (NOCs) i.e., benzene and dimethylpthalate (DMP), to study the effects of residence time and degree of water saturation on sorption nonequilibrium parameters, and observed that nonequilibrium model simulations closely matched the experimental results, while deviations between the equilibrium model simulations and the data points were significant.

# 2.4.4 Comparison of physical and chemical nonequilibrium approaches

Prior to studying the effects of sorption on the BTCs of reactive contaminants through a porous medium, the existence of the type of nonequilibrium (i.e., physical or sorption-related) must be established. It is relatively easy to interpret the results under the assumptions of a physical nonequilibrium but if the sorption-related nonequilibrium exists concurrently, isolating the effects of both is not trivial.

The immobile water fractions have been mostly associated with unsaturated conditions and aggregated media; therefore, most applications of the physical

nonequilibrium model have been in studies involving unsaturated flow conditions or in those utilizing aggregated media. In spite of the fact that evidences of immobile water fraction were found in these studies, the possibility of sorptive interactions could not be ruled out. For example Kamra et al. (2001) conducted displacement studies on the leaching of bromide and two pesticides (atrazine and isoproturon) under unsaturated steady flow conditions employing aggregated soils in 24 small undisturbed soil columns (5.7 cm in diameter and 10 cm long). Each soil sample differed in soil structure and organic carbon content. They inferred from the estimated parameters of the nonequilibrium model that 5-12% of water at one site, and 12% at the other site was immobile during displacement in non-preferential flow columns. The corresponding values for preferential flow columns of the two sites ranged between 25% to 51% determined by curve fitting with CXTFIT and 24% to 72% by the moment method. suggesting the role of certain mechanisms other than immobile water to be responsible for higher degrees of nonequilibrium. Several other studies e.g., (Bouchard et al., 1988; Brusseau et al., 1991a; Kamra et al., 2001; Lee et al., 1988; Maraqa et al., 1997; Maraqa et al., 1998) were not conclusive in ruling out the role of sorptive interactions as a cause of nonequilibrium. Maraga et al. (1999) demonstrated that nonequilibrium conditions resulted from slow sorptive interactions but not due to the slow diffusion into and out of immobile water regions thereby confirming the presence of a sorption-related nonequilibrium rather than a physical one. Majority of studies involving organic contaminants have preferred the use of sorption-related nonequilibrium models. The use of the MIM model in these studies has been limited to ruling out the possibility of existence of the immobile water fractions.

# 2.4.5 Multiple-process induced nonequilibrium

The inherent weakness in assuming a single process as being responsible for nonequilibrium has also been realized which results in a lumped kinetic term for a system being affected by more than one rate-limiting process. The effects of concurrent multiple processes contributing towards nonequilibrium have also been investigated. The multiprocess nonequilibrium model (MPNE) (Brusseau, 1989; Brusseau, 1991) was formulated to simulate solute transport in a porous medium where transport-related as well as sorption-related non-idealities were operative. In the MPNE model, the authors used a dual-porosity approach to represent physical non-ideality and a dual-domain approach for sorption non-ideality. The four dimensionless equations for the MPNE model are:

$$R_{a1} \frac{\partial C_a^*}{\partial T} + k_a^0 (C_a^* - S_a^*) + \omega (C_a^* - C_n^*) = \frac{1}{P} \frac{\partial^2 C_a^*}{\partial X^2} - \frac{\partial C_a^*}{\partial X}$$
 (2-38)

$$R_{n1}\frac{\partial C_n^*}{\partial T} + k_n^0 (C_n^* - S_n^*) = (C_a^* - C_n^*)$$
 (2-39)

$$R_{n2} \frac{\partial S_n^*}{\partial T} = k_n^0 (C_n^* - S_n^*)$$
 (2-40)

$$R_{a2} \frac{\partial S_a^*}{\partial T} = k_a^0 (C_a^* - S_a^*)$$
 (2-41)

where  $C^*$  is the dimensionless aqueous concentration,  $S^*$  is the dimensionless sorbedphase concentration, R is the retardation factor,  $k^0$  is the dimensionless Damköhler
number, subscripts a and n represent the advective and non-advective domains and the
subscripts I and I represent the instantaneous and rate-limited sorption sites respectively.

More details on the equation formulation and description of dimensionless variables can
be found in (Hu and Brusseau, 1996). The global retardation factor I is given by:

$$R = R_{a1} + R_{a2} + R_{n1} + R_{n2} = 1 + \frac{\rho}{\theta} K_d$$
 (2-42)

(Hu and Brusseau, 1996) investigated the transport of rate-limited sorbing solutes in a saturated, aggregated porous medium with an objective to isolate the effects of physical non-ideality and sorption non-ideality and to study the synergistic effects of multiple non-idealities on contaminant transport. The experimental procedures to test the multi-process non-ideality approach involved creating three separate systems i.e., with physical non-ideality (porous spheres), with sorption non-ideality (homogeneously packed soil columns) and with physical and sorption non-ideality (columns packed with a mixture of soil and porous spheres). The analysis involved independent determination of parameters from the physical and sorption non-ideality experiments and using these in the MPNE model in a predictive mode. The authors suggested that the MPNE model adequately described the processes controlling the transport of rate-limited sorbing solutes in an aggregated system. In another study, Johnson et al. (2003) used the MPNE model to determine the relative contributions of physical heterogeneity-related processes and nonlinear/rate-limited sorption-desorption of TCE in undisturbed cores. The authors were able to successfully describe the breakthrough curves using MPNE model.

Application of the MPNE model requires a large number of fitting parameters.

Although, the use of the model in lab-scale studies is possible, its use under field conditions in a real predictive sense is limited.

# 2.4.6 Irreversible sorption in transport models

The observations of irreversible sorption date back to the seventies, however, it has seldom been incorporated in transport models. It is only recently that some studies have focused on desorption-resistance in transport models. For example, Prata et al. (2003)

conducted batch and column experiments to study the sorption-desorption behavior of atrazine, with a focus on irreversible sorption. The results indicated that approximately 90% of atrazine desorbed in batch while in columns, desorption was only 53-65%. They attributed this increase in non-desorbable fraction in columns to an increased contact time, which contributed to a higher physical diffusion of atrazine in the humic substances. Mathematically, irreversible sorption is described as a first-order process. This approach will work only for systems in which there is no physical decay and irreversible sorption is the only sink. In the presence of a concurrent physical degradation/decay, the first order degradation rate coefficient will account for the lumped effects of irreversible sorption and decay/degradation.

#### 2.5 Statistical models

Statistical models generally employed include the temporal and spatial moments, the exponentially modified gaussian equation (EMG), the bi-exponentially modified gaussian equation (BEMG) and the nonlinear chromatography equation (NLC). Most applications of statistical models have been in the field of chromatography. The first two models, being the most widely used, are discussed in the subsequent paragraphs.

# 2.5.1 Temporal and spatial moments

Temporal moment analysis is a powerful method that may be utilized to evaluate various aspects of solute transport (Brusseau, 1989). Traditionally, these have been used in chemical engineering, soil sciences, hydrology and environmental engineering.

Statistical moments are classical functions that are used to describe the distribution of any data set with no assumptions about their functional form (Howerton et al., 2003).

Temporal moments may be used to evaluate the impact of nonequilibrium on solute

transport and to assess the differences between equilibrium and nonequilibrium models (Brusseau, 1989). One limitation however is, that moments can only be used for analysis and cannot be used in a predictive mode. A comparison of the temporal evolution of observed moments with the derived moments helps in deciding, if an equilibrium model is suited to describe the BTC or use of a nonequilibrium model is necessary. The observed temporal moments are calculated based on time-concentration data. The zeroth, first, second, third and fourth moments represent the mass, time of the center of mass, variance or degree of spreading, skewness or degree of asymmetry and kurtosis or a measure of degree of flatness of the peak respectively. These are defined by the following set of equations.

$$M_0 = \int C(t)dt \tag{2-43}$$

$$M_1 = \frac{\int tC(t)}{\int C(t)} \tag{2-44}$$

$$M_n = \frac{\int (t - M_1)^n C(t)dt}{\int C(t)dt}$$
 (2-45)

where the subscripts denote the moment numbers.

Analytical solutions exist in literature for temporal and spatial moments for advection-dispersion equation and its variations. These analytical solutions are equated to the observed moments for estimating the parameters. Srivastava et al. (2004) presented the analytical solutions for temporal moments for the MPNE model incorporating the rate-limited sorption, first-order mass transfer and first-order transformation with an objective to study the effects of rate coefficients on the observed moments. The authors found that in the presence of transformation reactions, rate coefficients are not monotonic functions of the temporal moments.

The analytical solutions for the spatial moments have also been derived for a multiprocess nonequilibrium case by Srivastava et al. (2002). The authors argue that the spatial heterogeneity of material properties can be satisfactorily accounted for by using an increasing macro-dispersivity function however, they also suggest that these analysis can be only used as a preliminary assessment tool for ascertaining the relative importance of various processes under consideration. They emphasize that spatial moments are obtained for the solute present in the solution phase and do not represent the entire solute in porous medium. The temporal moments have more practical value in column experiments, as it is more convenient to obtain the breakthrough curves rather than spatial solute distribution in columns. Even if spatial distribution of solute in columns is obtained, a limited number of data points donot offer the possibility of an analysis based on spatial moments. The effect of number of data points on the temporal moments has been investigated by Howerton et al. (2003). Another limitation of moment-based analysis is that precise analytical expressions have to be derived for the specific model employed to analyze the effect of different processes on the associated rate coefficients.

#### 2.5.2 Statistical models used in chromatography

The most widely used equation in chromatography is the exponentially modified gaussian equation (EMG), which is a convolution of a gaussian and an exponential function (Howerton et al., 2003) and is of the form:

$$C(t) = \frac{A}{2\tau} \exp\left[\frac{\sigma^2}{2\tau^2} + \frac{t_G - t}{\tau}\right] \left[erf\left(\frac{t - t_G}{\sqrt{2\sigma}} - \frac{\sigma}{\sqrt{2\tau}}\right) + 1\right]$$
(2-46)

where A is the area,  $t_G$  is the retention time of the gaussian component,  $\sigma$  is the standard deviation of the gaussian component (a quantitative measure of the zone broadening

arising from symmetrical processes such as diffusion, dispersion and mass transfer) and  $\tau$  is the standard deviation of the exponential component (parameter quantifying the zone broadening from asymmetrical processes (Howerton and McGuffin, 2004). BEMG and NLC are similar statistical models (not described here) used in chromatography. Howerton and McGuffin (2004) used these three statistical models to study the thermodynamic and kinetic behavior of a series of four-ringed PAHs with varying degrees of annelation and found that neither NLC nor BEMG provided a better description of zone profiles than EMG.

# 2.6 Focus of studies in contaminant transport

Numerous studies have been conducted involving nonequilibrium contaminant transport, which focused on different aspects. These aspects include but are not limited to retardation, dispersion, effects of nonlinear sorption, and mass transfer. A brief review of each of these aspects is presented in the following paragraphs.

#### 2.6.1 Retardation

The retardation coefficient R represents the average speed of contaminant in the porous medium relative to that of aqueous phase. For a conservative tracer, values of R less than unity indicate the existence of transport-related nonequilibrium between the mobile and immobile water regions (Nkedikizza et al., 1983). Controversies do exist regarding the appropriateness of determining R in batch or column experiments. R can be calculated with knowledge of  $K_d$  obtained through batch isotherms. Methods to calculate R using column data include: (1) the number of pore volumes eluted when  $C/C_0 = 0.5$  (2) the area between the elution curve and the step input curve (Nkedikizza et al., 1987) (3) the first moment of the BTC for a pulse type input (Valocchi, 1985) and (4) by curve-

fitting the equilibrium model to the observed BTC. Retardation coefficients computed by the above four methods will be identical for symmetric BTCs. For asymmetric BTCs, determination of R by the first method may be inappropriate (Nkedikizza et al., 1987). The second method cannot be used, if the applied boundary conditions did not permit the relative effluent concentration to reach unity. In column experiments, slow desorption rates compared with sorption result in a pronounced tailing in the BTCs. For pulse-type input, the column experiment is terminated when the quantification limit of the target compound is reached. In such a case, the BTCs may lack much of the tail data, although most of the solute has actually been recovered. Sorption parameters estimated by inverse modeling of column data are therefore subject not only to random errors but also to errors caused by the necessity to use a truncated data set.

Maraqa et al. (1998) utilized batch and column techniques to determine R for benzene and dimethylpthalate (DMP) and found that R values calculated using the batch data were consistently overestimated for the two compounds. Although, the author successfully ruled out previously reported causes of this discrepancy (i.e., sorption non-singularity, sorption nonequilibrium, presence of immobile water regions in the column, reduction in particle spacing in the columns) it still remained unclear, why the values of R determined by these two techniques were different. Altfelder et al. (2001) also used DMP to examine the compatibility of batch and column techniques for determining R. They estimated the sorption parameters by fitting a linear and a nonlinear model to 3-day and 14-day isotherms. The authors conclude that a major part of the apparent difference could be related to the analytical difficulties in determining the extensive tailing of the observed BTCs and recommend that batch technique is preferred over columns for determining the

retardation coefficients. Kamra et al. (2001) analyzed the BTCs of bromide under unsaturated steady state conditions in undisturbed soil columns using the equilibrium and the MIM model. They compared R values estimated using these models with those estimated by temporal moment analysis and concluded that the values of R did not differ significantly for the equilibrium model. They also report that the BTCs were better reproduced by the curve fitting than by moment method. In their case, although the moment method failed to capture the peak concentrations, it described the tail of BTCs better than the curve fitting approach. Nevertheless, for an ideal tracer like Tritium, the batch equilibration may not be sensitive enough to measure small values of  $K_d$  (Van Genuchten and Wierenga, 1976). For such a case, the column technique still remains preferable over the batch experiments.

To further explore the reasons for differences between the values of sorption distribution coefficient determined by batch and column techniques, Maraqa (2001) employed a circulation-through column in addition to the batch and miscible displacement experiments. The author used dimethylpthalate (DMP), diethylphathalate (DEP) and dipropylylphathalate (DPP) as contaminants and two natural soil samples with 0.36 % and 1.48 % organic carbon. Their  $K_d$  values determined from batch were higher than the column  $K_d$  values but were comparable with those determined by circulation-through columns. The author attributed the discrepancy between the batch and miscible displacement technique to a leftward shift of the BTCs after ruling out some of the factors originally viewed as a cause for this deviation; however, the identification of the exact cause still remained obscure.

R has also been found in some cases to be velocity-dependent, which may indicate the presence of an additional physical or chemical process currently not included in the nonequilibrium models, but becomes apparent only at relatively large spatial or time scales. Dependence of R on the flow rate is generally regarded as an indication of sorption-related nonequilibrium (Brusseau and Reid, 1991), in which case, R determined with the equilibrium model may not provide a good measure of actual retardation (Maraqa et al., 1999).

#### 2.6.2 Dispersion

Hydrodynamic dispersion coefficient (D) is the sum of mechanical dispersion  $(D_h)$  and effective diffusion coefficient  $(D_e)$ .

$$D = D_h + D_\rho \tag{2-47}$$

$$D_h = \lambda v^n \tag{2-48}$$

$$D_e = D_w \tau_w \tag{2-49}$$

where  $\tau_w$  is the tortuosity factor,  $\lambda$  is the dispersivity and n is an empirical constant whose value typically ranges between 1 and 1.2 (Freeze and Cherry, 1979). The tortuosity factor is assumed to account for the shape and length of the molecular path and depends on water content but not on velocity (Nielsen et al., 1986). The significance of molecular diffusion can be assessed with particle Peclet number i.e.,  $P = vd / D_e$  where d is the mean soil particle diameter. At higher P, the dispersion coefficient exhibits a linear increase with pore water velocity for non-aggregated sands or glass beads (Bear, 1972). Mechanical dispersion occurs, because water flow varies in magnitude and direction in soil pores as a result of meandering through the complex pore structure (Perfect et al., 2002). Mechanical dispersion is primarily caused by two mechanisms, i.e., kinematic and

dynamic (Sahimi et al., 1983). The kinematic mechanism results from variation in length of the streamlines that traverse the length of the column while, the dynamic mechanism results from a variation in the speed of the fluid movement from one streamline to the next. Longitudinal spreading of solute in a porous medium may also be caused by the existence of nonequilibrium processes. This spreading should not be incorporated into the dispersion coefficient if it is to be referred to as hydrodynamic dispersion coefficient (Maraga et al., 1997).

#### 2.6.3 Mass transfer

Dependence of mass-transfer coefficient on pore-water velocity has already been reported in the literature by many investigators e.g., (Brusseau, 1992; Brusseau and Reid, 1991; Van Genuchten et al., 1977). Maraga et al. (1999) report that, (1) sorption nonequilibrium appeared to be of a diffusive nature rather than due to a slow chemical reaction, (2) mass-transfer coefficients varied proportionally with pore-water velocity and (3) variations in the degree of water saturation had no impact on the value of the sorption mass-transfer coefficient other than what would be expected due to changes in the residence time. A strong correlation between the mass-transfer coefficient and residence time  $(LR/\nu)$  is also viewed to exist and may continue to decrease in a consistent way at large residence times. Maraqa et al. (1999) were able to overcome the inconsistencies in the column lengths in the previously reported data by regressing the  $\log(\omega)$  on the values of  $\log (LR/\nu)$  where  $\omega$  is the dimensionless mass transfer coefficient. They were able to explain 92% of the observed variations in  $log(\omega)$  but suggested that factors in addition to the residence time will be required to clarify the unexplained variations in log  $\omega$  values.

# 2.6.4 Effect of nonlinear sorption

Nonlinear sorption affects the shape of BTCs and may also mask the effects of nonequilibrium. A value of the Freundlich exponent less than unity (i.e., n < 1) sharpens the breakthrough front and spreads the elution front while the opposite is true for n > 1. These effects of nonlinearity complicate the assessment of solute dispersion by BTC analysis (Brusseau, 1989). Linearization of the nonlinear isotherm is an option in the absence of analytical solutions as advocated by Brusseau (1989). The effects of nonlinear sorption on other aspects of transport have also been studied. For example, Brusseau (1995) studied the effect of nonlinear sorption on contaminant transport in the presence of rate-limited sorption and first-order transformation, to investigate the coupled effect of these two processes. Mathematically, it was achieved by incorporating the Freundlich partitioning coefficient in the chemical two-site model. An important conclusion drawn from this theoretical analysis is that a model based on linear sorption cannot provide an accurate simulation of the transformation and transport of nonlinearly sorbing solutes when the Freundlich exponent is less than  $\sim 0.9$ . The author suggested that the relative impact of nonlinear sorption on the solute transport is mediated by the magnitude of transformation.

#### 2.7 Review of experimental techniques

In soil sciences the frequently used term of "miscible displacement" involves generating a breakthrough curve by injecting the solute of interest at a desired concentration until the relative concentration at the outlet is unity (i.e.,  $C/C_0=1$ ). The displacement of a non-reactive tracer is also carried out under identical conditions in order to determine the dispersive properties of the medium and the retardation of the

solute. Injecting a pulse of a finite duration and collecting effluent samples at the outlet to generate a complete time series for the entire residence time of the solute has also been resorted to in column studies. A sequential tracer experiment of Jaynes et al. (1995) was an attempt for in situ measurement of MIM parameters by Oliver and Smettem (2003). Most of such studies rely on employing a single conservative tracer. Recently, multiple tracer approach has been used by Fesch et al. (1998) to achieve independent information on the hydrodynamic properties of the columns and the relative importance of different sorbents, if more than one sorbent is present. It is also helpful in determining the accessibility and distribution of these sorbents on the pore scale. Tracer tests using multiple tracers with different diffusivities can also be used to help elucidate the relative contribution of diffusion-mediated mass transfer to solute transport. For a system, that is influenced by diffusional mass transfer process, it is expected that the solute with larger diffusion coefficient would be closer to the condition of equilibrium at a given time than the solute with a smaller diffusion coefficient (Nelson et al., 2003).

The flow interruption technique has also been used in many studies e.g., (Brusseau et al., 1989; Fesch et al., 1998; Fortin et al., 1997; Hu and Brusseau, 1996; Johnson et al., 2003). Flow interruption has been used to differentiate between dispersion and nonequilibrium effects and is based on the assumption that, during the periods of flow interruption, the solute transport proceeds only by diffusion. Changes in the aqueous concentration with increasing periods of flow interruption can be used to identify and quantify processes such as diffusion (Brusseau et al., 1989).

### 2.8 Summary

Multiple processes e.g., sorption, volatilization, and decay etc., affect the transport of reactive organic contaminants in the subsurface environment. A single process can be studied in the lab by designing experiments, which eliminates the possibility of existence of the non-desirable processes from the system. This approach helps in understanding the mechanisms controlling the process and can lead to the development of mechanistic models, which can be used to investigate the influence of an individual mechanism on the overall contaminant behavior. Sorption has been identified as a process with a significant influence on the fate and transport of hydrophobic organic compounds in subsurface. Treatment of sorption in transport models has traditionally been based on a bimodal approach, which is based on an equilibrium transfer and a rate-limited transfer of the contaminant between the solid and liquid phases. Evidence of desorption resistance/irreversible sorption influencing the desorption behavior in batch systems exists but its effects have not been evaluated in flow-through systems. The presence of a desorption-resistant fraction in the flow-through systems can have a significant effect on the transport of organic contaminants. It is likely to influence the nonequilibrium parameters as well as the natural attenuation of the contaminant in the field transport.

Hydrodynamic conditions exert major influence on the behavior of organic contaminants in transport through porous media. Velocity and residence time are viewed to affect the mass transfer rates, however, the influence of these variable on the extent of desorption-resistant fraction of the organic contaminants is unknown. Adequate understanding of these effects is essential in order to develop efficient remediation designs.

#### 2.9 References

- Ahn, I.S., Lion, L.W. and Shuler, M.L., 1999. Validation of a hybrid "two-site gamma" model for naphthalene desorption kinetics. Environmental Science & Technology, 33(18): 3241-3248.
- Akkanen, J. and Kukkonen, J.V.K., 2003. Measuring the bioavailability of two hydrophobic organic compounds in the presence of dissolved organic matter. Environmental Toxicology and Chemistry, 22(3): 518-524.
- Altfelder, S., 2000. Nonequilibrium sorption of non-ionic organic chemicals in soils: Experiments and modeling. Ph.D. Thesis, Technischen Universität Carolo-Wihelmina, Braunschweig, 151 pp.
- Altfelder, S., Streck, T., Maraqa, M.A. and Voice, T.C., 2001. Nonequilibrium sorption of dimethylphthalate Compatibility of batch and column techniques. Soil Science Society of America Journal, 65(1): 102-111.
- Ball, W.P., 1989. Equilibrium sorption and diffusion rate studies with halogenated organic chemicals and sandy aquifer material. Ph.D. Thesis, Stanford University, Stanford, 356 pp.
- Ball, W.P. and Roberts, P.V., 1991. Long-term sorption of halogenated organic chemicals by aquifer material .2. Intra-particle diffusion. Environmental Science & Technology, 25(7): 1237-1249.
- Bear, J., 1972. Dynamics of fluids in porous media. Dover Publications, Inc.
- Bouchard, D.C., Wood, A.L., Campell, M.L., Nkedikizza, P. and Rao, P.S.C., 1988. Sorption nonequilibrium during solute transport. Journal of Contaminant Hydrology, 2: 209-223.
- Brusseau, M.L., 1989. Sorption non-ideality during organic contaminant transport in porous media. Critical Reviews in Environmental Control, 19(1): 33-99.
- Brusseau, M.L., 1991. Application of a multi-process nonequilibrium sorption model to solute transport in a stratified porous medium. Water Resources Research, 27(4): 589-595.
- Brusseau, M.L., 1992. Nonequilibrium transport of organic chemicals The impact of pore-water velocity. Journal of Contaminant Hydrology, 9(4): 353-368.
- Brusseau, M.L., 1995. The effect of nonlinear sorption on transformation of contaminants during transport in porous media. Journal of Contaminant Hydrology, 17(4): 277-291.

- Brusseau, M.L., Jessup, R.E. and Rao, P.S.C., 1991a. Nonequilibrium sorption of organic chemicals Elucidation of rate-limiting processes. Environmental Science & Technology, 25(1): 134-142.
- Brusseau, M.L., Larsen, T. and Christensen, T.H., 1991b. Rate-limited sorption and nonequilibrium transport of organic chemicals in low organic-carbon aquifer materials. Water Resources Research, 27(6): 1137-1145.
- Brusseau, M.L. and Rao, P.S.C., 1989a. The Influence of sorbate-organic matter interactions on sorption nonequilibrium. Chemosphere, 18(9-10): 1691-1706.
- Brusseau, M.L. and Rao, P.S.C., 1989b. Sorption non-ideality during organic contaminant transport in porous media. Critical Reviews in Environmental Control, 19(1): 33-99.
- Brusseau, M.L., Rao, P.S.C., Jessup, R.E. and Davidson, J.M., 1989. Flow interruption: A method for investigating sorption equilibrium. Journal of Contaminant Hydrology, 4: 223-240.
- Brusseau, M.L. and Reid, M.E., 1991. Nonequilibrium sorption of organic chemicals by low organic-carbon aquifer materials. Chemosphere, 22(3-4): 341-350.
- Cameron, D.A. and Klute, A., 1977. Convective-dispersive solute transport with a combined equilibrium and kinetic adsorption model. Society of Petroleum Engineers Journal, 4: 73-84.
- Chiou, C.T., 1989. Theoretical considerations of the partition uptake of non-ionic organic compounds by soil organic matter, "In reaction and movement of organic chemicals in soils". Soil Science Society of America Journal, special publication #22: 1-30.
- Chiou, C.T., Peters, L.J. and Freed, V.H., 1979. Physical concept of soil-water equilibria for non-ionic organic compounds. Science, 206: 831-832.
- Chiou, C.T. and Schmedding, D.W., 1983. Partition equilibria of non-ionic organic compounds between soil organic matter and water. Environmental Science & Technology, 17(4): 227-231.
- Coats, K.H. and Smith, B.D., 1964. Dead end pore volume and dispersion in porous media. Society of Petroleum Engineers Journal, 4(73-84).
- Connaughten, D.F., Stedinger, J.R., Lion, L.W. and Schuler, M.L., 1993. Description of time-varying desorption kinetics: Release of naphthalene from contaminated soils. Environmental Science & Technology, 27(12): 2397-2403.

- Cornelissen, G., Rigterink, H., Ferdinandy, M.M.A. and Van Noort, P.C.M., 1998a.

  Rapidly desorbing fractions of PAHs in contaminated sediments as a predictor of the extent of bioremediation. Environmental Science & Technology, 32(7): 966-970.
- Cornelissen, G., Van Noort, P.C.M. and Govers, H.A.J., 1998b. Mechanism of slow desorption of organic compounds from sediments: A study using model sorbents. Environmental Science & Technology, 32(20): 3124-3131.
- Cornelissen, G., Van Noort, P.C.M., Parsons, J.R. and Govers, H.A.J., 1997. Temperature dependence of slow adsorption and desorption kinetics of organic compounds in sediments. Environmental Science & Technology, 31(2): 454-460.
- Culver, T.B., Hallisey, S.P., Sahoo, D., Deitsch, J.J. and Smith, J.A., 1997. Modeling the desorption of organic contaminants from long-term contaminated soil using distributed mass transfer rates. Environmental Science & Technology, 31(6): 1581-1588.
- Fesch, C., Simon, W., Haderlein, S.B., Reichert, P. and Schwarzenbach, R.P., 1998.

  Nonlinear sorption and nonequilibrium solute transport in aggregated porous media: Experiments, process identification and modeling. Journal of Contaminant Hydrology, 31(3-4): 373-407.
- Fettig, J. and Sontheimer, H., 1987. Kinetics of adsorption on activated carbon.I. Single solute system. Journal of Environmental Engineering, 113: 764.
- Fortin, J., M, F., Jury, W.A. and Streck, T., 1997. Rate-limited sorption of simazine in saturated soil columns. Journal of Contaminant Hydrology, 25: 219-234.
- Freeze, R.A. and Cherry, J.A., 1979. Groundwater, 603. Prentice-Hall Inc, N,J.
- Howerton, S.B., Lee, C. and McGuffin, V.L., 2003. Additivity of statistical moments in the exponentially modified Gaussian model of chromatography. Analytica Chimica Acta, 478(1): 99-110.
- Howerton, S.B. and McGuffin, V.L., 2004. Thermodynamics and kinetics of solute transfer in reversed-phase liquid chromatography Effect of annelation in polycyclic aromatic hydrocarbons. Journal of Chromatography, 1030(1-2): 3-12.
- Hu, Q.H. and Brusseau, M.L., 1996. Transport of rate-limited sorbing solutes in an aggregated porous medium: A multi-process non-ideality approach. Journal of Contaminant Hydrology, 24(1): 53-73.
- Jaynes, D.B., Logsdon, S.D. and Horton, R., 1995. Field method for measuring mobileimmobile water content and solute transfer rate coefficient. Soil Science Society of America Journal, 59: 352-356.

- Johnson, G.R., Gupta, K., Putz, D.K., Hu, Q. and Brusseau, M.L., 2003. The effect of local-scale physical heterogeneity and nonlinear, rate-limited sorption/desorption on contaminant transport in porous media. Journal of Contaminant Hydrology, 64(1-2): 35-58.
- Johnson, M., Keinath, T. and Weber, W.J., 2001. A distributed reactivity model for sorption by soils and sediments. 14. Characterization and modeling of phenanthrene desorption rates. Environmental Science & Technology, 35(8): 2734-2740.
- Kamra, S.K., Lennartz, B., Van Genuchten, M.T. and Widmoser, P., 2001. Evaluating nonequilibrium solute transport in small soil columns. Journal of Contaminant Hydrology, 48(3-4): 189-212.
- Karichoff, S.W., Brown, D.S. and Scott, T.A., 1983. Sorption of hydrophobic pollutants on natural sediments. Water Research, 13(241).
- Laird, D.A. and Fleming, P.D., 1999. Mechanisms of adsorption of organic bases on hydrated smectite surfaces. Environmental Toxicology and Chemistry, 18(1668-1672).
- Lee, L.S., Rao, P.S.C., Brusseau, M.L. and Ogwada, R.A., 1988. Nonequilibrium sorption of organic contaminants during flow through columns of aquifer materials. Environmental Toxicology and Chemistry, 7(10): 779-793.
- Maraqa, M.A., 1995. Transport of dissolved volatile organic compounds in the unsaturated zone. Ph.D. Thesis, Michigan State University, East Lansing, 154 pp.
- Maraqa, M.A., 2001. Prediction of mass-transfer coefficient for solute transport in porous media (vol 50, pg 1, 2001). Journal of Contaminant Hydrology, 53(1-2): 151-171.
- Maraqa, M.A., Wallace, R.B. and Voice, T.C., 1997. Effects of degree of water saturation on dispersivity and immobile water in sandy soil columns. Journal of Contaminant Hydrology, 25(3-4): 199-218.
- Maraqa, M.A., Wallace, R.B. and Voice, T.C., 1999. Effects of residence time and degree of water saturation on sorption nonequilibrium parameters. Journal of Contaminant Hydrology, 36(1-2): 53-72.
- Maraqa, M.A., Zhao, X., Wallace, R.B. and Voice, T.C., 1998. Retardation coefficients of nonionic organic compounds determined by batch and column techniques. Soil Science Society of America Journal, 62(1): 142-152.
- Means.J.C, Wood, S.G., Hasset, J.J. and Banwart, W.L., 1980. Sorption of polynuclear aromatic hydrocarbons by sediments and soils. Environmental Science & Technology, 14: 1524-1531.

- Mingelgrin, U. and Gerstl, Z.J., 1983. Re-evaluation of partitioning as a mechanism of non-ionic chemical adsorption in soils. Journal of Environmental Quality, 12: 1-11.
- Nelson, N.T., Hu, Q. and Brusseau, M.L., 2003. Characterizing the contribution of diffusive mass transfer to solute transport in sedimentary aquifer systems at laboratory and field scales. Journal of Hydrology, 276: 275-286.
- Nielsen, D.R., Van Genuchten, M.T. and Biggar, J.W., 1986. Water flow and solute transport processes in the unsaturated zone. Water Resources Research, 22(9): S89-S108.
- Nkedikizza, P. et al., 1983. Modeling tritium and chloride-36 transport through an aggregated oxisol. Water Resources Research, 19(3): 691-700.
- Nkedikizza, P., Rao, P.S.C. and Hornsby, A.G., 1987. Influence of organic cosolvents on leaching of hydrophobic organic chemicals through soils. Environmental Science & Technology, 21(11): 1107-1111.
- Oliver, Y.M. and Smettem, K.R.J., 2003. Parameterization of physically based solute transport models in sandy soils. Australian Journal of Soil Research, 41(4): 771-788.
- Park, J.H., 2000. Bioavailability of sorbed organic contaminants. Ph.D. Thesis, Michigan State University, East Lansing, 155 pp.
- Park, J.H., Zhao, X.D. and Voice, T.C., 2001. Biodegradation of non-desorbable naphthalene in soils. Environmental Science & Technology, 35(13): 2734-2740.
- Park, J.H., Zhao, X.D. and Voice, T.C., 2002. Development of a kinetic basis for bioavailability of sorbed naphthalene in soil slurries. Water Research, 36(6): 1620-1628.
- Perfect, E., Sukop, M.C. and Haszler, G.R., 2002. Prediction of dispersivity for undisturbed soil columns from water retention parameters. Soil Science Society of America Journal, 66(3): 696-701.
- Pignatello, J.J., 1998. Soil organic matter as a non-porous sorbent of organic pollutants. Environmental Science & Technology, 76-77: 445-467.
- Pignatello, J.J. and Xing, B., 1996. Mechanisms of slow sorption of organic chemicals to natural particles. Environmental Science & Technology, 30: 1-11.
- Plaehn, W.A., Zhao, X.D., Dale, B.E. and Voice, T.C., 1999. Impact of dissolved organic matter on the desorption and mineralization rates of naphthalene. Journal of Soil Contamination, 8(4): 491-507.

- Prata, F., Lavorenti, A., Jan, V., Burauel, P. and Vereecken, H., 2003. Miscible displacement, sorption and desorption of atrazine in a Brazilian oxisol. Vadose Zone Journal, 2: 728-738.
- Rao, P.S.C., Davidson, J.M., Jessup, R.E. and Selim, H.M., 1979. Evaluation of conceptual models for describing nonequilibrium adsorption-desorption of pesticides during steady flow in soils. Soil Science Society of America Journal, 43(1): 22-28.
- Saffron, C., 2005. Plant-enhanced remediation of naphthalene. Ph.D. Thesis, Michigan State University, East Lansing.
- Sahimi, M., Hughes, B.D., Scriven, L.E. and Davis, H.T., 1983. Stochastic transport in disordered systems. Journal of Chemical Physics, 78(11): 6849-6864.
- Schawarzenbach, R.P., Gschwend, P.M. and Imboden, D.M., 1993. Environmental Organic Chemistry. John Willey & Sons inc., New York.
- Schawarzenbach, R.P. and Westall, J., 1981. Transport of non-polar organic compounds from surface water to groundwater. Laboratory sorption studies. Environmental Science & Technology, 15(11): 1360-1367.
- Srivastava, R., Sharma, P.K. and Brusseau, M.L., 2002. Spatial moments for reactive transport in heterogeneous porous media. Journal of Hydrologic Engineering, 7(4): 336-341.
- Srivastava, R., Sharma, P.K. and Brusseau, M.L., 2004. Reactive solute transport in macroscopically homogeneous porous media: Analytical solutions for the temporal moments. Journal of Contaminant Hydrology, 69(1-2): 27-43.
- Valocchi, A.J., 1985. Validity of the local equilibrium assumption for modeling sorbing solute transport through homogeneous soils. Water Resources Research, 21(6): 808-820.
- Van Genuchten, M.T. and Wagenet, R.J., 1989. Two-site/two-region models for pesticide transport and degradation: Theoretical development and analytical solutions. Soil Science Society of America Journal, 53(5): 1303-1310.
- Van Genuchten, M.T. and Wierenga, P.J., 1976. Mass transfer studies in sorbing porous media .1. Analytical solutions. Soil Science Society of America Journal, 40(4): 473-480.
- Van Genuchten, M.T., Wierenga, P.J. and Oconnor, G.A., 1977. Mass transfer studies in sorbing porous media .3. Experimental evaluation with 2,4,5-T. Soil Science Society of America Journal, 41(2): 278-285.

- Van Noort, P.C.M. et al., 2003. Slow and very slow desorption of organic compounds from sediment: influence of sorbate planarity. Water Research, 37(10): 2317-2322.
- Voice, T.C., Rice, C.P. and Weber, W.J., 1983. Effect of solids concentration on the sorptive partitioning of hydrophobic pollutants in aquatic systems. Environmental Science & Technology, 17(9): 513-518.
- Weber, T.W. and Chakravorti, R.K., 1974. Pore and solids diffusion models for fixed-bed adsorbers. American Institute of Chemical Engineers journal, 20(2): 228-238.
- Weber, W.J. and Huang, W., 1996. A distributed reactivity model for sorption by soils and sediments. 4. Intraparticle heterogeneity and phase-distribution relationships under non-equilibrium conditions. Environmental Science & Technology, 30(3): 881-888.

#### **CHAPTER 3**

# DESORPTION KINETICS OF NAPHTHALENE IN BATCH AND COLUMN EXPERIMENTS

#### **Abstract**

Differences in the desorption behavior of naphthalene in batch and column systems were investigated using three sandy soils containing different organic matter content. Soil-naphthalene equilibration for both systems was done in batch for three days to ensure identical conditions during the sorption phase. In addition, three-day sorption isotherms were also conducted on all soils. Solvent extraction with methanol was performed at the end of desorption to account for non-desorbable naphthalene. Kinetic parameters were estimated using nonlinear regression with the two-site and the three-site model. Tritiated water was used to obtain independent estimates of dispersion. Sorption isotherms were linear and consistent with respective organic matter content for all soils. A significant amount of naphthalene could be recovered by methanol extraction in all soils after desorption from soil columns, which suggests that the traditional approach of assuming the solid matrix comprising of only two domains (i.e., an equilibrium domain and a rate-limited domain) is questionable. In all soils, the three-site model incorporating a non-desorption domain described desorption better than the two-site model. The results also provide evidence that longer diffusion path lengths due to packing in columns limit the ability of the contaminant to diffuse into the bulk solution resulting in a greater number of sorption sites to behave as rate-limited sites.

#### 3.1 Introduction

Three regimes of behavior i.e., fast, slow and very slow are known to exist in batch desorption rate studies involving an equilibration period of 2 to 15 days (Ahn et al., 1999; Connaughten et al., 1993; Park, 2000; Park et al., 2003; Park et al., 2001). Rates of desorption associated with the release of hydrophobic organic compounds (HOCs) from soils and sediments are at least biphasic, with an initial rapid sorption phase that occurs over a few hours or days, followed by an extremely slow desorption that can take months or years to reach the end point (Johnson et al., 2001). Very slow desorption is sometimes referred to as non-desorption (Park et al., 2001), desorption-resistant or irreversible sorption (Kan et al., 1997). Although "true" sorption equilibrium may take a very long time to reach, formation of a desorption-resistant fraction within 24 hours (Sharer et al., 2003a; Sharer et al., 2003b) to 3 days (Park et al., 2003) has been observed in batch studies.

Numerous mathematical models exist in the literature that describe desorption in batch systems. These can be categorized based on the different conceptualizations e.g., chemical site models, kinetic models, distributed-rate models and pore diffusion models. The assumption in chemical site models is that the rate-limited sorption/desorption is chemically controlled and a rate-limited sorption/desorption reaction explains the behavior of organic compounds from the soil matrices (Brusseau and Rao, 1989). The chemical two-site and three-site models (Park, 2000) are based on a mathematical formulation that uses a driving force formulation based on the linear distribution coefficient  $K_d$ . Kinetic models i.e., the three-parameter kinetic model (Cornelissen et al.,

1998a) and the five-parameter kinetic model (Cornelissen et al., 1998b) represent two and three regimes of desorption behavior by characterizing these as rapid, slow and very slow processes. These models are based on kinetic rate formulations that are independent of  $K_d$ . The distributed-rate models include a gamma-distribution model (Connaughten et al., 1993) and a hybrid gamma-distribution model (Ahn et al., 1999). In these models, the soil matrix is assumed to contain a series of compartments and desorption from each of these compartments is described by a unique desorption rate coefficient. In addition, one, two and three-parameter pore diffusion models are based on Fick's law and describe one, two and three desorption regimes respectively.

All of these models are mathematical approximations of desorption behavior in batch systems incorporating one, two or three-regimes of behavior. In a recent study (Saffron, 2005), it was shown by a comparison of nine different models applied to the desorption data for four soils and two contaminants that three-regime models describe the observed desorption behavior better than the two-regime models. The conclusion drawn from this study was based on the "Akaike information criterion" (AIC) (Burnham and Anderson, 1998). AIC is a statistical tool to decide if increasing the number of model parameters to improve the description of observed data is justified. The experimental limitations however, limit our ability to draw a distinction between different categories of models if these models are based on equivalent regime description.

In the past, with the exception of a few studies e.g., (Ahn et al., 1999; Prata et al., 2003), flow-through systems have been typically modeled following the dual-domain approach. For contaminant-soil combinations, if three regimes of behavior are observed in batch systems, there is a high probability that these regimes will also exist in the flow-

through systems. In such cases, the adequacy of the dual-domain model becomes questionable. A mathematical description of these regimes, that is compatible with observations, is essential to accurately describe the transport of contaminants in flow-through systems.

In this study, our objective is to experimentally verify, the presence and extent of the third desorption regime (i.e., non-desorption) in flow-through systems. We also evaluate the differences in kinetic parameters between batch and column systems.

# 3.2 Materials and methods

**Solute**. Unlabeled and  $^{14}$ C-naphthalene with uniformly labeled carbons, procured from Sigma Aldrich Co., was utilized as a representative HOC for batch and column desorption experiments due to its suitability compared with other 16 PAHs in the EPA's list for priority pollutants. The solubility of naphthalene in water is approximately 31.6 mg/L at 25 C and its  $K_{OW}$  is about 2300.

Sorbents. Three natural soils i.e., Kalkaska-A, SPCF and an aquifer sand from the Plume-A site Schoolcraft, MI (Dybas et al., 2002) hereafter referred to as Plume-A sand, containing different amounts of soil organic matter (SOM) were used for this study. Mechanical characteristics and SOM of these soils are presented in Table 3-1. These soils represent two different classes in terms of their origin. Kalkaska-A and SPCF are surface soils while Plume-A sand is of aquifer origin obtained from approximately 60 feet below surface. Soil samples were passed through U.S series sieve No. 20 (> 850 microns) to remove larger components after air drying and were irradiated in 20 mL glass vials by  $\gamma$ -irradiation ( $^{60}$ Co source) at a dosage of 5 Mrad at Radiation Science & Engineering Center (RSEC), Pennsylvania State University. Sealed vials were stored at room temperature and were opened immediately before use. Sterility of soil was verified once by plating and no colonies were observed after 3 days.

**Spiking solutions.** The spiking solutions were prepared by mixing unlabeled and  $^{14}$ C-naphthalene in methanol. The spiking solution for the isotherms (4925 mg/L total naphthalene concentration) contained an activity of 2281 dpm/ $\mu$ L and 0.0984%  $^{14}$ C-naphthalene. The spiking solution for rate and transport studies (4939.1 mg/L total

naphthalene concentration) contained approximately 2%  $^{14}$ C-naphthalene and an activity of 52092 dpm/ $\mu$ L

Table 3-1: Characteristics of soils and packed columns

Soil	Organic content (%)	Sand* (%)	Silt* (%)	Clay (%)	Density (g/cm <sup>3</sup> )	Porosity (cm <sup>3</sup> /cm <sup>3</sup> )
Kalkaska-A	3.9	91	7.7	1.7	$0.572 \pm .045$	$0.413 \pm 0.025$
SPCF	1.9	78	17	5	$1.385 \pm 0.009$	$0.436 \pm 0.016$
Plume-A sand	ND	97.6	0	2.4	$1.811 \pm 0.016$	$0.354 \pm 0.016$

Analysis done at the Plant and Soil Sciences laboratory, Michigan State University Sorption isotherms. Three-day sorption isotherms were conducted in 5 mL vials with Teflon caps. Soil-to-water ratios were carefully selected to achieve an equal mass distribution at the end of equilibration period. The aliquots of sterile soil (i.e.,  $0.348 \pm 0.028$  g of Kalkaska-A,  $0.844 \pm 0.095$  g of SPCF, and  $2.64 \pm 0.0283$  g of Plume-A sand) were used in triplicate for the isotherms. Liquid phase volume used for these three soils was  $4.589 \pm 0.034$  mL,  $4.179 \pm 0.022$  mL and  $2.464 \pm 0.028$  mL respectively. The vials were spiked with naphthalene to achieve an initial liquid-phase concentration between 0.5 mg/L to 31 mg/L. Maximum volume of the spiking solution did not exceed  $30 \mu$ L and minimum activity in the liquid phase at the end of equilibration period was always greater than 200 dpm/mL in all samples except one sample of Kalkaska-A, which contained an activity of 120 dpm/mL. Vials were tumbled end-over-end in dark at 6 rpm for 72 hours. At the end of mixing period, these vials were centrifuged at  $1163 \times g$  for 5 minutes for solids separation. The supernatant was sampled and analyzed for naphthalene by liquid

scintillation counting (LSC) and selected samples were verified by high performance liquid chromatography (HPLC) using a reverse phase C-18 column with a mobile phase consisting of 80% acconitrile and 20% acidified water at a flow rate of 1.3 mL/min. Naphthalene was detected by UV absorption at a wavelength of 220 nm.

**Batch desorption.** Desorption rate studies in batch were conducted in 25 mL centrifuge vials with mininert valves equipped with Teflon liners. The vials were autoclaved for 30 minutes and oven-dried for 24 hours prior to use. Soil slurries were prepared in these vials in triplicate by mixing an aliquot of sterile soil with CaCl<sub>2</sub> (0.01M) prepared in deionized water. Soil mass used was 1.0 g  $\pm$  0.002 g for Kalkaska-A, 4.603 g  $\pm$  0.02 g for SPCF, and  $15.004 \pm 0.00045g$  for Plume-A sand and the liquid-phase volume used was  $28.165 \pm 0.0034$  mL for Kalkaska-A,  $27.996 \pm 0.001$  mL for SPCF, and  $22.999 \pm$ 0.0015mL for Plume-A sand. These soil slurries were spiked with naphthalene to achieve an initial liquid-phase concentration of 1500 µg/L. After spiking, vials were tumbled endover-end in dark for 72 hours, centrifuged at 1076 x g for 10 minutes and the supernatant was analyzed by LSC. Sorbed-phase concentration was calculated by difference. After completion of sorption step, the remaining liquid was decanted to the extent possible, vials were topped up with naphthalene free CaCl<sub>2</sub> and were tumbled again at 6 rpm as described earlier. A periodic sampling of the supernatant at 0.5,1,2,3,4,6,12,24,36,48 and 72 hours was done to monitor the liquid-phase concentration over time. At the end of 72 hours of sampling, vials were once again decanted and methanol extraction was performed to determine the concentration of non-desorbable naphthalene.

An independent test to verify the extraction efficiency of methanol was also conducted on separate batch samples for a three-day equilibration period (initial liquid-

phase concentration between 1-5 mg/L). Methanol was found to be  $100 \pm 5\%$  efficient in recovering sorbed naphthalene. This test also confirmed that calculation of sorbed-phase concentration by difference in the sorption isotherms was appropriate.

Column desorption. Column desorption studies were performed using stainless steel columns (15 cm length and 1.1 cm i.d.), with reducing unions at both ends fitted with 25-micrometer frits, to prevent loss of fine particles (Figure 3-1). The column fittings included stainless steel tubing 1/16 inches outer diameter (i.d. 1.27 mm) and Teflon valves. The columns and fittings were autoclaved for 30 minutes at 120 °C and were dried at 105 °C for 24 hours prior to use. Soil-naphthalene equilibration was done in 50 mL Corex centrifuge vials with mininert valves containing Teflon liners. Soil slurry was prepared by mixing a known mass of each soil with 0.01m CaCl<sub>2</sub> and spiking each vial so as to achieve an initial liquid-phase concentration of 5 mg/L. The vials were then tumbled end-over-end in dark for three days. At the end of equilibration period, the vials were centrifuged at 1076 x g for 10 minutes and the liquid phase was analyzed for naphthalene by LSC and HPLC.

Columns were packed with pre-equilibrated wet soil. Approximately 2 mL of the liquid phase was initially poured in the column and the wet soil was transferred using a spatula accompanied by gentle tapping of the column surface with a steel rod, so that soil could settle at bottom. Scooping of the soil continued until the column was filled with wet soil and the liquid phase initially poured in, could overflow.

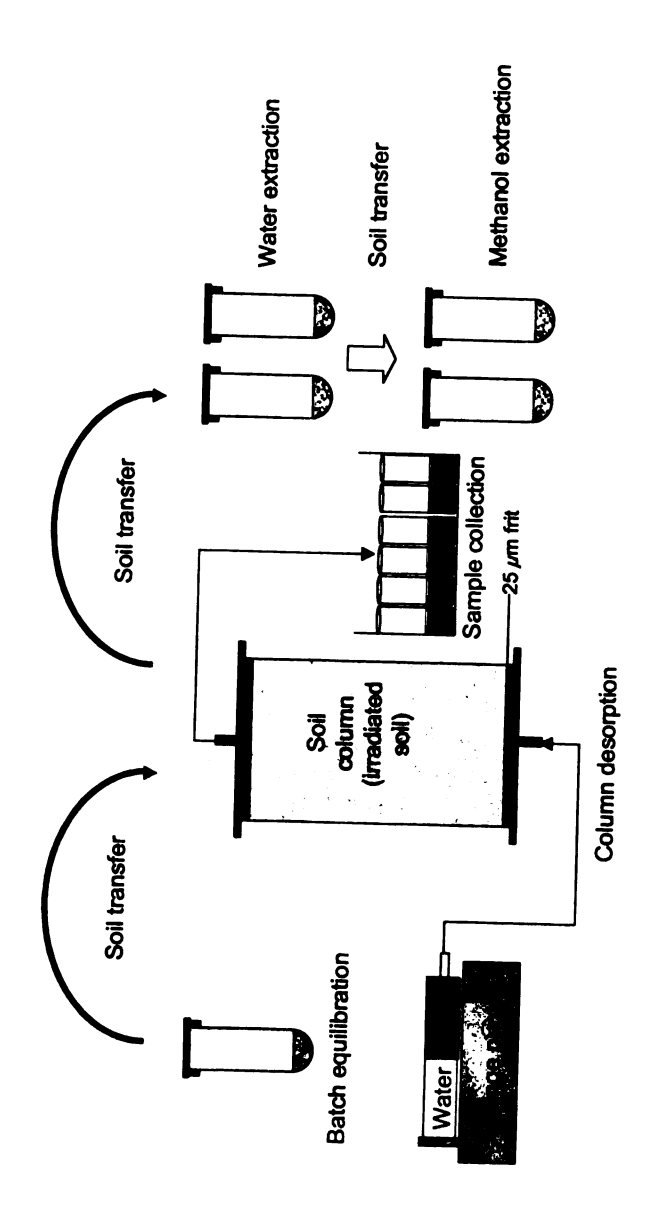


Figure 3-1: Experimental setup for column desorption

The columns were then capped and desorption was initiated by injecting 0.01M CaCl<sub>2</sub> at a constant flow rate of 0.1 mL/min using a syringe pump. Samples were collected over time using a fraction collector in glass tubes pre-filled with scintillation fluid. Sample so collected could settle at the bottom of scintillation cocktail preventing the loss due to volatilization. These samples were then transferred to scintillation vials and analyzed for naphthalene by LSC. Desorption from soil columns continued until the activity in the liquid phase was less than 200 dpm/mL. Columns were then removed and soil was pushed out using a stainless steel rod in pre-weighed 50 mL Corex centrifuge vials. These vials were filled with CaCl<sub>2</sub> to the top and were tumbled at 6 rpm for 24 hours, centrifuged at 1076 x g for 10 minutes and the liquid phase was analyzed for naphthalene, which represented water-extractable fraction. After two to three successive water extractions, solvent extraction was performed using methanol to measure the non-desorbable naphthalene.

To measure the density and porosity of each soil, four separate columns were wet-packed with naphthalene-free soil using the method described above for the spiked soil and were weighed before and after packing. The soil was then pushed out of columns in pre-weighed glass beakers that were oven-dried and re-weighed. Density and porosity for each soil was determined gravimetrically and is reported in Table 3-1. Each soil was also characterized for retardation and dispersion by employing identical soil columns for tritiated water breakthrough. Approximately, two pore volumes of tritiated water with an activity of 28000-31000 DPM/mL were injected and the effluent was sampled every five minutes. The activity of  $^3\text{H}_2\text{O}$  was analyzed by LSC.

# 3.3 Analysis

Mathematical models. In a three-site batch desorption model, the soil matrix is assumed to comprise of three types of desorption sites i.e., equilibrium sites, rate-limited sites and non-desorption sites (Park, 2000). The equilibrium and non-desorption partitioning in this model are described by:

$$S_{eq} = f_{eq} K_d C_{des} (3-1)$$

$$S_{nd} = f_{nd} K_d C_{eq} (3-2)$$

while the release from the rate-limited sites follows the first-order expression:

$$\frac{dS_{neq}}{dt} = \alpha \left[ f_{neq} K_d C_{des} - S_{neq} \right]$$
 (3-3)

where  $S_{eq}$ ,  $S_{neq}$  and  $S_{nd}$  are the sorbed-phase concentrations ( $\mu g/Kg$ ) in equilibrium, rate-limited and non-desorption sites respectively,  $C_{des}$  is the liquid-phase concentration ( $\mu g/L$ ) in the desorption assay,  $C_{eq}$  is the liquid-phase concentration ( $\mu g/L$ ) at sorption equilibrium;  $f_{eq}$ ,  $f_{neq}$  and  $f_{nd}$  are the equilibrium, rate-limited and non-desorption site fractions,  $\alpha$  is the first order desorption rate coefficient (hr<sup>-1</sup>) for the rate-limited sites and  $K_d$  is the linear sorption distribution coefficient. For a linear sorption case,  $K_d$  in the batch systems is given by:

$$K_d = \frac{S_{eq}}{C_{eq}} \tag{3-4}$$

For desorption from a soil column,  $K_d$  can be calculated by (Zhao and Voice, 2000):

$$K_d = \frac{(M_e - P_\nu C_0)1000}{m_{soil} C_0} \tag{3-5}$$

where  $M_e$  is the contaminant mass calculated from the effluent desorption curves (µg),  $m_{soil}$  is the soil mass in column (g) and  $C_0$  is the average liquid-phase concentration in soil column prior to desorption (µg/L) and  $P_v$  is the volume of liquid phase (equal to one pore volume) in the column at the start of desorption (mL). Solute transport through a porous medium is typically based on the advection-dispersion equation:

$$\frac{\partial C}{\partial t} + \frac{\rho}{\theta} \frac{\partial S}{\partial t} = D \frac{\partial^2 C}{\partial x^2} - v \frac{\partial C}{\partial x}$$
 (3-6)

where C is liquid-phase concentration ( $\mu g/L$ ), S is sorbed-phase concentration ( $\mu g/Kg$ ),  $\nu$  is average linear pore-water velocity (cm/hr), D is hydrodynamic dispersion coefficient (cm<sup>2</sup>/hr), x is the distance along principal direction of flow (cm) and t is time (hr).

Equation 3-6 is referred to as the equilibrium model, if the condition of local equilibrium is assumed between the liquid phase and sorbed phase. The dimensionless form of the equilibrium model is:

$$R\frac{\partial C_1}{\partial T} = \frac{1}{P} \frac{\partial^2 C_1}{\partial Z^2} - \frac{\partial C_1}{\partial Z}$$
 (3-7)

where:

$$C_1 = \frac{C}{C_o}, \ Z = \frac{x}{L}, \ T = \frac{vt}{L}, \ R = 1 + \frac{\rho K_d}{\theta}, \ P = \frac{vL}{D}$$

In lab and field studies, the asymmetry in the observed breakthrough curves (BTCs) is believed to be a result of a slower desorption rate compared to sorption. The most widely used model to describe these rate limitations is the two-site model (Selim et al., 1977; Van Genuchten and Wagenet, 1989) in which, the solid matrix is divided into two domains i.e., an equilibrium domain comprising of instantaneous sorption/desorption

sites and a rate-limited domain comprising of sorption sites for which sorption/desorption is rate-limited. For a homogeneous soil, the governing equations for a linearly adsorbed solute are:

$$(1 + \frac{f_{eq}\rho K_d}{\theta})\frac{\partial C}{\partial t} = D\frac{\partial^2 C}{\partial r^2} - v\frac{\partial C}{\partial r} - \frac{\alpha\rho}{\theta}[(1 - f_{eq})K_dC - S_{neq}]$$
(3-8)

$$\frac{\partial S_{neq}}{\partial t} = \alpha [(1 - f_{eq})K_dC - S_{neq}]$$
(3-9)

where  $S_{neq}$  is solid-phase concentration in the rate-limited domain ( $\mu g/Kg$ ),  $\alpha$  is the first order kinetic rate coefficient (hr<sup>-1</sup>) governing the rate of solute exchange between liquid phase and solid matrix in rate-limited domain and  $f_{eq}$  is fraction of exchange sites that are at equilibrium. Using the dimensionless parameters, the two-site model reduces to following form:

$$\beta R \frac{\partial C_1}{\partial T} = \frac{1}{P} \frac{\partial^2 C_1}{\partial Z^2} - \frac{\partial C_1}{\partial Z} - \omega (C_1 - C_2)$$
(3-10)

$$(1-\beta)R\frac{\partial C_2}{\partial T} = \omega(C_1 - C_2) \tag{3-11}$$

where:

$$C_1 = \frac{C}{C_o}, C_2 = \frac{S_{neq}}{(1 - f_{eq})K_dC_o}, \beta = \frac{\theta + f_{eq}\rho K_d}{\theta + \rho K_d}, \omega = \frac{\alpha(1 - \beta)RL}{\nu}$$

Subscripts I and I refer to the equilibrium and rate-limited sites respectively, I is the dimensionless partitioning coefficient and I is the dimensionless mass transfer coefficient. The parameters I, I, I and I are the same as described for Equation 3-7. Some studies have utilized a first order degradation rate coefficient to mimic non-

desorption e.g., (Prata et al., 2003), however, in the presence of degradation, mass disappearance due to irreversible sorption has to be separated from that due to degradation/decay. This can be achieved by incorporating a non-desorption site fraction  $(f_{nd})$  in the soil matrix (Figure 5-2). The governing equations for the three-site model then become:

$$(1 + \frac{f_{eq}\rho K_d}{\theta})\frac{\partial C}{\partial t} = D\frac{\partial^2 C}{\partial x^2} - v\frac{\partial C}{\partial x} - \frac{\alpha_1 \rho}{\theta}[(1 - f_{eq} - f_{nd})K_dC - S_{neq}]$$

$$-\frac{\alpha_3 \rho}{\theta} f_{nd}K_dC$$
(3-12)

$$\frac{\partial S_{neq}}{\partial t} = \alpha_1 [(1 - f_{eq} - f_{nd}) K_d C - S_{neq}]$$
(3-13)

$$\frac{\partial S_{nd}}{\partial t} = \alpha_3 f_{nd} K_d C \tag{3-14}$$

The dimensionless equations for the three-site model for the flow-through systems are:

$$\beta_1 R \frac{\partial C_1}{\partial T} = \frac{1}{P} \frac{\partial^2 C_1}{\partial Z^2} - \frac{\partial C_1}{\partial Z} - \omega_1 (C_1 - C_2) - \omega_3 C_1 \tag{3-15}$$

$$R(1-\beta_1-\beta_2/R)\frac{\partial C_2}{\partial T} = \omega_1(C_1-C_2)$$
(3-16)

$$\beta_2 \frac{\partial C_3}{\partial T} = \omega_3 C_1 \tag{3-17}$$

where:

$$C_{1} = \frac{C}{C_{o}}, C_{2} = \frac{S_{neq}}{(1 - f_{eq} - f_{nd})K_{d}C_{o}}, C_{3} = \frac{S_{nd}}{f_{nd}K_{d}C_{o}}$$

$$\beta_{1} = \frac{\theta + f_{eq}\rho K_{d}}{\theta + \rho K_{d}}, \beta_{2} = \frac{\rho f_{nd}K_{d}}{\theta}, \omega_{1} = \frac{\alpha_{1}LR}{\nu}(1 - \beta_{1} - \beta_{2}/R), \omega_{3} = \frac{\alpha_{3}L}{\nu}\beta_{2}$$

Desorption from soil columns filled with wet pre-equilibrated soil represents only the desorption phase. The three-site model equations have to be modified to represent this

special case by eliminating the term that represents solute flux from the liquid phase to the non-desorption sites. The governing equations for this special case are:

$$(1 + \frac{f_{eq}\rho K_d}{\theta})\frac{\partial C}{\partial t} = D\frac{\partial^2 C}{\partial x^2} - v\frac{\partial C}{\partial x} - \frac{\alpha_1 \rho}{\theta}[(1 - f_{eq} - f_{nd})K_dC - S_{neq}]$$
(3-18)

$$\frac{\partial S_{neq}}{\partial t} = \alpha_1 [(1 - f_{eq} - f_{nd}) K_d C - S_{neq}]$$
(3-19)

and the dimensionless equations for the three-site model representing column desorption become:

$$\beta_1 R \frac{\partial C_1}{\partial T} = \frac{1}{P} \frac{\partial^2 C_1}{\partial Z^2} - \frac{\partial C_1}{\partial Z} - \omega_1 (C_1 - C_2)$$
(3-20)

$$R(1 - \beta_1 - \beta_2 / R) \frac{\partial C_2}{\partial T} = \omega_1 (C_1 - C_2)$$
 (3-21)

Solution technique. The solution of the advection dominated transport problems generated by simple finite-difference and finite element methods typically contain spurious oscillations and/or numerical diffusion near steep concentration gradients (Fischer et al., 1979). In addition, there are additional truncation errors in solving transient problems that arise from approximating the time derivative term (Croucher and O'Sullivan, 1998). Higher-order accurate schemes (greater than second-order) guarantee much better convergence towards grid-independence along with better wave number resolution (Demuren et al., 2001). For this study, the governing three-site model equations, with initial and boundary conditions, were solved using a high-resolution numerical scheme. The spatial derivatives were approximated using a fourth-order compact scheme with spectral like resolution (Lele, 1992) and a fourth-order Runge-Kutta scheme was used for temporal differencing. Higher accuracy was achieved by implicitly solving the fourth-order compact relations for the first and second derivatives

of the concentrations, which form a system of equations solvable by tri-diagonal matrix solvers (Phanikumar and Hyndman, 2003). The well-known Thomas algorithm (Roache, 1998) was used to solve the system of equations resulting in a tri-diagonal matrix form. A uniform grid of 301 points was used for all model runs.

Parameter estimation. Parameters for the batch desorption (i.e.,  $\alpha$ ,  $f_{eq}$  and  $f_{neq}$ ) were estimated by nonlinear regression of the three-site model for batch systems (Equations 3-1 to 3-3). Column desorption data were analyzed to determine the optimized parameter values using nonlinear regression with two-site model and three-site model for the flow-through systems. Parameters for the two-site model ( $\beta$  and  $\omega$ ) were estimated using the  $K_d$  values obtained from batch isotherms and those calculated from the column desorption. A nonlinear least squares inversion program CXTFIT (Toride et al., 1999) was used for estimating these parameters. Parameters for the three-site model ( $\beta_1$ ,  $\beta_2$  and  $\omega$ ) were estimated using variable-metric methods (also called sequential quadratic programming, SQP) as implemented in MATLAB. A script was developed in MATLAB to run the FORTRAN code based on the dimensionless equations of the three-site model and to minimize the following objective function:

$$F(\phi) = \sum_{i=1}^{n} \left[ C(\phi)_i - C_{obs} \right]$$
 (3-22)

in which  $\phi$  is the parameter set  $\left[\beta_{1},\beta_{2},\omega\right]$ ,  $C_{obs}$  is the vector of observed concentrations,  $C(\phi)$  is a vector of the predicted model concentrations for the sampling times. The SQP algorithm converged to a minimum in approximately 500-1000 iterations with a relative tolerance of  $10^{-5}$ . The details of measured, estimated and calculated parameters for

column desorption using two-site and three-site model are tabulated in Table A-1 in Appendix-A.

# 3.4 Results and discussion

**Isotherms**. Sorption of naphthalene was linear in all the three soils (Figure 3-2).

Distribution coefficients calculated using linear regression were 9.22 mL/g for Kalkaska-A, 5.82 mL/g for SPCF and 1.46 mL/g for Plume-A sand respectively. The  $K_d$  values for all soils are consistent with their respective SOM i.e., 1.9 % and 3.9 % and < 0.03% for Kalkaska-A, SPCF and Plume-A sand respectively. Our value for SPCF is comparable with the previously reported value of 4.26 mL/g (Park et al., 2001) but is different for Kalkaska-A (i.e., 25.6 mL/g). The reason for this difference was attributed to a different batch of soil collected from the same location but at a different time of the year, which is likely to alter SOM.

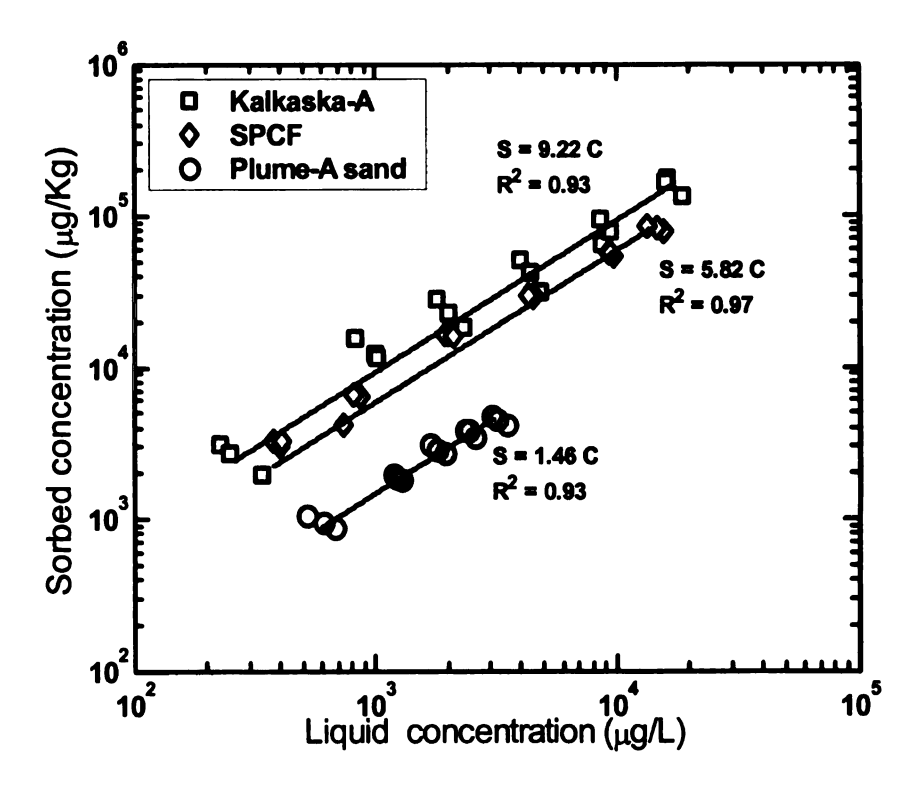


Figure 3-2: Three-day sorption isotherms of naphthalene

**Batch desorption.** In batch desorption rate studies, an equilibrium regime and a nondesorption regime could be observed in all soils, however, the rate-limited regime was relatively insignificant in SPCF (Figure 3-3). This indicates that the release of naphthalene occurred faster in SPCF than in Kalkaska-A. Parameters for the three-site model (Table 3-2) indicate that the site fractions for Kalkaska-A and Plume-A sand were remarkably similar. These two soils are similar in their mechanical characteristics but different in SOM and origin. Out of the two surface soils, the soil with low SOM (i.e., SPCF) displayed larger fractions of equilibrium sites (i.e., 0.63 compared with 0.29) and lower fraction of non-desorption sites (i.e., 0.35 against 0.59) compared with Kalkaska-A. The fraction of rate-limited sites for Kalkaska-A and SPCF was 0.12 and 0.02 respectively. Desorption rate coefficient for Kalkaska-A was significantly lower than that of SPCF indicating a slower desorption. These observations are contrary to what has been observed by Park et al. (2001), who reported that the estimated non-desorption site fractions obtained by a nonlinear regression based on a chemical three-site model were remarkably similar, in spite of the soils bearing different organic content. Park et al. (2003) reported a systematic increase in the fraction of equilibrium (0.20 to 0.73) sites, desorption rate coefficients (0.002 to 0.0029 min<sup>-1</sup>) and the linear distribution coefficient  $K_d$  with an increase in the organic carbon (1.29% to 38.3%). They also report a narrow range of rate-limited sites (i.e., 0.14 to 0.17) for their soils excluding the Kmontmorillonite and Housten. However, no conspicuous trend was observable for the fraction of non-desorption sites and the authors donot offer any explanation in this regard. Sharer et al. (2003b) suggested the presence of a specific physical or chemical sorption interaction rather than slow diffusion based on a rapid formation of a desorption-resistant

fraction (i.e., 0.17-0.27) within 24 hours. This could probably be explained by the behavior of the soil with almost no organic matter content (i.e., Plume-A sand), for which the fraction of non-desorption sites was the highest. The preferred sorption mechanism for HOCs is partitioning to organic matter; however, immediate formation of non-desorbable naphthalene suggests that some fraction of naphthalene mass interacts with active mineral surface sites. It also hints at the possibility that these two processes occur simultaneously. The equilibrium and rate-limited site fractions in Plume-A sand were 25 % and 15% respectively while the desorption rate coefficient was approximately 5 times lower than that of Kalkaska-A and approximately 28 times lower than SPCF. This indicates a dominant surface adsorption mechanism rather than SOM partitioning in Plume-A sand that appears to follow comparatively slower kinetics.

Table 3-2: Fractions of equilibrium, rate-limited and non-desorption sites and the desorption rate coefficients for batch desorption of naphthalene estimated by fitting the three-site model

Soil	Si	ite fractio	ns	Desorption rate coefficient	R <sup>2</sup>
	$f_{eq}$	$f_{neq}$	$f_{nd}$	$\alpha (hr^{-1})$	
Kalkaska-A	0.29	0.12	0.59	0.364	0.955
SPCF	0.63	0.02	0.35	2.163	-
Plume-A sand	0.25	0.15	0.60	0.077	0.983

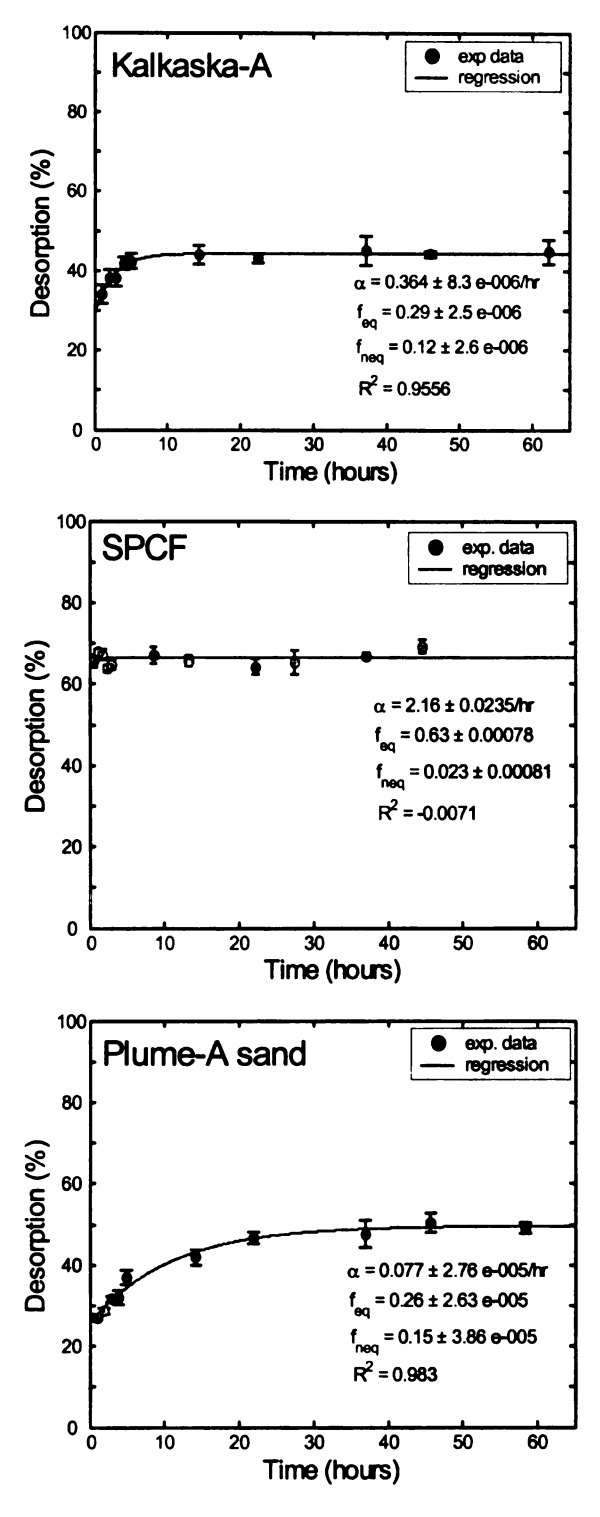


Figure 3-3: Best fits of the three-site model to the observed naphthalene desorption data in batch experiments

Analysis of tracer data. In column desorption experiments, it is important to rule out the possibility of a physical process being the cause of rate limitations (e.g., entrapment of water into relatively stagnant zones). In addition, the dispersive properties of the medium must be determined. To rule out the possibility of a physical process responsible for rate-limited desorption, the equilibrium model was fitted to tritiated water BTCs (Figure 3-4) using the nonlinear least squares inversion program CXTFIT (Toride et al., 1999) and the retardation coefficients were determined. Values of R less than unity indicate that all the pores do not participate in flow (Maraga et al., 1998). Values of R less than unity for tritiated water have been reported (Nkedikizza et al., 1983) and have been attributed to transport-related nonequilibrium created by the presence of mobile and immobile water regions. In our data, no evidence of a transport-related nonequilibrium was found in any of the soils. The retardation factors for Kalkaska-A and Plume-A sand were not different than unity (Table 3-3). For SPCF, the estimated R was significantly greater than unity. Values greater than unity for tritiated water have been reported. For example, Seyfried and Rao (1987) reported R for tritiated water between 1.10-1.18 for their columns. We also observed a velocity-dependent R for SPCF (i.e., 1.083 to 1.282) in our experiments conducted at four different velocities ranging between 3.16 – 15.79 cm/hour in a separate study (all data not reported here). We attribute this to the isotopic exchange of tritiated water with crystallatic hydroxyls of clay particles as proposed by Van Genuchten and Wierenga (1977). We note that SPCF has a clay content of 5 %, which is slightly higher than the other two soils. Based on the analysis of retardation, the dispersion coefficients for Kalkaska-A and Plume-A sand were estimated using the equilibrium model in CXTFIT with a value of R fixed to unity. Due to a significant

velocity-dependent R in SPCF, the dispersion coefficient was estimated by using R=1.083 estimated in first step. These estimated dispersion coefficients were used in all the subsequent model applications to calculate Peclet numbers.

Table 3-3: Retardation factors and dispersion coefficients estimated using the equilibrium model

Soil	Velocity (cm/hr)	Retardation factor R	Dispersion coefficient $D \text{ (cm}^2/\text{hr)}$
Kalkaska-A	18.34	0.970 (0.961-0.980)	5.66 (4.56-6.77)
SPCF	15.80	1.083 (1.078-1.088)	1.67 (1.47-1.86)
Plume-A Sand	17.18	0.995 (0.986-1.003)	12.33 (11.30-13.36)

Note: The values in parentheses represent lower and upper bounds based on 95% confidence intervals

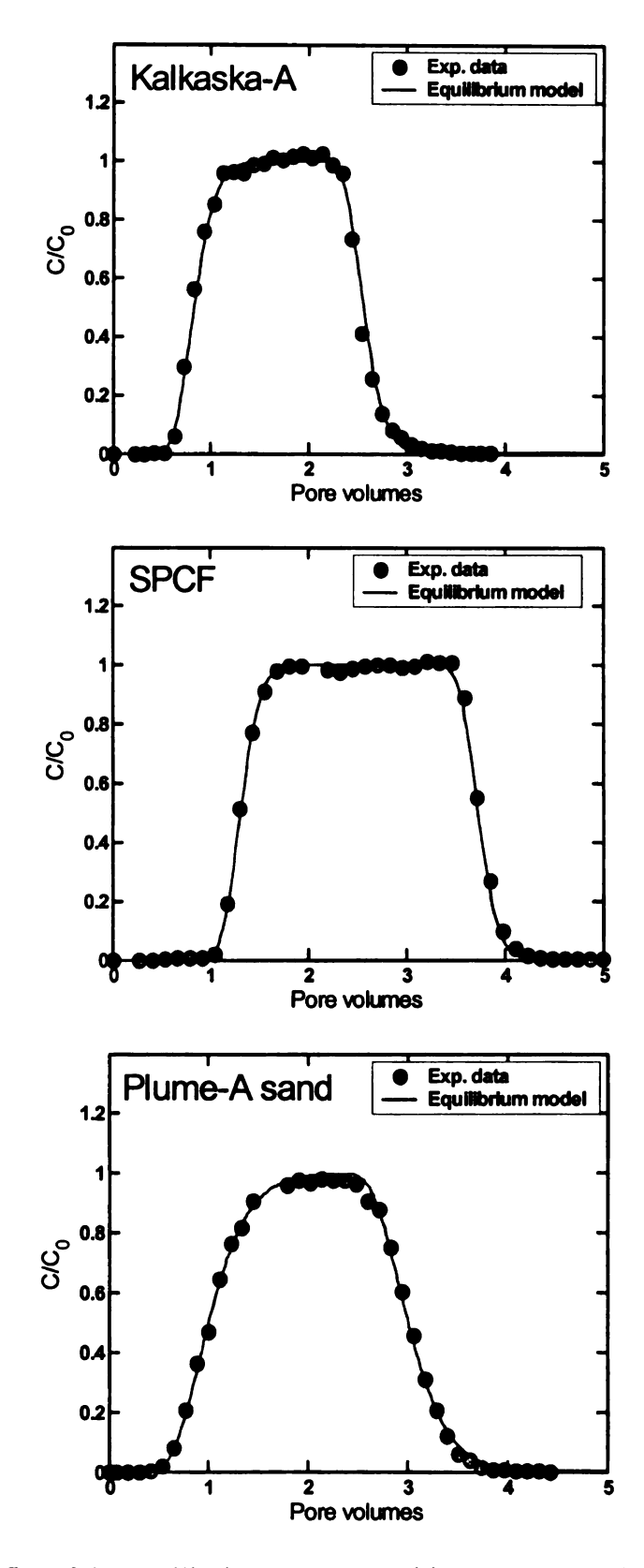


Figure 3-4: Best fits of the equilibrium model to tritiated water BTCs at 0.1 mL/min

Column desorption. Desorption of naphthalene from soil columns continued for approximately 65 to 70 pore volumes for Kalkaska-A and SPCF while for plume-A sand it took approximately 30 pore volumes. The desorption curves from the columns for the three soils exhibited different shapes (Figure 3-5) but were consistent with what would be expected based on the organic matter partitioning for the two surface soils (i.e., Kalkaska-A and SPCF) and with that of surface adsorption for Plume-A sand.

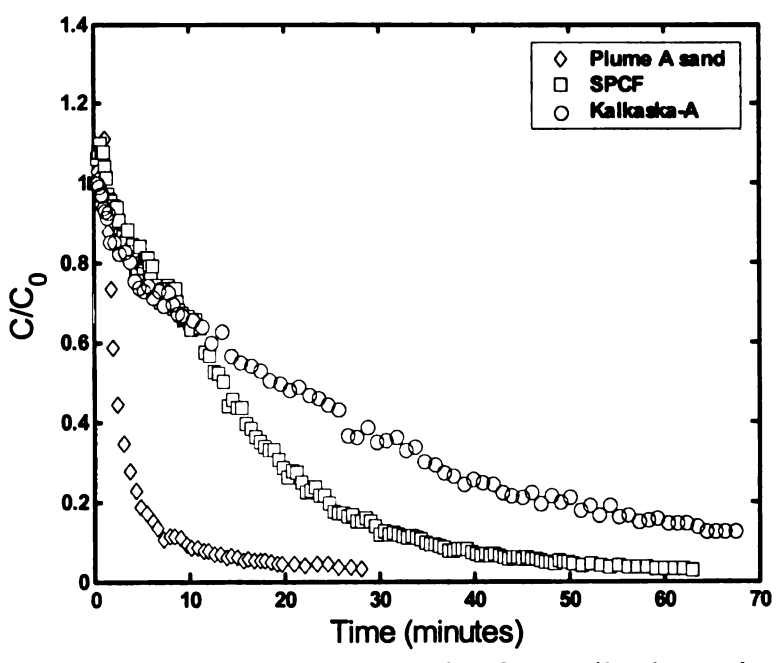


Figure 3-5: Naphthalene desorption from soil columns in the three soils

The degree of sorption nonequilibrium in non-ionic organic compounds (NOCs) has been shown to increase with an increase in SOM (Bouchard, 1998). In soil with a higher SOM (i.e., Kalkaska-A), the methanol extractable mass was higher compared to SPCF (Table 3-4). A higher mass elution in column desorption for SPCF compared with Kalkaska-A (i.e., 88.01 % compared with 65.41%) when almost equal number of pore volumes have eluted, indicates comparatively slower desorption for Kalkaska-A soil than

SPCF. Methanol extractable mass at the end of column desorption was also greater for Kalkaska-A than SPCF (i.e., 23.59% compared to 8.26%) suggesting a strong correlation between SOM and desorption-resistance.

Table 3-4: Desorbable, water-extractable and solvent-extractable naphthalene mass for each soil in column desorption experiments

Soil	Mass from column desorption	Mass from batch water extraction	Mass from methanol extraction	Recovery
	(%)	(%)	(%)	(%)
Kalkaska-A	64.51	11.90	23.59	70.4
SPCF	88.01	3.72	8.26	60.7
Plume-A sand	41.50	13.92	44.59	86.6

Sorption distribution coefficient  $K_d$  is a fundamental parameter in some of the mathematical models that use a driving force formulation of the form  $(K_d C-S_{neq})$  to describe desorption in batch and column systems.  $K_d$  values derived from batch isotherms can be used in transport models in the absence of sorption nonlinearity and nonsingularity. In our case, isotherms for all three soils were linear over the concentration range employed; therefore, modifying the governing transport equations to incorporate the effects of nonlinear isotherms in transport models was not considered essential. However, in all three soils, an evidence of sorption non-singularity existed as confirmed by solvent-extractable naphthalene in all batch and column experiments. It was, therefore, essential to investigate which  $K_d$  value is appropriate to use in the transport model. As an initial step, a comparison was made between the isotherm  $K_d$  and the column desorption  $K_d$  for each soil. The column desorption  $K_d$  was calculated with Equation 3-5 using the desorbable mass calculated by integrating the time-concentration data from the column

desorption. Sorption non-singularity affects the value of  $K_d$  in column desorption experiments, because a significant fraction of contaminant mass is unaccounted for. This is evident from the values listed in Table 3-5. Column  $K_d$  values calculated using Equation 3-5 were 15-55 % lower than the isotherm  $K_d$  values when only the naphthalene mass desorbing from soil columns was used. The column desorption  $K_d$  values for Kalkaska-A and SPCF become comparable with the batch isotherm  $K_d$  values, once the total mass is accounted for. We note that the total naphthalene mass includes the mass desorbed from soil column, the mass recovered by water extraction that follows column desorption and the mass recovered by methanol extraction.

Table 3-5: Comparison of batch and column sorption distribution coefficients

	Batch $K_d$		Column desor	otion $K_d$
Soil	From isotherm	Using desorbable mass	Using desorbable and water-extractable mass	Using desorbable, water-extractable and solvent- extractable mass
Kalkaska-A	9.22	6.45	7.69	10.14
SPCF	5.82	4.93	5.55	5.65
Plume-A sand	1.46	0.65	0.93	1.83

In our experiments, we were able to establish that the conditions of physical equilibrium exist in the system, as the equilibrium model was able to describe tritiated water BTCs for all three soils. Therefore, we analyzed the column desorption data under an assumption of sorption-related nonequilibrium. Retardation factor R is model a parameter that needs to be assigned correctly for estimating other parameters in equilibrium or nonequilibrium models. In columns, conventional methods to estimate R

include (1) number of pore volumes eluted at which  $C/C_0$  equal 0.5 (2) area above the curve for a step input and (3) the mean (first moment) for a pulse input. For columns, wet-filled with pre-equilibrated soil, none of these methods is suitable to use. In the absence of an ability to estimate R by any of these three methods, one of the available options is estimation of R by curve fitting. However, due to non-desorption, R estimated by curve fitting is underestimated, as was the case for all three soils. The R values estimated by curve fitting with two-site model were 28.18 ( $\pm 0.47$ ) for Kalkaska-A, 16.40 ( $\pm 0.26$ ) for SPCF and 4.306 ( $\pm 0.307$ ) for Plume-A sand. These R values result in  $K_d$  values of 7.14, 4.85 and 0.65 for the three soils respectively and are significantly lower than isotherm  $K_d$  or column desorption  $K_d$  values.

In nonequilibrium models that are based on either a two-domain or a three-domain conceptualization, the driving force controlling the mass flux from liquid phase to solid phase and vise versa is represented by the term  $(K_dC-S_{neq})$ . This representation is inadequate, if  $K_d$  values are calculated based on the mass eluting form the column only and water-extractable and solvent-extractable mass is neglected. We calculated R for naphthalene in two different ways; (1) using the isotherm  $K_d$  and (2) using the column desorption  $K_d$  that was calculated from the total naphthalene mass (i.e., desorbable mass + water-extractable mass + solvent-extractable mass), both being physically measured parameters. In our model applications, R and hence  $K_d$  was not estimated as a fitting parameters.

Table 3-6: Parameters for the two-site and the three-site models in column desorption experiments

Soil	Model	R	В	β2	ø	feg	fneg	$f_{nd}$	$\alpha (hr^{-1})$	$\mathbb{R}^2$
	2-site with	36.09	0.0839		1.358	90.0	0.94		0.0419	0.950
Kalkaska-A	$V_d$ (Isomerm)		(±0.0127)		(±0.131)					
17-pucpupu	2-site with	706	0.0921		1.188	700	000		0.0227	000
	$K_d$ (column)	39.0	$(\pm 0.0158)$		$(\pm 0.137)$	0.0	0.93		0.0337	0.92
	3- site with	206	0.061	020 7	. 6	3000	0.017	0.157	00500	3000
	$K_d$ (column)	35.0	0.031	0.070	70.1	0.023	0.023 0.017	0.137		0.993
:	2-site with	10.40	0.1428		2.148	010	000		0.1241	7200
SPCE	$K_d$ (isotherm)	19.49	$(\pm 0.0198)$		$(\pm 0.17)$	0.10	0.50		0.1241	0.970
SI CI	2-site with	10.01	0.1427		2.215	000	0.01		0.1217	000
	$K_d$ (column)	10.74	$(\pm 0.0188)$		$(\pm 0.161)$	0.03	0.91			0.70
	3- site with	10 04	0.104	73E C	2 7240	600		0.130		7000
	$K_d$ (column)	16.94	0.104	7.330	2.1349	0.034	0.014	0.130	0.1000	0.994
	2-site with	6 47	0.281		0.1283	0.10	600	a ·	0.0351	0.070
Plume-A	$K_d$ (isotherm)	0.4/	$(\pm 0.0155)$		$(\pm 0.0031)$	0.10	70.0			0.273
Sand	2-site with		0.2328		0.1160	0.16	300			0.00
	$K_d$ (column)	10.27	$(\pm 0.0131)$		$(\pm 0.0286)$	0.13	0.00		0.0173	0.770
	3- site with	10.07	3000	077.5	73260	0.14	0 230	0690	0 1001	0000
	$K_d$ (column)	10.27	0.443	3.740	0.2307	41.0		0.020		0.75

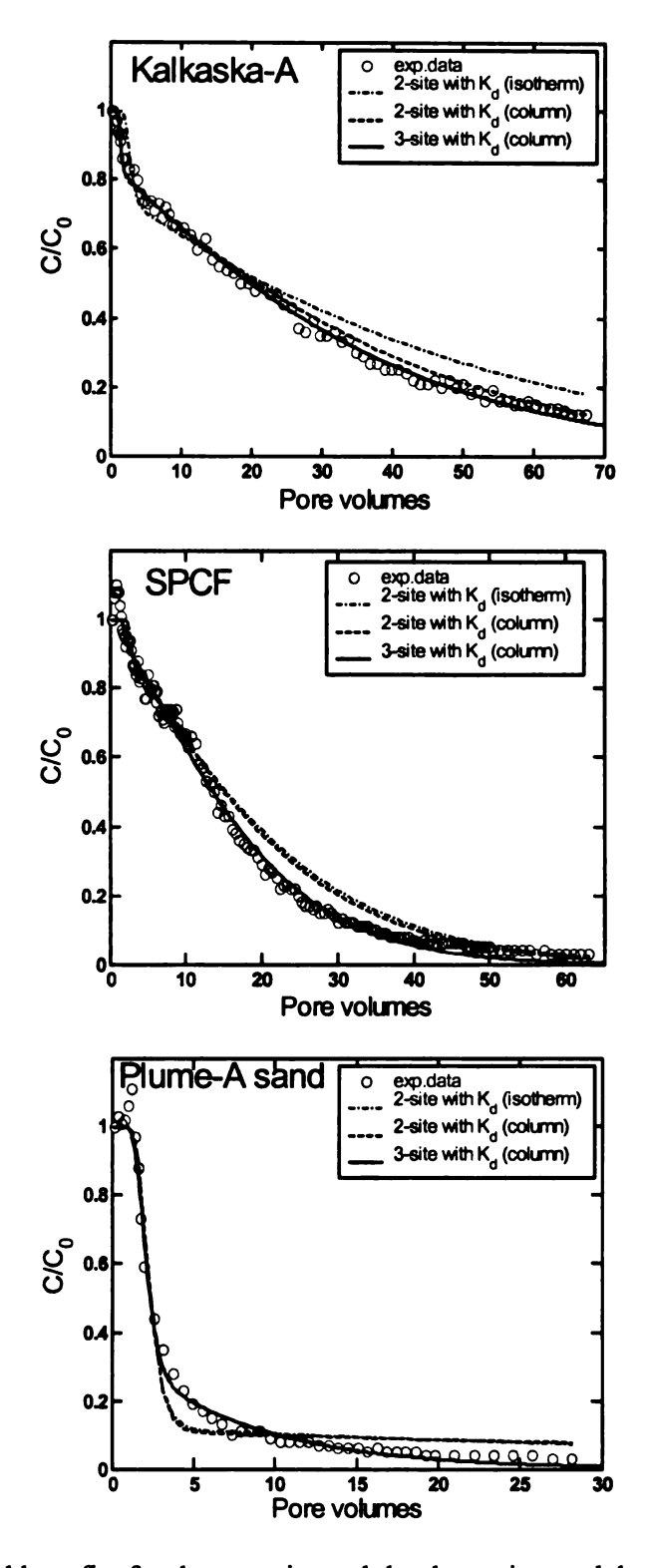


Figure 3-6: Model best fits for the two-site and the three-site models to the observed naphthalene desorption data in soil columns

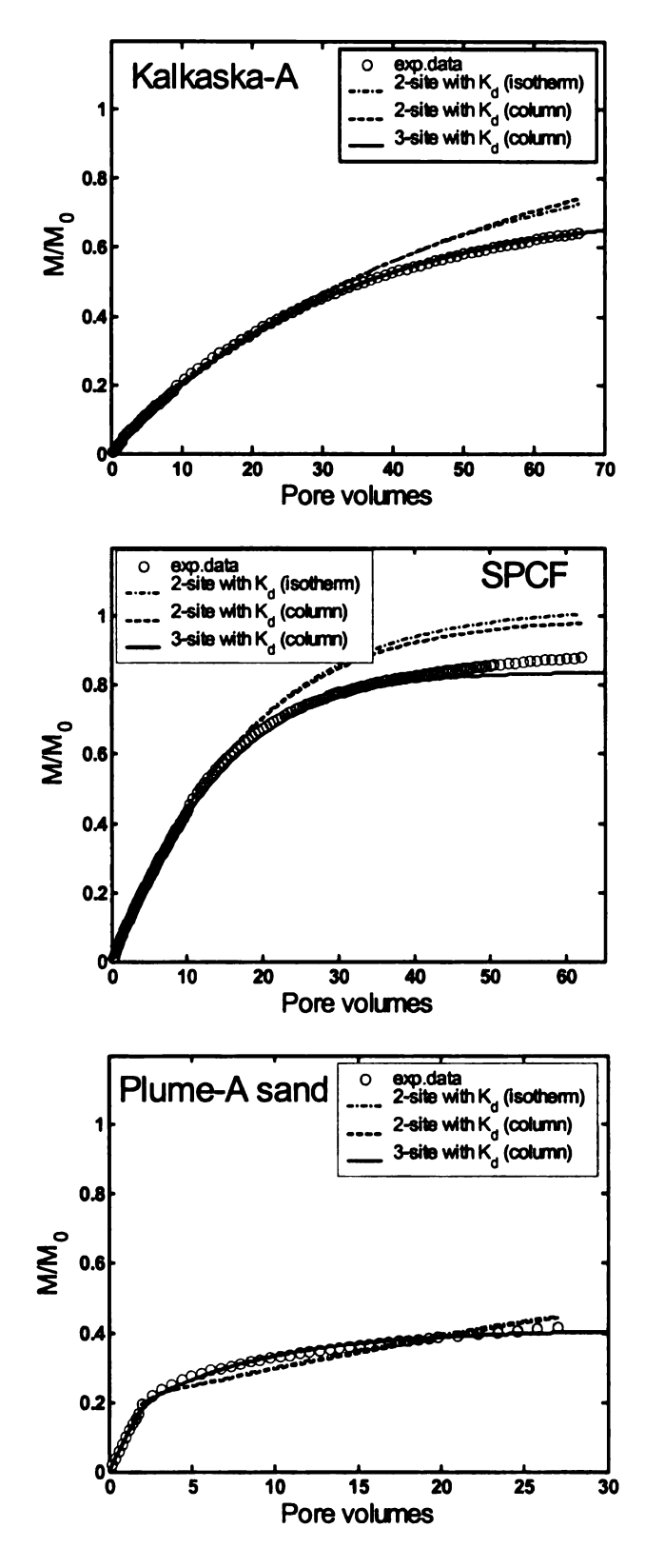


Figure 3-7: Model best fits of the two-site and the three-site models to the observed naphthalene desorption data in soil columns showing the cumulative mass desorbed

Comparison of mathematical models. The two-site model with an R based on isotherm  $K_d$  poorly described the observed time-concentration data (Figure 3-6) as is evident from the relatively low values of correlation coefficient (i.e., R<sup>2</sup> between 0.95-0.97). However, the inability of the two-site model to describe naphthalene desorption is not due to the use of isotherm  $K_d$  to calculate R, because the isotherm  $K_d$  and column desorption  $K_d$  for the three soils do not differ significantly. The two-site model does not account for the residual contaminant mass due to non-desorption and results in a greaterthan-actual mass elution. This is evident for all soils in cumulative mass desorption plots (Figure 3-7) and is more pronounced for SPCF, which desorbs faster compared to the other two soils. Both applications of two-site model (i.e., with isotherm and column desorption  $K_d$ ) result in almost identical desorption curves. This supports the hypothesis that absence of a third domain rather than the difference in batch and column  $K_d$  is the reason for the relatively inferior description of the desorption data with the two-site model. But we caution here that our column  $K_d$  values should not be compared with the column  $K_d$  in miscible displacement experiments, in which case, the sorption equilibrium is achieved by injecting the solute of interest until the influent and the effluent concentrations are equal. In our case, we equilibrated soil with naphthalene in batch for column desorption as well, therefore, drawing a similarity between the column  $K_d$  in our experiments and that in the conventional miscible displacement experiments is not appropriate. The naphthalene desorption in columns could be best described by the proposed three-site model ( $R^2 = 0.995$  for all soils).

The degree of nonequilibrium in a solid matrix exhibiting rate-limited mass transfer depends on the size of rate-limited domain as well as the mass transfer rate between the liquid phase and rate-limited domain. Only a slight variation exists in the fraction of equilibrium, rate-limited and non-desorption sites, estimated using the three-site model, for Kalkaska-A and SPCF while for Plume-A sand the variation is significant. Another notable difference is a three-times lower desorption rate coefficient ( $\alpha$ ) for Kalkaska-A compared with SPCF (i.e., 0.0588 hr<sup>-1</sup> compared with 0.1806 hr<sup>-1</sup>). A lower  $\alpha$  is consistent with the higher SOM content in Kalkaska-A as compared to SPCF. Plume-A sand exhibited the maximum desorption resistance (i.e.,  $f_{nd} = 0.62$ ) which, we attribute to a different sorption mechanism in the absence of SOM. The fraction of rate-limited domain was much smaller (i.e.,  $f_{neq} = 0.24$ ) compared to what was observed in organic soils.

Comparison of batch and column parameters. A comparison between the batch and column parameters was also done to assess the suitability of use of batch parameters in transport models. For a given soil, the batch and column-derived parameters are expected to be similar, if identical conditions for equilibration exist in sorption phase and the desorption parameters are estimated using mathematical models based on similar conceptualization of the porous medium. The results from our experiments were, however, to the contrary. For all three soils, the fraction of equilibrium sites was higher in batch and fraction of rate-limited sites was consistently lower in columns. This can probably be explained based on the limited ability of the contaminant molecules to access bulk liquid in columns as compared to batch. In a well-mixed batch environment, the onset of desorption results in instantaneous desorption from all of the equilibrium sites as

the desorption process is not physically hindered. On the other hand, the packing in soil columns results in longer-than-normal diffusion path lengths, which a contaminant molecule needs to traverse in order to diffuse to the bulk solution (Figure 3-8). An evidence of sorption to equilibrium or rate-limited sites is provided by the naphthalene mass extracted in water-extraction step in column desorption experiments. Another possible explanation for the differences in the equilibrium and rate-limited site fractions is that high  $f_{eq}$  values in batch could be due to an abrupt change of concentration gradient when the vials are decanted at the end of sorption process and desorption is started by adding a known volume of contaminant free liquid which is approximately 3-20 times greater than the volume of soil in the vial. In the column experiments it is not practical to achieve this difference due to the packed nature of the soil matrix. Desorption in columns is started by resuming the flow with a contaminant-free liquid and the exposure of soil matrix to the liquid is not instantaneous, as is the case in batch systems.

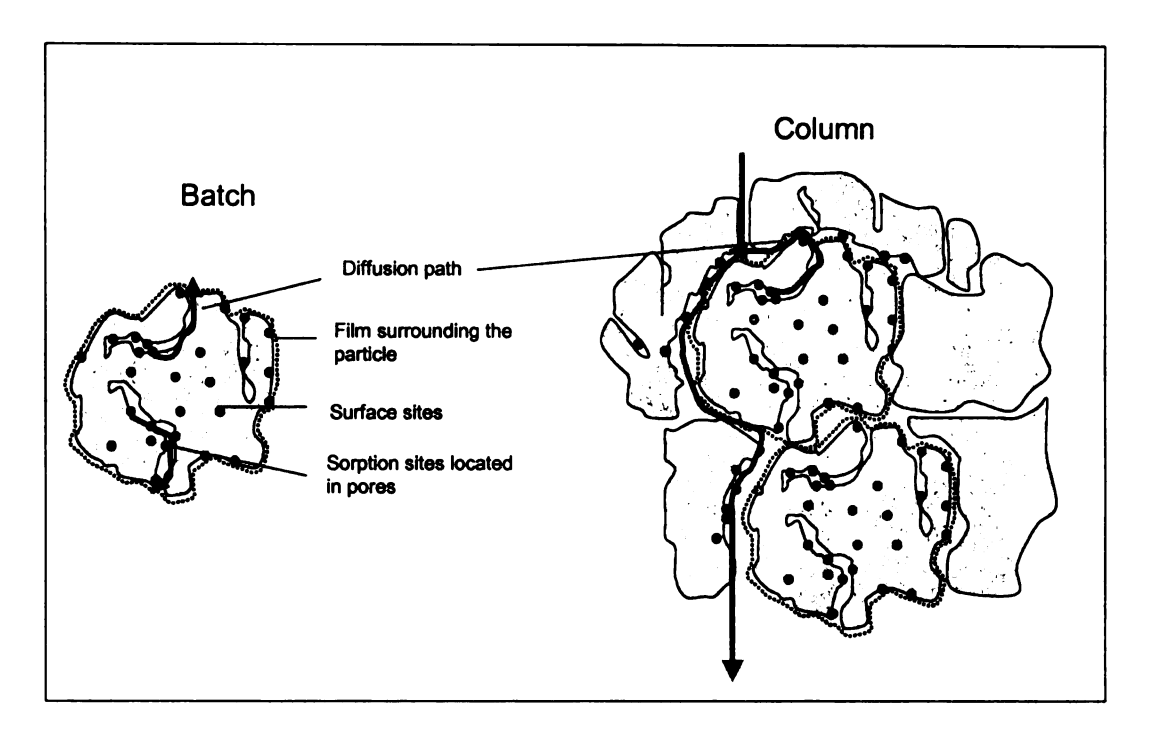


Figure 3-8: Schematic showing an increase in diffusion path lengths as a result of packing in soil columns

The fraction of non-desorption sites was higher in batch for the two surface soils i.e., Kalkaska-A and SPCF while it was almost similar for plume-A sand (Figure 3-9). It is difficult to explain the differences in the non-desorption site fractions for the two soils and the similar  $f_{nd}$  values for one soil. A similar explanation can be offered for the higher desorption rate coefficients in batch than in column for the two surface soils as was the case for equilibrium sites and rate-limited sites, but again, it is difficult to justify the opposite trend in Plume-A sand, in which case, the desorption rate coefficient values were higher in column compared to batch. In general, due to differences in the environments between the two systems, it is viewed that it is not appropriate to use the batch parameters in transport models even if these have been estimated using the same mathematical formulations based on similar conceptualizations.

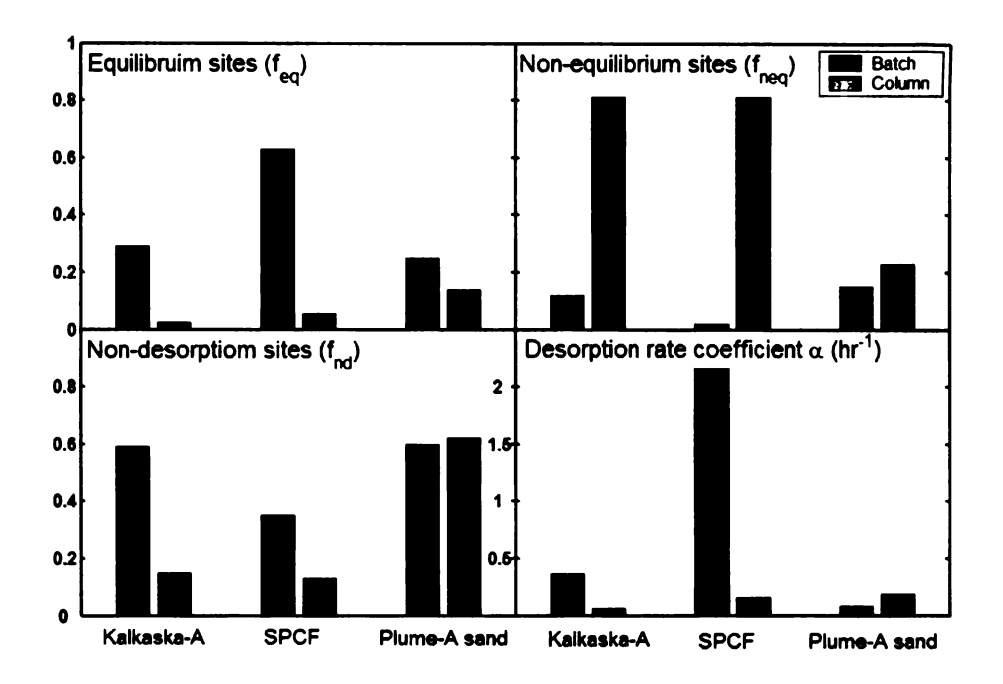


Figure 3-9: Comparison of batch and column parameters obtained by nonlinear regression using the three-site model

## 3.5 Conclusions

Based on our results we conclude that the traditional approach of viewing the solid matrix consisting of an equilibrium domain and a rate-limited domain is questionable and that incorporating a non-desorption domain in transport models enhances the predictive ability of the models. We also conclude that inadequate representation of the observational regimes rather than the difference in  $K_d$  is the reason for the inferior description of desorption by the two-site model. This is supported by minor differences in batch and column  $K_d$  values. We also conclude that batch parameters other than  $K_d$  are not comparable with their column counterparts even if these have been estimated by application of mathematical models based on the same conceptualization. We found that

in soil columns, a higher degree of rate limitations is expected due to a greater fraction of the soil matrix behaving in rate-limited mode.

### 3.6 References

- Ahn, I.S., Lion, L.W. and Shuler, M.L., 1999. Validation of a hybrid "two-site gamma" model for naphthalene desorption kinetics. Environmental Science & Technology, 33(18): 3241-3248.
- Bouchard, D.C., 1998. Sorption kinetics of PAHs in methanol-water systems. Journal of Contaminant Hydrology, 34(1-2): 107-120.
- Brusseau, M.L. and Rao, P.S.C., 1989. Sorption non-ideality during organic contaminant transport in porous media. Critical Reviews in Environmental Control, 19(1): 33-99.
- Burnham, K.P. and Anderson, D.R., 1998. Model selection and inference. Springer-Verlag, New York City, 353 pp.
- Connaughten, D.F., Stedinger, J.R., Lion, L.W. and Schuler, M.L., 1993. Description of time-varying desorption kinetics: Release of naphthalene from contaminated soils. Environmental Science & Technology, 27(12): 2397-2403.
- Cornelissen, G., Rigterink, H., Ferdinandy, M.M.A. and Van Noort, P.C.M., 1998a.
  Rapidly desorbing fractions of PAHs in contaminated sediments as a predictor of the extent of bioremediation. Environmental Science & Technology, 32(7): 966-970.
- Cornelissen, G., Van Noort, P.C.M. and Govers, H.A.J., 1998b. Mechanism of slow desorption of organic compounds from sediments: A study using model sorbents. Environmental Science & Technology, 32(20): 3124-3131.
- Croucher, A.E. and O'Sullivan, M.J., 1998. Numerical methods for contaminant transport in rivers and estuaries. Computers & Fluids, 27(8): 861-878.
- Demuren, A.O., Wilson, R.V. and Carpenter, M., 2001. Higher-order compact schemes for numerical simulation of incompressible flows, part 1: Theoretical development. Numerical Heat Transfer., Part B, Fundamentals, 39: 207-230.
- Dybas, M.J. et al., 2002. Development, operation, and long-term performance of a full-scale biocurtain utilizing bioaugmentation. Environmental Science & Technology, 36(16): 3635-3644.
- Fischer, B.H., List, E.J., Koh, R.C.Y., Imberger, J. and Brooks, N.H., 1979. Mixing in inland and coastal waters. Academic Press Inc., New York.
- Johnson, M., Keinath, T. and Weber, W.J., 2001. A distributed reactivity model for sorption by soils and sediments. 14. Characterization and modeling of phenanthrene desorption rates. Environmental Science & Technology, 35(8): 2734-2740.

- Kan, A.T., Fu, G., Hunter, M.A. and Tomson, M.B., 1997. Irreversible adsorption of naphthalene and tetrachlorobiphenyl to Lula and surrogate sediments. Environmental Science & Technology, 31(8): 2176-2185.
- Lele, S.K., 1992. Compact finite difference schemes with spectral-like resolution. Journal of Computational Physics, 103: 16-42.
- Maraqa, M.A., Zhao, X., Wallace, R.B. and Voice, T.C., 1998. Retardation coefficients of nonionic organic compounds determined by batch and column techniques. Soil Science Society of America Journal, 62(1): 142-152.
- Nkedikizza, P. et al., 1983. Modeling tritium and chloride-36 transport through an aggregated oxisol. Water Resources Research, 19(3): 691-700.
- Park, J.H., 2000. Bioavailability of sorbed organic contaminants. Ph.D. Thesis, Michigan State University, East Lansing, 155 pp.
- Park, J.H., Feng, Y.C., Ji, P.S., Voice, T.C. and Boyd, S.A., 2003. Assessment of bioavailability of soil-sorbed atrazine. Applied and Environmental Microbiology, 69(6): 3288-3298.
- Park, J.H., Zhao, X.D. and Voice, T.C., 2001. Biodegradation of non-desorbable naphthalene in soils. Environmental Science & Technology, 35(13): 2734-2740.
- Phanikumar, M.S. and Hyndman, D.W., 2003. Interactions between sorption and biodegradation: Exploring bioavailability and pulsed nutrient injection efficiency. Water Resources Research, 39(5): art. no.-1122.
- Prata, F., Lavorenti, A., Jan, V., Burauel, P. and Vereecken, H., 2003. Miscible displacement, sorption and desorption of atrazine in a Brazilian oxisol. Vadose Zone Journal, 2: 728-738.
- Roache, P.J., 1998. Fundamentals of computational fluid dynamics. Hermosa Publishers, New Mexico.
- Saffron, C., 2005. Plant-enhanced remediation of naphthalene. Ph.D. Thesis, Michigan State University, East Lansing.
- Selim, H.M., Davidson, J.M. and Rao, P.S.C., 1977. Transport of reactive solutes through multilayered soils. Soil Science Society of America Journal, 41(1): 3-10.
- Seyfried, M.S. and Rao, P.S.C., 1987. Solute transport in undisturbed columns of an aggregated tropical soil Preferential flow effects. Soil Science Society of America Journal, 51(6): 1434-1444.
- Sharer, M., Park, J.H., Voice, T.C. and Boyd, S.A., 2003a. Aging effects on the sorption-desorption characteristics of anthropogenic organic compounds in soil. Journal of Environmental Quality, 32(4): 1385-1392.

- Sharer, M., Park, J.H., Voice, T.C. and Boyd, S.A., 2003b. Time dependence of chlorobenzene sorption/desorption by soils. Soil Science Society of America Journal, 67(6): 1740-1745.
- Toride, N., Leij, F.J. and Van Genuchten, M.T., 1999. The CXTFIT code for estimating transport parameters from laboratory or field tracer experiments. 137, U.S Salinity Laboratory, Riverside, California.
- Van Genuchten, M.T. and Wagenet, R.J., 1989. Two-site/two-region models for pesticide transport and degradation: Theoretical development and analytical solutions. Soil Science Society of America Journal, 53(5): 1303-1310.
- Van Genuchten, M.T. and Wierenga, P.J., 1977. Mass transfer studies in sorbing porous media .2. Experimental evaluation with tritium (<sup>3</sup>H<sub>2</sub>O). Soil Science Society of America Journal, 41(2): 272-278.
- Zhao, X.D. and Voice, T.C., 2000. Assessment of bioavailability using a multicolumn system. Environmental Science & Technology, 34(8): 1506-1512.

### **CHAPTER 4**

## EFFECTS OF AGING ON DESORPTION KINETICS IN SOIL COLUMNS

#### Abstract

A study was conducted to explore the effects of aging on desorption kinetics in saturated soil columns. Sorption isotherms, batch series-dilution desorption and column desorption experiments were conducted with naphthalene on three sandy soils with different organic content involving different equilibration periods. Each soil was characterized for dispersion and retardation using tritiated water. Increased soil-naphthalene contact time resulted in an increase in the total naphthalene distribution to sorbed phase in all soils. A significant increase in the non-desorbable (solvent-extractable) naphthalene due to an increase in the equilibration period was evident in batch as well as column desorption. This increase in non-desorbable naphthalene was accompanied by a corresponding decrease in the desorbable naphthalene.

Nonlinear regression of the column desorption data with the conventional two-site model and the three-site model indicate that data are difficult to reconcile using the two-site model. The three-site model, which incorporates non-desorption sites, described naphthalene desorption better than the two-site model in all nine cases (i.e., three soils at three aging periods). We conclude from parameters of the three-site model, that aging results in a shift of contaminant from nonequilibrium domain to non-desorption domain, while the effect of aging on the size of equilibrium domain and desorption rate coefficients is minimal.

## 4.1 Introduction

Soil-contaminant contact time, commonly referred to as aging, is an important variable influencing different aspects of the sorption and the desorption process. These aspects include the extent of sorption, isotherm linearity, the distribution of the contaminant in equilibrium, nonequilibrium and non-desorption compartments, the rate of release from the solid matrix and the reversibility of the sorption process. The effect of aging on the extent of sorption is well known, as the equilibrium sorption distribution coefficient  $(K_d)$  has been shown to increase with an increase in the contact time. For example, (Xing and Pignatello, 1996) evaluated the sorption isotherms for dichlorobenzene and dichlorophenol over periods of 1 and 30 days and found that the sorption coefficient,  $K_F$ , increased 1.3 times for dichlorobenzene and 2.7 times for dichlorophenol. Similar observations exist for other organic compounds in studies involving the aging effects on sorption/desorption kinetics e.g., (Sharer et al., 2003a; Sharer et al., 2003b). The increase in  $K_d$ , however, has been reported to be compoundspecific and not necessarily related to aging. For example, (Sharer et al., 2003a) reported a significant increase for 2,4 D over a 14 month period, a decrease in  $K_d$  for attrazine over a 30 day period, and no change for chlorobenzene. The effect of aging on the isotherm linearity produced mixed results with some supporting an increase in non-linearity e.g., (Weber and Huang, 1996; Xing and Pignatello, 1996) with aging while others found no significant effect e.g., (Sharer et al., 2003a; Sharer et al., 2003b).

Three aspects are important with reference to desorption viz., (1) how quickly a fraction of contaminant becomes desorption-resistant (2) how the size of the desorption-

resistant fraction of the matrix changes over time and (3) how the rate of desorption from rate-limited compartment changes over time. Formation of a desorption-resistant fraction has been observed over equilibration times of 24 hours (Kan et al., 1997; Park et al., 2003; Park et al., 2001). An increase in the desorption-resistant fraction with an increase in soil-contaminant contact time has also been reported e.g., (Johnson et al., 2001; Pignatello, 1990b; Sharer et al., 2003a; Sharer et al., 2003b). (Pignatello, 1990a) studied the slowly reversible or the non-labile fraction of non-polar halogenated hydrocarbons on soils and observed that non-labile fraction increased nonlinearly with the incubation time and applied concentration. (Sharer et al., 2003b) studied the effects of aging on desorption kinetics in lab-controlled environment on chlorobenzene (CB) using four soils ranging in OC from 0.69% to 13.4%. The authors found that 17-27% of non-desorbable fraction was observable after only 24 hours and increased to 28-45% after 14 months of aging. Observations for a slower desorption in aged soils compared to freshly contaminated soils also exist. Aging is also believed to affect the desorption rates for the non-equilibrium compartment. For example, (McCall and Agin, 1985) observed a decrease in the desorption rate coefficient with aging. Similar findings exist in the work of (Carmichael et al., 1997) who found an order of a magnitude difference between the desorption rates of fresh and field weathered PAHs. Sharer et al. (2003a) found that aging appeared to affect the desorption rates of chlorobenzene, ethylene dibromide and atrazine but did not affect 2,4 D.

Most of the studies referred aimed at exploring the effects of aging on desorption kinetics of short and long-term aged soils in batch systems. Despite the significant implications of aging on desorption, there are very few long-term laboratory studies, that

have focused on analyzing the influence of aging on desorption parameters in soil columns. In this study, we conducted column desorption experiments with short and long-term aged soils. Our approach was to ensure identical conditions for sorption in batch except the equilibration time so that we could explicitly measure the kinetic desorption parameters for differentially-aged soils. By employing sorbents with different organic content, we also aimed at evaluating the role of SOM in the desorption process.

## 4.2 Materials and methods

Solute and sorbents. Unlabeled and <sup>14</sup>C-naphthalene with uniformly labeled carbons procured from Sigma Aldrich Co. was utilized as a representative HOC for the batch and column desorption experiments. Three sandy soils i.e., Kalkaska-A, SPCF and an aquifer sand from the Plume-A site, Schoolcraft, MI (hereafter referred to as Plume-A sand) containing different organic matter content were used for the study. The methods of pretreatment for these sorbents, their mechanical characteristics and the respective organic matter content have been reported in Chapter 3.

Sorption isotherms. Three-day, 2-month and 5-month sorption isotherms were conducted on three soils. The protocol for the three-day isotherms has been discussed in detail in Chapter 3. The same protocol was adhered to for 2-month and 5-month isotherms. Soil mass and liquid-phase volume used for the batch isotherms for each soil are presented in Table 4-2.

Series-dilution desorption in batch. The series-dilution desorption experiments were performed on all three soils at differential equilibration periods ranging from 10 minutes to 12 days to monitor a change in the non-desorbable concentration. Triplicate soil slurries were prepared in 5 mL vials with mininert valves equipped with Teflon liners. An aliquot of sterile soil was mixed with  $CaCl_2$  (0.01M) prepared in deionized water. The details of soil mass and liquid-phase volume for each soil are presented in Table 4-2. The resulting soil-to-water ratios were 0.075. 0.214 and 0.712 for Kalkaska-A, SPCF and Plume-A sand respectively. The soil slurries so prepared were spiked with 4  $\mu$ L of naphthalene spiking solution resulting in an initial liquid-phase concentration of 3815 ± 63.9  $\mu$ g/L for Kalkaska-A, 4183.68 ± 99.8  $\mu$ g/L for SPCF and 4986.05 ± 208.35  $\mu$ g/L for

Plume-A sand respectively. After spiking, the vials were tumbled end-over-end in dark for different equilibration periods between 10 minutes and 12 days. At the end of respective equilibration periods, the vials were centrifuged at 1163 x g for 5 minutes and the supernatant was analyzed by liquid scintillation counting (LSC). The sorbed-phase concentration was calculated by difference. On completion of the sorption step, the remaining liquid-phase was decanted to the extent possible. Vials were refilled with naphthalene-free CaCl<sub>2</sub>, tumbled at 6 rpm for 18-24 hours and the liquid-phase was analyzed again for naphthalene after centrifugation. Approximately, 4-6 successive dilutions were done in each case except for the sorption time of 10 minutes; in which case, the low radioactivity after two consecutive dilutions did not warrant further dilutions.

Table 4-1: Details of the soil mass and the liquid-phase volumes used for the isotherms and series-dilution desorption experiments

	Batch i	sotherms	Series-dilution desorption		
Soil	Soil mass (g)	Liquid volume (mL)	Soil mass (g)	Liquid volume (mL)	
Kalkaska-A	$0.348 \pm 0.028$	$4.589 \pm 0.034$	$0.342 \pm 0.0216$	$4.512 \pm 0.074$	
SPCF	$0.844 \pm 0.095$	$4.179 \pm 0.022$	$0.889 \pm 0.027$	$4.1514 \pm 0.099$	
Plume-A sand	$2.64 \pm 0.0283$	$2.464 \pm 0.028$	$2.487 \pm 0.032$	$3.490 \pm 0.146$	

Column desorption. A detailed description of the method used for column desorption experiments involving an equilibration period of three-days has been presented in Chapter 3. The same procedure was adopted for column desorption studies for the

equilibration period of 2 months and 5 months. The dispersive properties of the three soils were also determined using tritiated water as discussed in Chapter 3.

Independent tests to verify the extraction efficiency of methanol after 3 days and 5 months were also carried out on separate batch samples by spiking the soil with an initial liquid-phase concentration between 1-5 mg/L. Methanol was found to be  $100 \pm 5\%$  efficient in recovering sorbed naphthalene for the three soils after 3 days of equilibration. However, after 5 months of equilibration period, methanol could recover  $80.9 \pm 2.71\%$  of naphthalene for Kalkaska-A,  $76.1 \pm 4.34\%$  for SPCF and  $77.0 \pm 2.46\%$  for Plume-A sand respectively.

# 4.3 Analysis

In this study, the desorption of naphthalene from soil columns for the three different aging periods (i.e., three days, two months and five months) was analyzed using the two-site and the three-site models. The three-site model assumes that (1) the solid matrix can be divided into equilibrium, nonequilibrium and non-desorption sites (2) the equilibrium sites achieve an instantaneous equilibrium with the aqueous phase that can be described by a linear distribution coefficient (3) the release from the non-equilibrium sites is described by the concentration gradient between the two phases and (4) the release from the non-desorption sites (designated as irreversible sorption) is insignificant during the experimental time scales. The dimensional and dimensionless equations for these models, the solution technique and the parameter estimation technique have been described in detail in chapter 3. The two-site model was used with two different parameters i.e., (1)

with isotherm  $K_d$  and (2) with column desorption  $K_d$ . The three-site model was used with column desorption  $K_d$  only.

## 4.4 Results and discussion

Aging isotherms. The slope of the sorption isotherms was calculated by using linear regression from the plots of the amount of naphthalene sorbed (µg/Kg) versus the concentration in aqueous phase (µg/L). This corresponds to the sorption distribution coefficient  $K_d$ . Sorption of naphthalene was linear for all three soils for all aging periods.  $K_d$  calculated using linear regression was 9.22 mL/g for Kalkaska-A, 5.82 mL/g for SPCF and 1.46 mL/g for Plume-A sand respectively based on a three-day isotherm (Figure 4-1). There appears to be a considerable effect of aging on sorption capacity of naphthalene for all the three soils. A comparison of  $K_d$  values for the three aging periods provides evidence that an apparent equilibrium appears to have been reached quickly on all three soils, however, the "true" equilibrium takes a much longer time and the tested period of aging (5 months) may not be sufficient to reach the true equilibrium state, for surface soils containing SOM. The  $K_d$  values at different aging periods for naphthalene indicate a rapid initial sorption phase followed by a slow and continuous uptake. One notable difference is for the Plume-A sand, for which  $K_d$  increased by almost 100% from 3 days to 2 months but showed no increase thereafter. This contradicts the findings of (Loehr and Webster, 1996) but is consistent with the findings of (Xing and Pignatello, 1996) who observed that largest relative increase in sorption coefficient  $(K_p)$  for dichlorophenol occurred for a mineral soil (OC 1.74%) rather than the soil with OC as high as 54.1%. In several other studies also, an increase in the extent of sorption as a

consequence of aging has been found e.g., (Sharer et al., 2003a; Sharer et al., 2003b;

Xing and Pignatello, 1996)

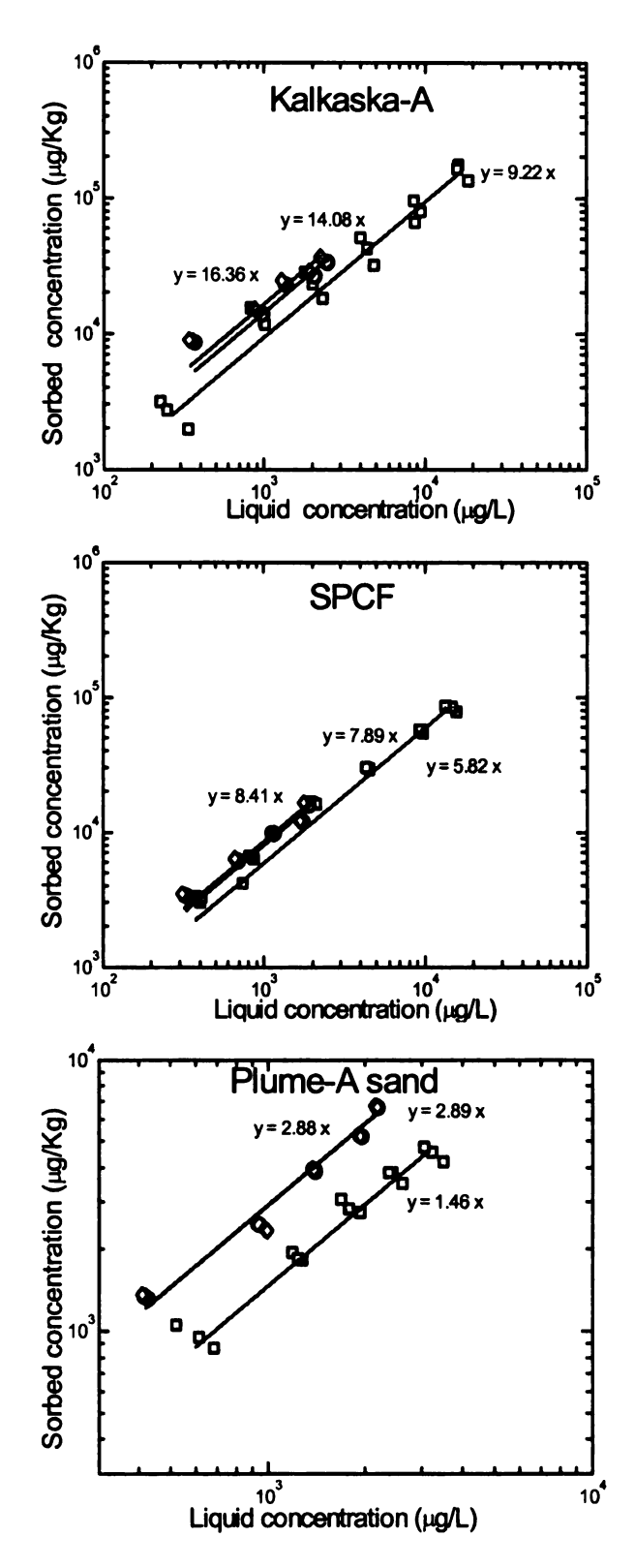


Figure 4-1: Sorption isotherms for the three soils. Squares, circles and diamonds represent 3-day, 2-month and 5-month equilibration period respectively

Series-dilution desorption. In series-dilution desorption experiments, an increase in the sorbed naphthalene with an increase in the sorption period is evident for all soils (Figure 4-2 to Figure 4-4). The slope of sorption line increased from 4.41 to 10.64 for Kalkaska-A corresponding to an increase in the sorption equilibration period from 10 minutes to 12 days. A similar trend is evident for SPCF and Plume-A sand, in which case, the increase in slope is 4.30 to 9.07 and 0.28 to 2.0 respectively. The  $K_d$  values based on the three-day sorption isotherms for the three soils also lie within this range. Desorption isotherms donot coincide with sorption data in all cases providing an evidence of hysteresis. The non-desorbable naphthalene concentration was calculated by the intercept of the desorption isotherms and was found to be 1196  $\mu$ g/Kg for Kalkaska-A, 779.68  $\mu$ g/Kg for SPCF and 447.9  $\mu$ g/Kg for plume-A sand respectively for the least sorption time of 10 minutes.

A change in the slope of the desorption isotherms with an increase in soil-naphthalene contact time is also apparent in all three soils. The sorption and desorption lines appear to converge at lower equilibration periods and start to diverge at longer equilibration periods. This divergence is a result of an increase in the intercept, which identifies the non-desorbable naphthalene concentration  $(S_{nd})$ . A consistent increase in the non-desorbable concentration can be observed for all three soils (Figure 4-5). This is consistent with previous studies e.g., (Carmichael et al., 1997; Connaughten et al., 1993; Farrell and Reinhard, 1994; Grathwohl and Reinhard, 1993; Harmon and Roberts, 1994; Pignatello, 1990a; Pignatello, 1990b; Pignatello et al., 1993; Wu and Gschwend, 1986). Although, the extent of desorption as affected by aging in these studies has been different in laboratory-spiked and field-contaminated samples, the phenomena has been noted in

both. Carmichael et al. (1997) in their sequential desorption experiments found that 15-30% of <sup>14</sup>C-phenanthrene and 15-40% of <sup>14</sup>C-Chrysene had become non-labile over a contact period of 85 days.

The rate of increase in the non-desorbable concentration  $(S_{nd})$  appeared to be fast for equilibration periods up to three days and tends to slow down at later periods. Non-desorbable fraction of the soil matrix  $(f_{nd})$ , was calculated for each series-dilution experiment by the relation  $S_{nd}$  /  $S_T$ . A significant fraction of the soil matrix appeared to behave as non-desorption sites i.e., 0.095 for Kalkaska-A, 0.081 for SPCF and 0.38 for plume-A sand. The increase in the non-desorption site fractions revealed a consistent but nonlinear trend over time for all three soils (Figure 4-5). For a differential equilibration time spanning over 12 days, the ranges of  $f_{nd}$  displayed by Kalkaska-A, SPCF and Plume-A sand were 0.095-0.33, 0.081-0.25 and 0.38-0.55 respectively. It is to be noted that the range of  $f_{nd}$  for Plume-A sand with no SOM is the highest among the three soils.

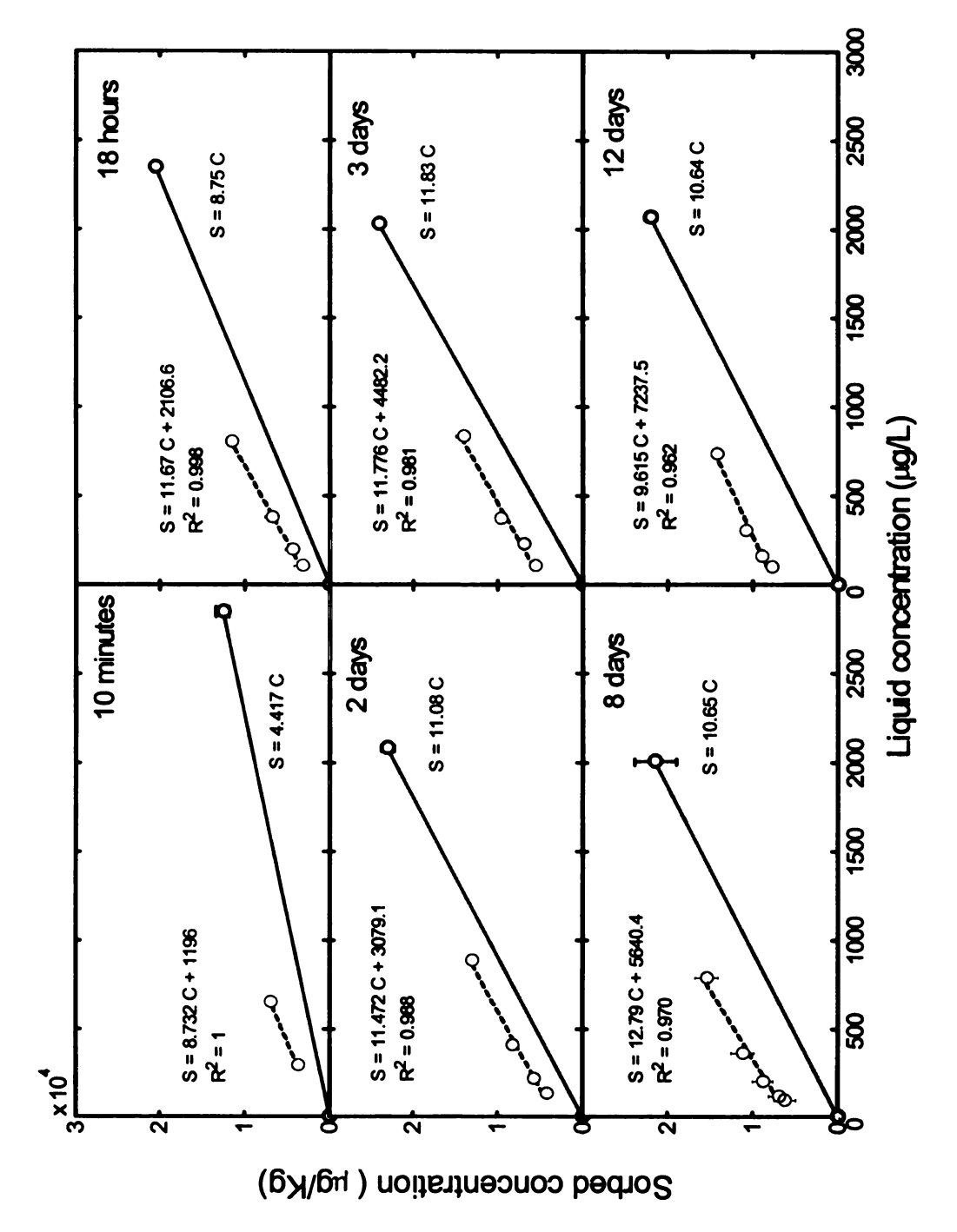


Figure 4-2: Series-dilution desorption in Kalkaska-A for different equilibration periods. The solid lines represent the sorption phase and the dashed lines represent the desorption isotherms

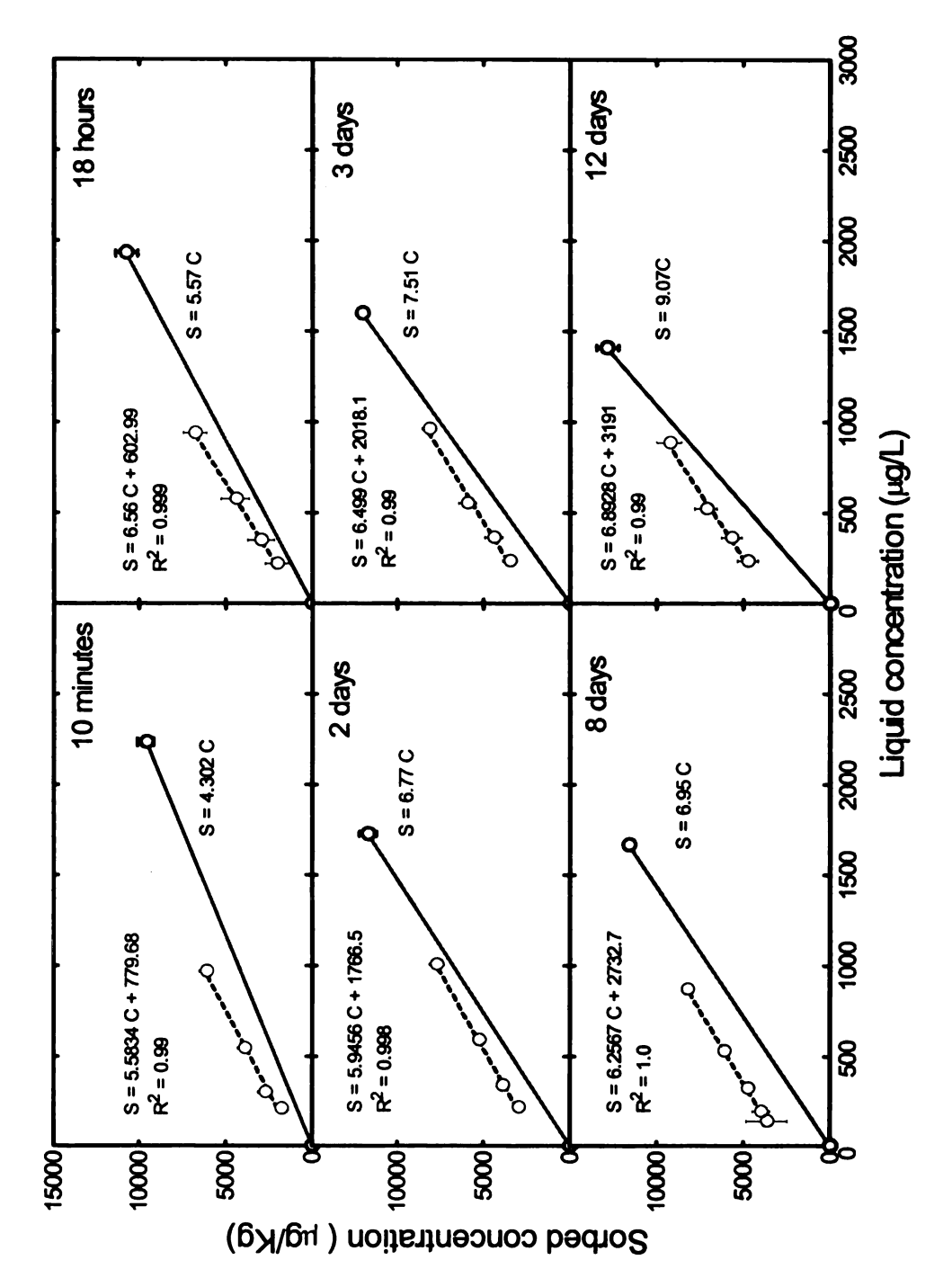


Figure 4-3: Series-dilution desorption in SPCF for different equilibration periods. The solid lines represent the sorption phase while the dashed lines represent the desorption isotherms

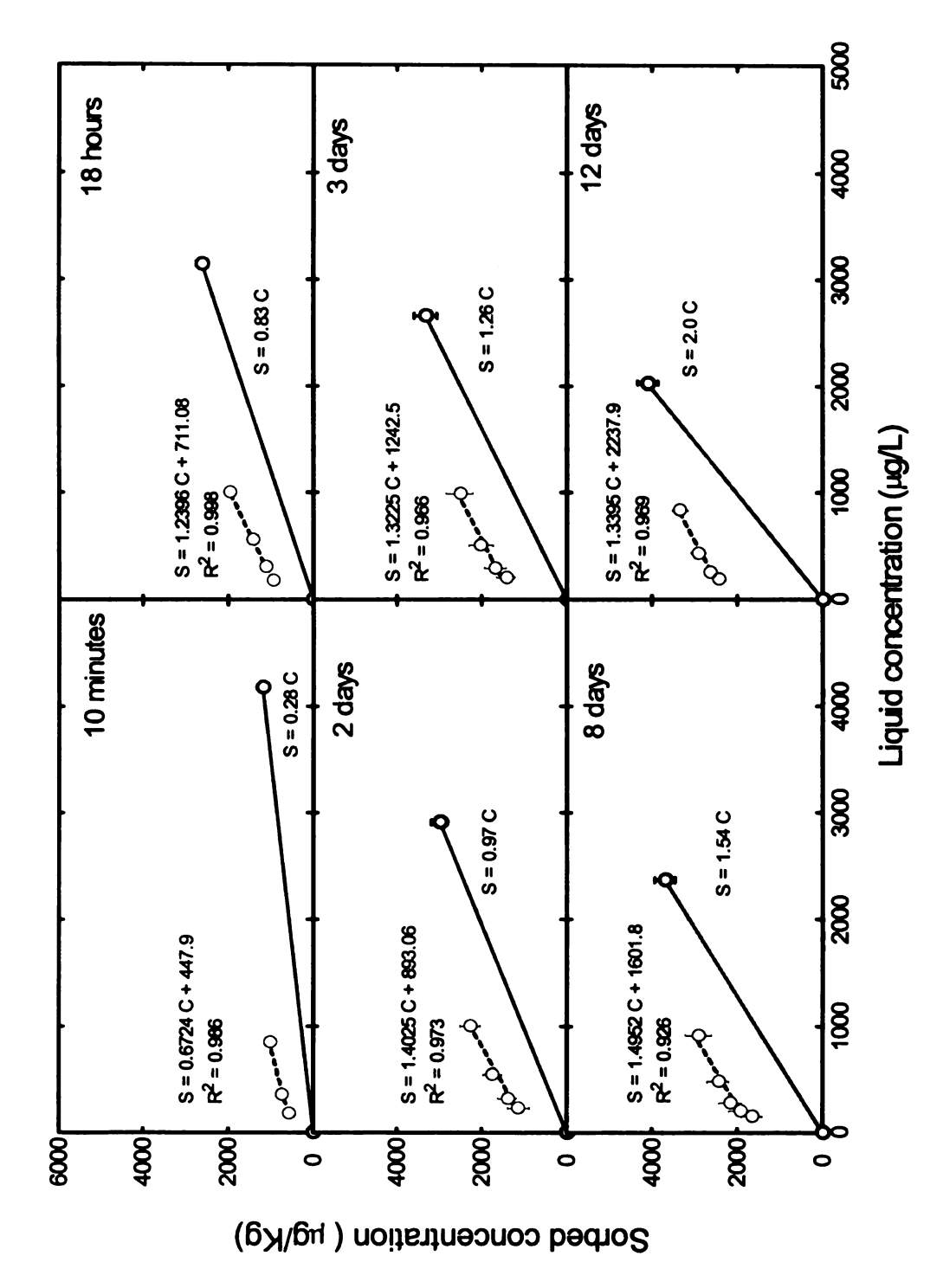


Figure 4-4: Series-dilution desorption in Plume-A sand for different equilibration periods. The solid lines represent the sorption phase while the dashed lines represent the desorption isotherms

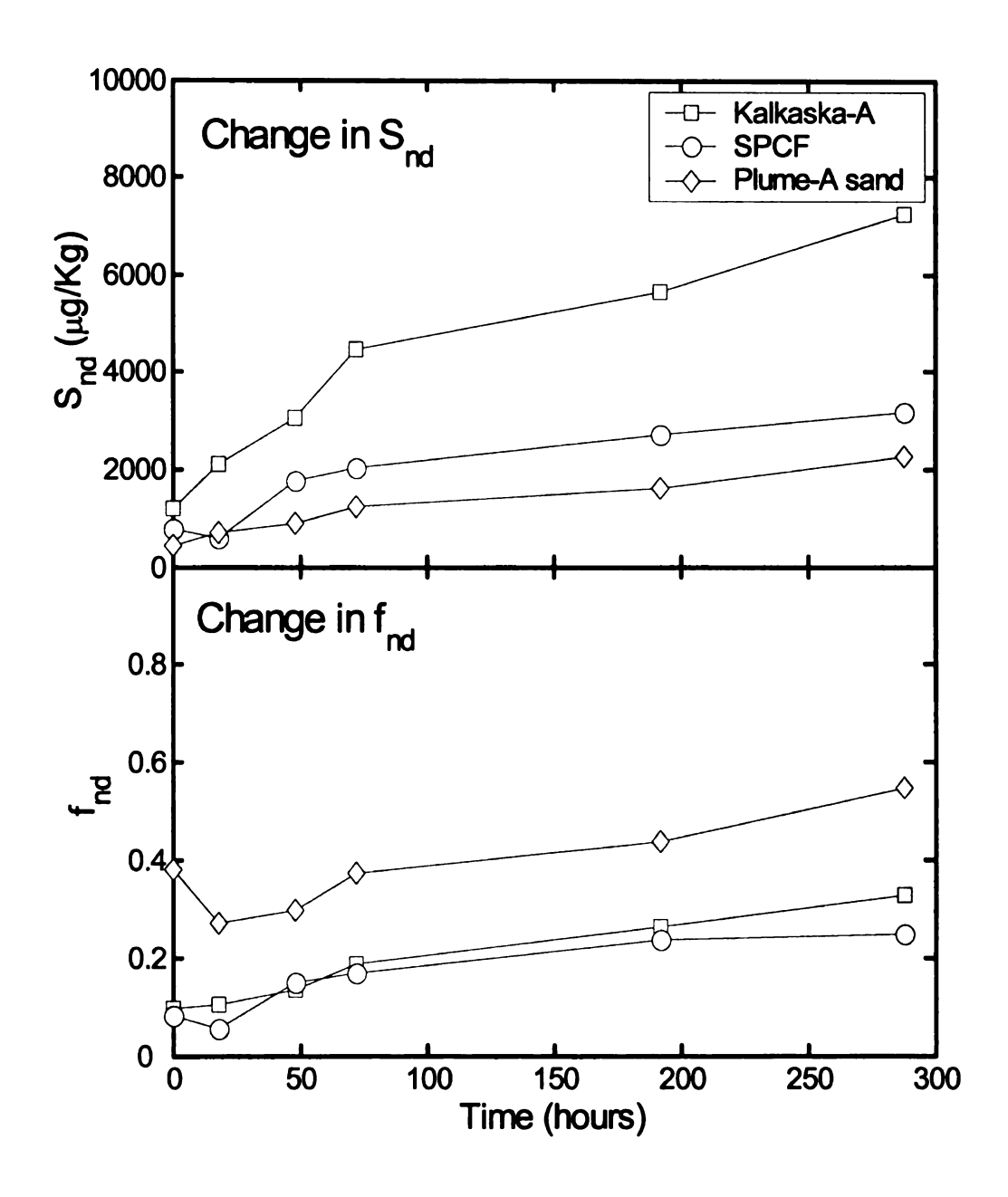


Figure 4-5: Change in the non-desorbable concentration  $(S_{nd})$  and the fraction of non-desorption sites  $(f_{nd})$  with an increase in aging period

Column desorption. A systematic reduction in the liquid-phase concentration and a corresponding increase in the sorbed-phase concentration with an increase in the aging time from three days to five months occurred during the sorption phase for column desorption ( $C_{eq}$  values in Table 4-2). This reduction is consistent with the observation of an increase in the sorptive uptake for each soil in sorption isotherms. It is to be noted that Plume-A sand did not exhibit an increase in the uptake for the period from 2 months to five months as the liquid-phase concentration decreased form 3 days to 2 months but a slight increase is noted thereafter. A similar trend is observed in our aging isotherms for Plume-A sand.

 $C_{init}$  in Table 4-2 represents the initial liquid-phase concentration at the start of column desorption (i.e., the mean of first three samples from column desorption). The process of column packing using pre-equilibrated wet soil spanned over an average time of 20 minutes, exposing the soil slurry to air and causing volatilization of naphthalene. A lower  $C_{init}$  at the start of column desorption than the corresponding  $C_{eq}$  values is due to volatilization that occurred during the process of column packing. The  $C_{init}$  in column desorption was lower than corresponding  $C_{eq}$  values in all cases with the exception of one i.e., Kalkaska-A at three-day equilibration period, where a higher  $C_{init}$  at the start of column desorption than  $C_{eq}$  value was noted. For the three-day equilibration period, bulk of naphthalene is considered to be reversibly sorbed and a loss of naphthalene due to volatilization might induce desorption from sorbed-phase prior to the start of column desorption.

Desorption of naphthalene in Kalkaska-A and SPCF continued for approximately 70 to 80 pore volumes, while for plume-A sand it occurred over approximately 35 to 40 pore volumes for all aging periods. The desorption curves from the soil columns exhibited different shapes for the three soils (Figure 4-7). Column  $K_d$  values were calculated using Equation 3-5 (Chapter 3) for all desorption experiments and compared with the isotherm  $K_d$  values for the corresponding aging times. Our results confirm a previously drawn conclusion based on comparison of the three-day batch and column desorption experiments that the reason for the normally lower  $K_d$  values reported in literature might be due to differences in solute accessibility in batch and column environments. Furthermore, we calculated the desorption  $K_d$  values based on the three different mass fractions. The column  $K_d$  values in Table 4-2 represent those calculated by accounting for the naphthalene mass desorbed from columns, the mass recovered by water extraction at the end of a column desorption and the mass recovered by solvent extractions. In our experiments, the difference between the batch and column  $K_d$  ranged between 2.61% to 24.21% for all nine cases compared. This highlights that, if a common method of equilibration employed for both batch and column studies, the resulting  $K_d$  values for a soil-contaminant combinations are likely to be comparable.

Aging had a significant effect on the reversibility of sorption process as noted by the differences in the desorbable naphthalene (i.e., mass of naphthalene desorbed from the soil columns plus mass extracted by water extractions at the end of column desorption) and non-desorbable naphthalene for all three soils. For Kalkaska-A, the desorbable naphthalene mass decreased from 76.41% to 49.74% with a corresponding

increase in the non-desorbable mass from 23.59% to 50.26% over a period of 5 months, while for SPCF, the desorbable mass decreased from 91.73% to 68.56% with a corresponding increase in the non-desorbable mass from 8.26% to 31.44% (Figure 4-6). For Plume-A sand, a similar increase is noted in the non-desorbable mass form 44.59% to 64.31%.

Table 4-2: Summary of column conditions and the calculated column distribution coefficients at 3 days, 2 months and 5 months aging time

Soil	Liquid-phase concentration at the end of sorption equilibration in batch	Liquid-phase concentration at the start of column desorption	*Column desorption distribution coefficient	Recovery
	$C_{eq}$	Cinit	$K_d$ (column)	
	(μg/L)	(μg/L)	(mL/g)	(%)
Kalkaska-A (3 days)	318.8	354.7	10.14	70.70
Kalkaska-A (2 months)	228.9	190.0	13.46	62.74
Kalkaska-A (5 months)	197.6	182.2	12.49	58.79
SPCF (3 days)	604.6	550.3	5.65	60.71
SPCF (2 months)	513.5	460.2	9.02	84.89
SPCF (5 months)	448.0	448.0	8.63	88.38
Plume-A (3 days)	1548.6	1198.8	1.81	86.64
Plume-A (2 months)	1201.2	1003.3	2.48	76.99
Plume-A (5 months)	1288.7	908.1	2.86	83.24

Calculated using equation (3-5) in Chapter 3

Out of the two surface soils, the desorbable naphthalene mass was consistently lower by 21-28% for Kalkaska-A than for SPCF and the non-desorbable mass was consistently higher by 15-20% for all aging times. The water-extractable mass fraction was also

higher for Kalkaska-A compared with SPCF for all aging periods, although the difference between the two is not as significant as is the case for the desorbable and non-desorbable mass fractions. The effect of variation in SOM and hence the distribution of naphthalene to the organic phase rather than pore diffusion is apparently supported by these consistent differences in the naphthalene mass distribution of the two soils. Another notable difference consistent with the variation in isotherm  $K_d$  values over time is the behavior of Plume-A sand with almost no SOM. Compared with Kalkaska-A and SPCF, the least amount of mass was desorbable for Plume-A sand (28.34% to 41.5%).

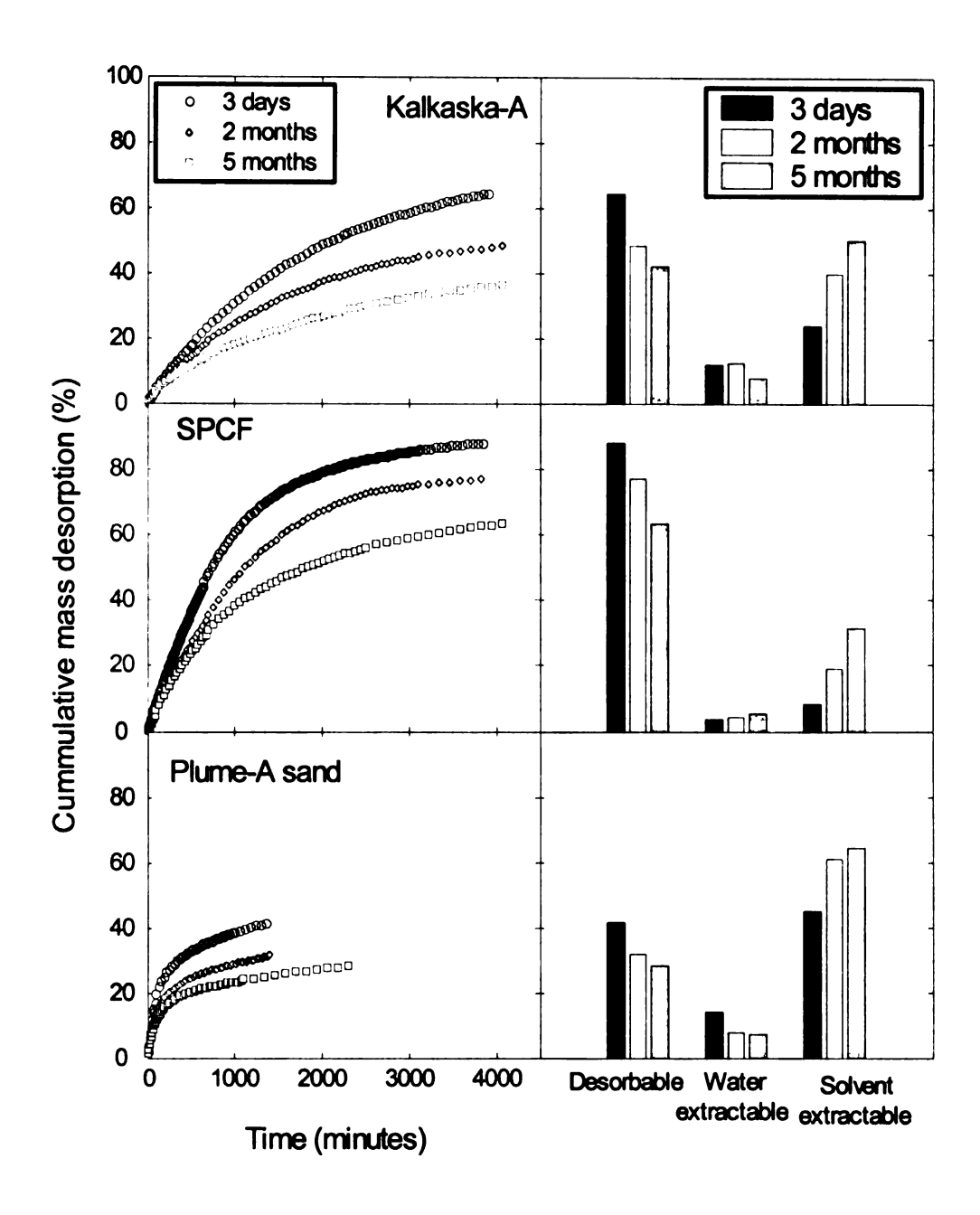


Figure 4-6: Cumulative naphthalene desorption from the soil columns at an aging time of 3 days, 2 months and 5 months. A summary of desorbable, water-extractable and solvent-extractable naphthalene mass from each column desorption experiment is also shown

Model comparisons. In applying the mathematical models to column desorption data. we minimized the number of estimated parameters by supplying independently determined dispersion coefficients obtained through independent tracer tests involving tritiated water and the sorption distribution coefficients for each soil. Our first goal was to isolate a difference, if any existed, between the model outputs obtained by  $K_d$  values determined through batch isotherms and those determined from the column desorption data. The two-site model was not able to describe desorption from soil columns with isotherm  $K_d$  as well as the column  $K_d$  and resulted in a higher-than-actual naphthalene mass elution for all nine cases (Figure 4-7 to Figure 4-9). Owing to minor differences in the isotherm  $K_d$  values and the column  $K_d$  values, the description of desorption data with the two-site model for both cases was not significantly different. With isotherm  $K_{\boldsymbol{d}}$  , the R<sup>2</sup> values ranged between 0.83-0.95 for Kalkaska-A, 0.92-0.97 for SPCF and 0.97-0.98 for Plume-A sand respectively. A reduction in the R<sup>2</sup> values is also observed for all soils with an increase in aging time, although, it is more pronounced in high organic soil (i.e., Kalkaska-A), comparatively less pronounced in SPCF and almost insignificant in Plume-A sand. The deterioration in the two-site model fits for Kalkaska-A at an aging period of 5 months is expected due to a greater deviation between the isotherm and the column  $K_d$  values.

All applications of the three-site model were also based on measured column  $K_d$  values. The three-site model described naphthalene desorption from soil columns better than the two-site model for all nine cases (Figure 4-7 to Figure 4-9). The

 $R^2$  values for all nine cases (i.e., three soils at three aging times) ranged between 0.98-0.99. We conclude based on the comparison of the two-site and three-site model best fits, that an inadequate representation of the observational regimes rather than differences in  $K_d$  values, is the reason for a less accurate description of the naphthalene desorption in soil columns. Therefore, in the subsequent analysis, we base our analysis on the parameters of the three-site model only.

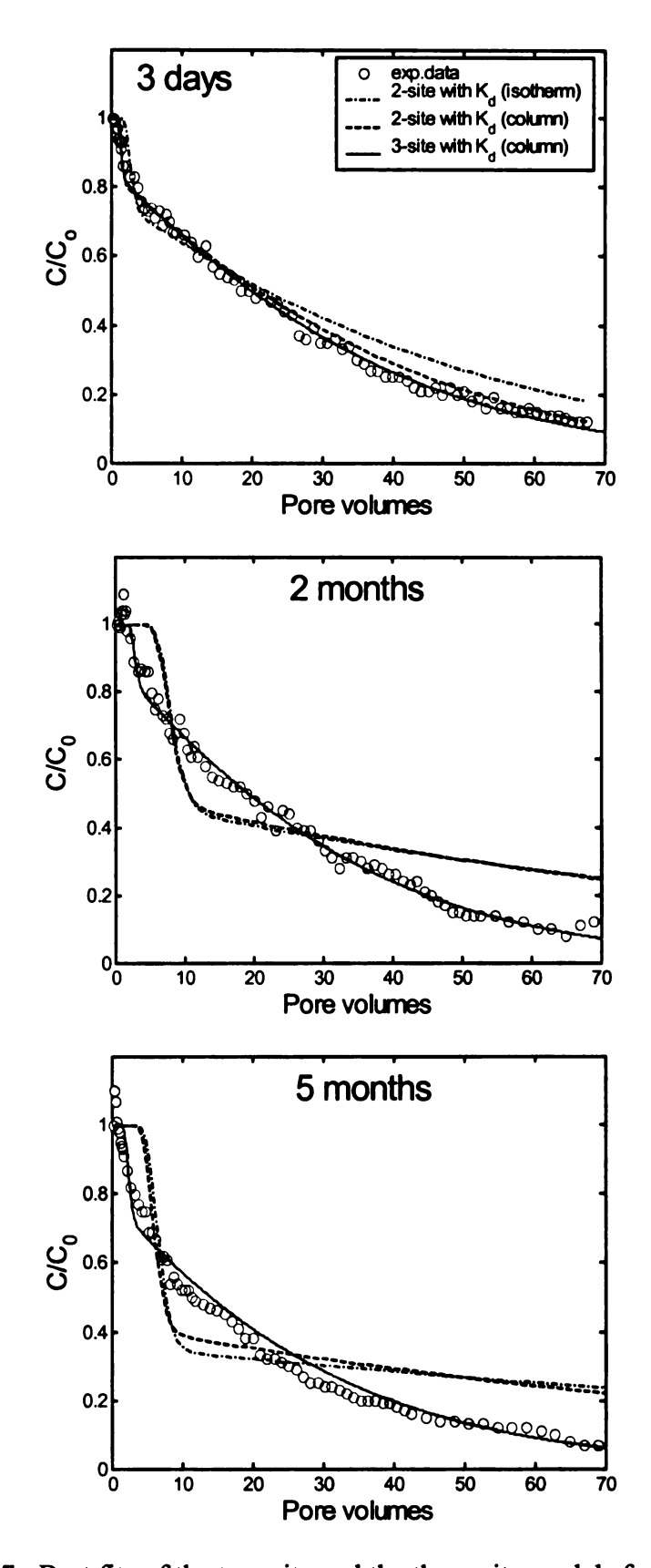


Figure 4-7: Best fits of the two-site and the three-site models for Kalkaska-A

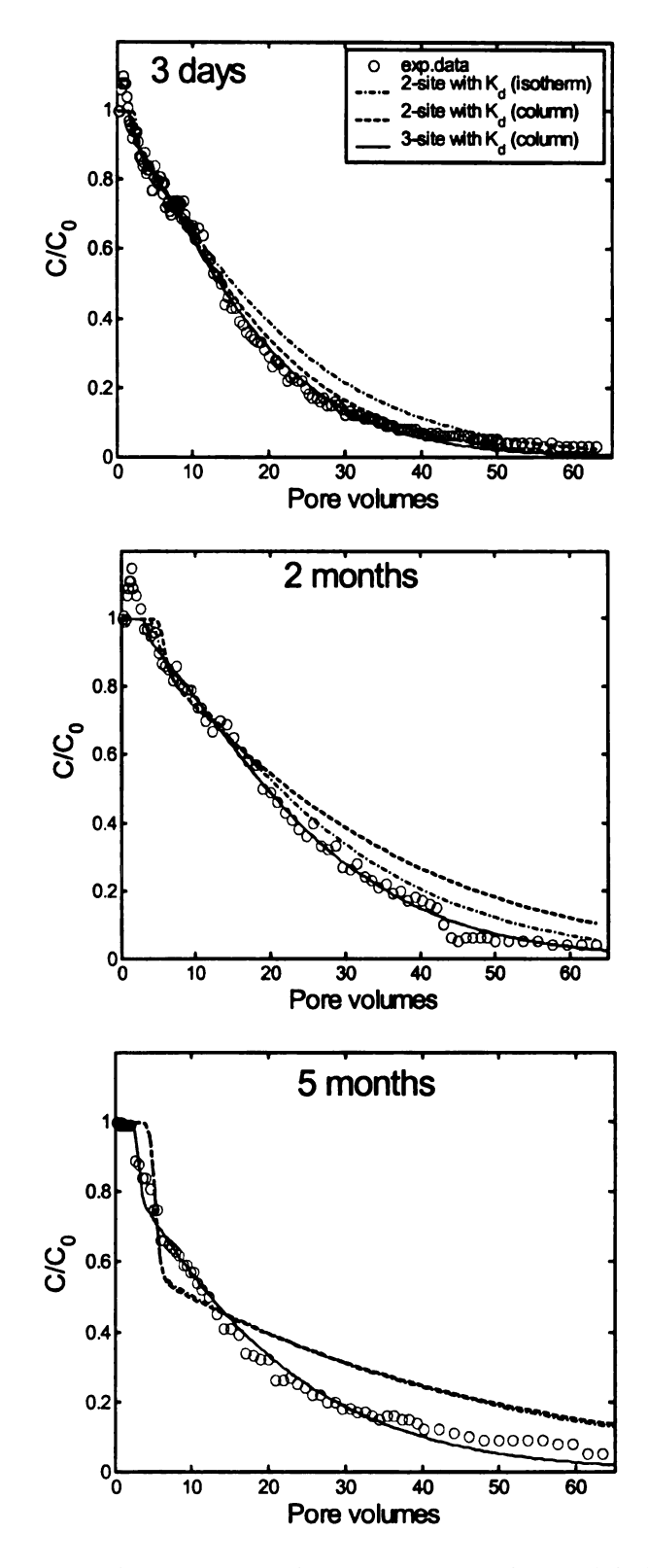


Figure 4-8: Best fits of the two-site and the three-site models for SPCF

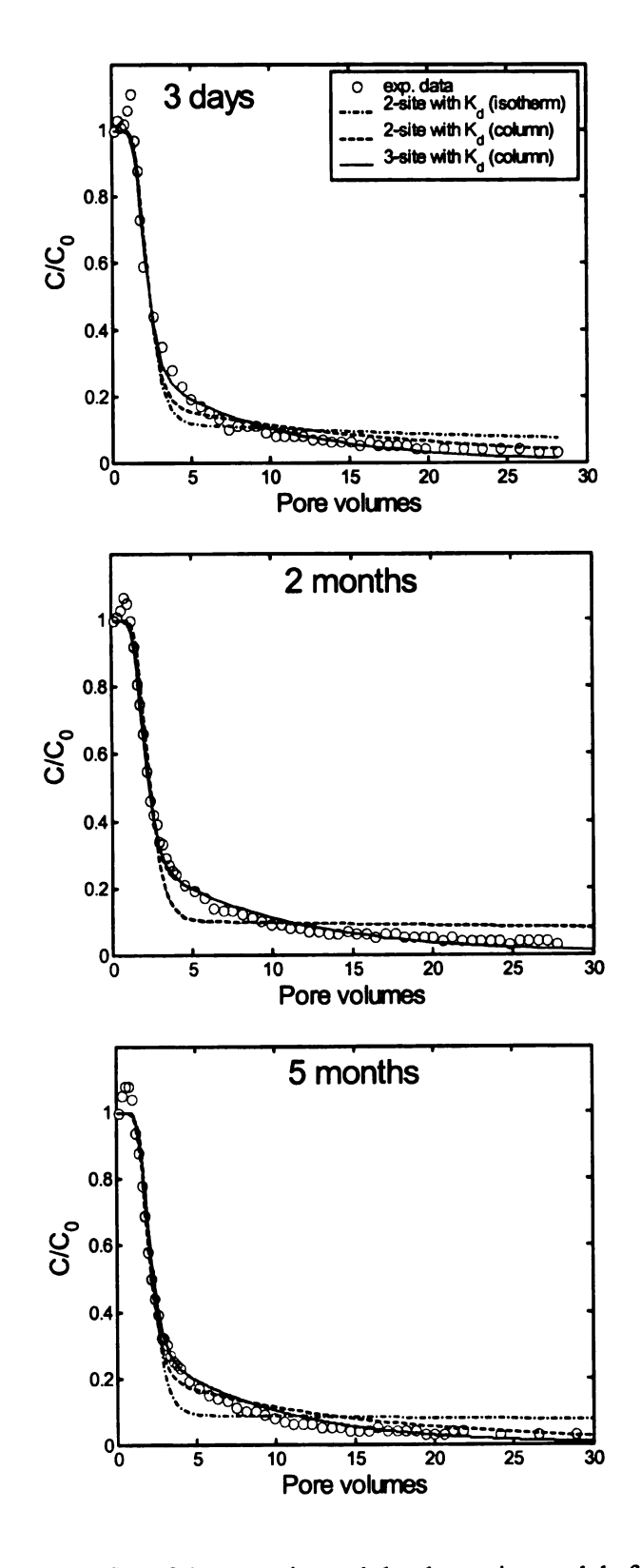


Figure 4-9: Best fits of the two-site and the three-site models for Plume-A sand

The parameter estimation described earlier in chapter 3 was done using the nondimensional equations. The fractions of equilibrium/rate-limited/non-desorption sites and desorption rate coefficients were calculated based on the estimated parameters  $\beta_1$ ,  $\beta_2$  and  $\omega$ . The effect of aging was neither significant nor systematic on the fraction of equilibrium site ( $f_{eq}$ ) in all three soils, which displayed a narrow range i.e., 0.025-0.043 for Kalkaska-A, 0.054-0.094 for SPCF and 0.089-0.14 for Plume-A sand. On the contrary, the decrease in nonequilibrium site fractions ( $\Delta f_{neq}$ ) with a corresponding increase in the non-desorption sites ( $\Delta f_{nd}$ ) was evident in all soils. For example, Kalkaska-A showed  $\Delta f_{neq}$  of 0.345 and 0.03 with a corresponding  $\Delta f_{nd}$  of 0.32 and 0.03, for a period of 2 and 5 months. This is in agreement with some previous batch studies e.g., (Pignatello, 1990b; Sharer et al., 2003a). Similar correspondence was observed in the estimated site fractions for other two soils overtime, however, this change is not consistent for the three soils studied. For example, in Kalkaska-A, the change is more than 90% in the first two months while for SPCF and Plume-A sand, the change in nonequilibrium sites ( $\Delta f_{neq}$ ) and the corresponding change in non-desorption sites  $(\Delta f_{nd})$  is almost equal. These results explain the resistance to desorption exhibited by contaminants in long-term contaminated soils and support the hypothesis that increased soil-contaminant contact time is likely to limit desorption due to an increased probability for contaminant molecules to "diffuse" deeper into intra-aggregate micro-pores.

Table 4-3: Parameters of the two-site and the three-site models for Kalkaska-A in column desorption experiments

Model	Time	B	Я	β	8	$f_{eq}$	feq fneq	$f_{nd}$	$lpha$ (hr $^{-1}$ )	$\mathbb{R}^2$
			0.0839		1.358					
	3 days	36.09	(±0.0199)		±0.131)	90.0	0.94		0.0419	0.950
2-site with $K_d$			0.1575		0.6057					
(isotherm)	2 months	54.59	$(\pm 0.0146)$		$(\pm 0.096)$	0.14	98.0		0.0134	0.868
•	1		0.1094		0.4284					
	5 months	63.27	$(\pm 0.01)$		$(\pm 0.073)$	0.10	06.0		0.0078	0.837
			0.0921		1.188					
	3 days	39.60	$(\pm 0.0158)$		$(\pm 0.137)$	0.07	0.93		0.0337	0.92
2-site with $K_d$			0.1591		0.640					
(column)	2 months	52.22	$(\pm 0.015)$		$(\pm 0.099)$	0.14	0.86		0.0149	0.97
•			0.1294		0.5135					
	5 months	48.56	(±0.0127)		$(\pm 0.081)$	0.11	0.89		0.0124	0.97
	3 days	39.6	0.051	6.07	1.82	0.025	0.817	0.157	0.0588	0.995
3-site with $K_d$	2 months	52.22	0.063	24.76	1 706	670	0.042 0.472	0.483	0.0756	0000
(column)			0.007		1./30	0.040	0.472	6.5	0.0730	0.392
	5 months	48.85	0.054	24.99	1.364	0.035	0.035 0.442	0.520	0.065	0.985

Table 4-4: Parameters of the two-site and the three-site models for SPCF in column desorption experiments

Model	Time	×	А	β2	æ	feq	feg Ineg Ind	$f_{nd}$	$\alpha$ (hr <sup>-1</sup> )	R <sup>2</sup>
2 17:	3 days	19.49	0.1428 (±0.0198)		2.148 (±0.17)	0.10	0.90		0.1241	0.976
$\lambda$ -site with $\lambda_d$ (isotherm)	2 months	26.06	0.1935 (±0.039)		2.298 (±0.339)	0.16	0.84	i	0.1055	0.979
	5 months	27.72	0.1889 (±0.016)		0.8328 (±0.1231)	0.16	0.84		0.0358	0.922
7 direction C	3 days	18.94	0.1427 (±0.0188)		2.215 (±0161)	0.09	160		0.1317	0.98
(column)	2 months	29.66	0.2048 (±0.038)		1.796 (±0.334)	0.18	0.82		0.0735	0.94
	5 months	28.41	0.1878 (±0.0162)		0.8054 (±0.122)	0.16	0.84		0.0337	0.917
	3 days	18.94	0.104	2.356	2.735	0.054	0.054 0.815 0.131	0.131	0.1807	0.994
3-site with $K_d$ (column)	2 months	29.67	0.125	6.260	2.913	0.094	0.688	0.218	0.1427	0.991
	5 months	28.41	0.109	10.690	1.588	0.077	0.077 0.533 0.390	0.390	0.1049	0.991

Table 4-5: Parameters of the two-site and the three-site models for Plume-A sand in column desorption experiments

Model	Time	R	В	$eta_2$	ø	feq	feq Ineq	fnd	$\alpha$ (hr <sup>-1</sup> )	R <sup>2</sup>
	3 days	8.47	0.2810 (±0.0155)		0.1283 (±00314)	0.18	0.82		0.0251	0.979
2-site with $K_d$ (isotherm)	2 months	15.78	0.155 (±0.0057)		0.1043 (±0.0219)	0.10	06.0		0.0093	0.970
	5 months	15.73	0.1473 (±0.006)		0.0935 (±0.022)	0.09	0.91		0.0083	0.969
	3 days	10.277	0.2174 (±0.0095)		0.3826 (±0.066)	0.13	0.87		0.0566	0.99
2-site with $K_d$ (column)	2 months	13.68	0.1784 (±0.0066)		0.1684 (±0.0227)	0.11	0.89		0.0178	0.974
	5 months	15.57	0.1384 (±0.0042)		0.2456 (±0.0306)	0.08	0.92		0.0218	0.989
	3 days	10.27	0.225	5.748	0.337	0.14	0.238	0.621	0.1881	0.993
3-site with $K_d$ (column)	2 months	13.679	0.1675	8.994	0.3412	0.10	0.10 0.190	0.710	0.1695	966.0
	5 months	15.575	0.148	11.048	0.337	0.089	0.152	0.758	0.1802	0.991

A comparison of desorption rate coefficient ( $\alpha$ ) estimated using the three-site model also reveals that unlike the change in the size of the rate-limited and non-desorption domains, the change in desorption rate coefficients is not significant. This coefficient decreased systematically with aging for SPCF while the minor variations in case of Kalkaska-A and Plume-A sand would not render it to be statistically different. The variations in  $\alpha$ observed for Kalkaska-A and Plume-A sand was not systematic either (Figure 4-10). Aging appeared to affect the size of the rate-limited compartment more than desorption rates. These findings are, to some extent, in conflict with those of Sharer et al. (2003b) who found a decrease in the desorption rate coefficient for chlorobenzene, ethylene dibromide and atrazine but no change for 2.4.D. Similar observations exist in other studies e.g., (Carmichael et al., 1997; Johnson et al., 2001; McCall and Agin, 1985) about a slight reduction in desorption rate coefficients for some cases, while no change in others. For example, (Johnson et al., 2001) found that the desorption rate coefficient for slowly desorbing fractions decreased by a factor of 2 with increased aging for a humic topsoil but remained unaffected for an aging time beyond three months for a shale. In the light of these results as well as findings of some previous studies, it can be said that the effect of aging on the desorption rates is likely to be a function of compound-sorbentaging period combination and cannot be generalized based on a limited set of observations.

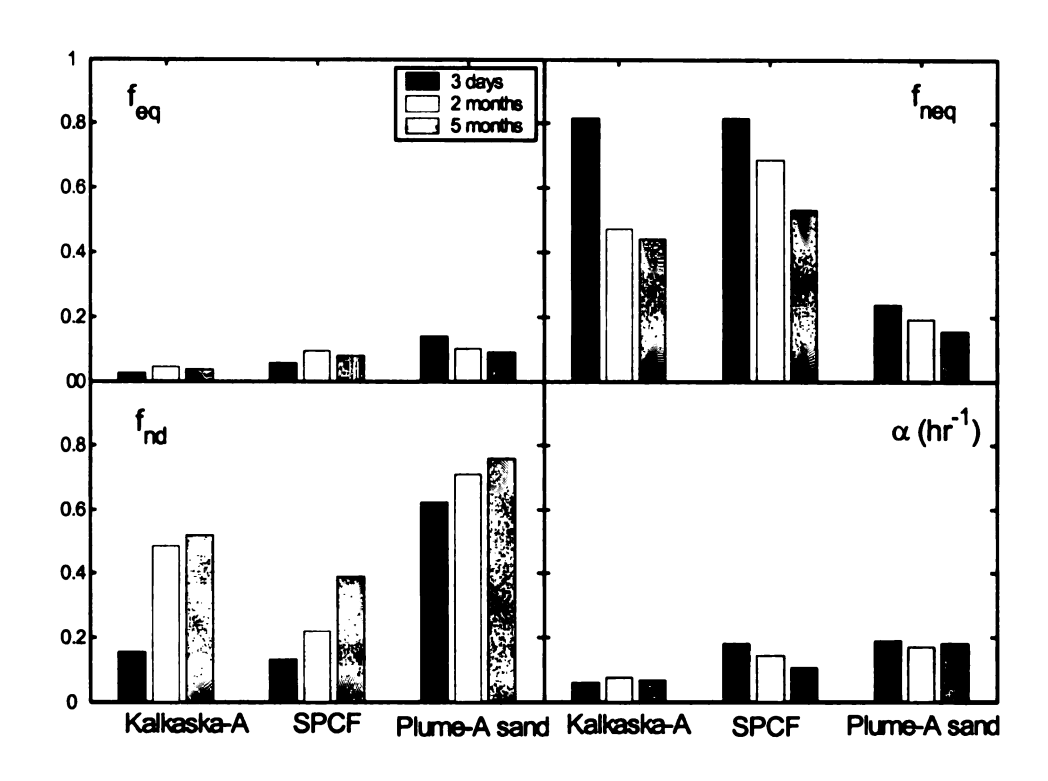


Figure 4-10: Changes in the fractions of equilibrium, rate-limited and non-desorption sites and the desorption rate coefficients with aging

### 4.5 Conclusions

The results from this study provide evidence that partitioning of HOCs to the solid phase is a time-dependent process and the extent of sorption is likely to increase with soil contact time. Contrary to some previous findings, aging did not cause a reduction in the isotherm linearity; however, a significant effect of aging was noted on the distribution of contaminant in various compartments in the solid matrix. A significant amount of naphthalene was rendered non-desorbable over a very short equilibration time suggesting that the formation of a desorption-resistant fraction could be instantaneous for some matrix-contaminant combinations. This highlights the presence of a specific physical or chemical interaction as suggested by (Sharer et al., 2003b).

We also conclude based on the comparison of the two-site and the three-site models, that for contaminants exhibiting significant non-desorption, a compatible mathematical model results in a better description and the data are difficult to reconcile with the dual domain approach. We also suggest that, our aging conceptual model, in which, a shift of contaminant from nonequilibrium domain to non-desorption domain occurs over time is consistent with our observations and explains the resistance to desorption exhibited by contaminants over long-term contact times.

### 4.6 References

- Carmichael, L.M., Christman, R.F. and Pfaender, F.K., 1997. Desorption and mineralization kinetics of phenanthrene and chrysene in contaminated soils. Environmental Science & Technology, 31: 126-132.
- Connaughten, D.F., Stedinger, J.R., Lion, L.W. and Schuler, M.L., 1993. Description of time-varying desorption kinetics: Release of naphthalene from contaminated soils. Environmental Science & Technology, 27(12): 2397-2403.
- Farrell, J. and Reinhard, M., 1994. Desorption of halogenated organics from model solids, sediments, and soil under unsaturated conditions .2. Kinetics. Environmental Science & Technology, 28(1): 63-72.
- Grathwohl, P. and Reinhard, M., 1993. Desorption of trichloroethylene in aquifer material Rate limitation at the grain scale. Environmental Science & Technology, 27(12): 2360-2366.
- Harmon, T.C. and Roberts, P.V., 1994. The effect of equilibration time on desorption rate measurements with chlorinated alkenes and aquifer particles. Environmental Progress, 13: 1-8.
- Johnson, M., Keinath, T. and Weber, W.J., 2001. A distributed reactivity model for sorption by soils and sediments. 14. Characterization and modeling of phenanthrene desorption rates. Environmental Science & Technology, 35(8): 2734-2740.
- Kan, A.T., Fu, G., Hunter, M.A. and Tomson, M.B., 1997. Irreversible adsorption of naphthalene and tetrachlorobiphenyl to Lula and surrogate sediments. Environmental Science & Technology, 31(8): 2176-2185.
- Loehr, R.C. and Webster, M., 1996. Behavior of fresh vs. aged chemicals in soils. Journal of Soil Contamination(5): 361-383.
- McCall, P.J. and Agin, G.L., 1985. Desorption kinetics of picloram as affected by residence time in the soil. Environmental Toxicology and Chemistry, 4: 37-44.
- Park, J.H., Feng, Y.C., Ji, P.S., Voice, T.C. and Boyd, S.A., 2003. Assessment of bioavailability of soil-sorbed atrazine. Applied and Environmental Microbiology, 69(6): 3288-3298.
- Park, J.H., Zhao, X.D. and Voice, T.C., 2001. Biodegradation of non-desorbable naphthalene in soils. Environmental Science & Technology, 35(13): 2734-2740.
- Pignatello, J.J., 1990a. Slowly reversible sorption of aliphatic halocarbons in soils .2. Mechanistic aspects. Environmental Toxicology and Chemistry, 9(9): 1117-1126.

- Pignatello, J.J., 1990b. Slowly reversible sorption of aliphatic halocarbons in soils. 1. Formation of residual fractions. Environmental Toxicology and Chemistry, 9: 1107-1115.
- Pignatello, J.J., Ferrandino, F.J. and Huang, L.Q., 1993. Elution of Aged and Freshly Added Herbicides from a Soil. Environmental Science & Technology, 27(8): 1563-1571.
- Sharer, M., Park, J.H., Voice, T.C. and Boyd, S.A., 2003a. Aging effects on the sorption-desorption characteristics of anthropogenic organic compounds in soil. Journal of Environmental Quality, 32(4): 1385-1392.
- Sharer, M., Park, J.H., Voice, T.C. and Boyd, S.A., 2003b. Time dependence of chlorobenzene sorption/desorption by soils. Soil Science Society of America Journal, 67(6): 1740-1745.
- Weber, W.J. and Huang, W., 1996. A distributed reactivity model for sorption by soils and sediments. 4. Intraparticle heterogeneity and phase-distribution relationships under non-equilibrium conditions. Environmental Science & Technology, 30(3): 881-888.
- Wu, S.C. and Gschwend, P.M., 1986. Sorption kinetics of hydrophobic organic compounds to natural sediments and soils. Environmental Science & Technology, 20(7): 717-725.
- Xing, B. and Pignatello, J.J., 1996. Time-dependent isotherm shape of organic compounds in soil organic matter: Implications for sorption mechanism. Environmental Toxicology and Chemistry, 15: 1282-1288.

#### **CHAPTER 5**

# EFFECTS OF PORE-WATER VELOCITY ON SORPTION NONEQUILIBRIUM Abstract

The contaminant residence time in flow-through soil columns is considered analogous to the equilibration time or "aging" in batch and is controlled by the varying pore-water velocity. Because of this analogy, we evaluated the effect of pore-water velocity on desorption-resistance and sorption non-equilibrium of naphthalene using three natural sorbents (i.e., two surface soils and one of an aquifer origin). Each soil was characterized for retardation and dispersion at four different velocities by injecting a pulse of approximately two pore volumes of tritiated water (<sup>3</sup>H<sub>2</sub>O). Dispersion coefficients were estimated by curve fitting the equilibrium model to the observed BTCs. Pulse injections for naphthalene were conducted at three pore-water velocities ranging between 7-36 cm/hr and solvent extractions were performed after each column desorption to measure the amount of non-desorbable naphthalene mass.

Nonequilibrium was evident in the breakthrough curves for all soils, although the degree of asymmetry and nonequilibrium was different in each case. Similarly, non-desorption was also evident in all soils, as evidenced by solvent-extractable naphthalene at the end of column desorption. For the two surface soils, an increase in the non-desorbable naphthalene mass with a decrease in pore-water velocity could not be established, as velocity varied over a narrow range (14.80-16.3% for Kalkaska-A and 3.54-5.83% for SPCF). On the contrary, a significant increase in the non-desorbable naphthalene mass (6.33% to 18.31%) with a reduction in pore-water velocity was evident in case of Plume-A sand.

The observed time-concentration data for naphthalene was analyzed using the two-site model and four different formulations of the three-site model. In general, the three-site model describes naphthalene breakthrough better than the two-site model for all nine cases (i.e. three soils at three different pore-water velocities). An interesting finding in our work is that all four formulations of the three-site model resulted in identical fits to observed naphthalene breakthrough curves. This suggests that an increase in the number of model parameters to improve the description of observed sorption/desorption behavior is not justified in this case. However, an analysis of the estimated parameters suggests that a mathematical formulation that accounts for a shift of contaminant from the equilibrium domain to the non-desorption domain and formulated with time- independent parameters, is preferred over the driving force formulations based on the linear distribution coefficient  $K_d$ .

### 5.1 Introduction

Processes governing the fate and transport of organic contaminants have been investigated in the past to develop a better understanding of the mechanisms involved. Slow desorption compared to sorption greatly affects the shape of the breakthrough curves in lab and field studies. Sorption is typically known to follow biphasic behavior while good evidence for the three desorption regimes has been found in a number of batch studies. These three regimes include a fast regime, a slow regime and a very slow/non-desorption regime. In recent batch studies, formation of a desorption-resistant fraction within 24 hours (Sharer et al., 2003a; Sharer et al., 2003b) to 3 days (Park et al., 2003) has also been observed. The extent of sorption, distribution of contaminant to different domains, the extent of desorption as well as desorption rates are believed to be greatly affected by soil-contaminant contact time.

Batch experiments to study the sorption-desorption behavior in laboratory normally utilize the equilibrium concept, in which desorption is induced after sorption equilibrium or at least an "apparent equilibrium" between the solute in aqueous phase and solid phase has been achieved. The column studies are normally conducted to apply these findings to the flow-through systems. These involve either the miscible displacement technique or pulse-type injections. In miscible displacement, an "apparent equilibrium" is achieved by injecting the solute of interest long enough so that the effluent concentration equals the influent concentration prior to cutting off the solute injection. The pulse-type experiments on the other hand, represent a case, where the "apparent equilibrium" is dependent on the duration of injected solute pulse. For shorter pulse duration, the "apparent equilibrium" is not reached and a condition of nonequilibrium is viewed to

exist between the sorptive and desorptive fluxes. For such cases, the description of the solute behavior using model formulations that are based on equilibrium partitioning coefficient are questionable. Equilibrium sorption distribution coefficient ( $K_d$ ) may increase 1.3 to 10 times between short and long-term soil contact times and sorption isotherms may become non-linear with increased contact time (Xing and Pignatello, 1996). Similar observations exist for the variations in domain size as a result of an increased contact time. For example, an increase in the desorption-resistant fraction with an increase in soil-contaminant contact time has been reported e.g., (Pignatello, 1990b; Sharer et al., 2003a; Sharer et al., 2003b). In such a case, the mathematical formulations that are based on time independent parameters may be more appropriate to use.

A variety of mathematical models, based on different conceptualizations of the porous medium, have been used to describe desorption in batch systems. These models include chemical site models i.e., two-site model (Rao et al., 1979; Van Genuchten and Wagenet, 1989) and the three-site model (Park, 2000; Park et al., 2001; Park et al., 2002), two and three-parameter pore diffusion models (Johnson et al., 2001), three-parameter kinetic model (Cornelissen et al., 1998a; Cornelissen et al., 1998b), five-parameter kinetic model (Cornelissen et al., 1998a; Cornelissen et al., 1997), gamma-distribution model (Connaughten et al., 1993) and hybrid gamma-distribution model (Ahn et al., 1999).

Most applications of these models have been limited to batch systems. On the contrary, with the exception of a few studies e.g., (Ahn et al., 1999; Prata et al., 2003),

Transport of organic contaminants through porous media has typically been modeled following the dual domain approach that neglects the desorption-resistant domain.

For this work, we have utilized pore-water velocity as a variable to control the soil-naphthalene contact time and study its effects on the extent of non-desorption and nonequilibrium. In the process, we compared different mathematical models for the flow-through systems based on the three regimes of behavior. These formulations utilize the equilibrium distribution coefficient and the kinetic rate coefficients to describe the solute flux between the aqueous phase and the solid phase.

### 5.2 Materials and methods

Solute and geosorbents. The three soils described in Chapter 3 were employed in this phase of study. The properties of dry packed soil columns are summarized in Table 5-1. For this study also, unlabeled and <sup>14</sup>C-naphthalene with uniformly labeled carbons, (procured from Sigma Aldrich Co.) was used as a representative hydrophobic organic compound (HOC). The method of pretreatment and sterilization for the soils has been described in Chapter 3. The same method was followed for this phase of the study.

Table 5-1: Properties of the packed soil columns

Soil	Organic content (%)	Density (g/cm <sup>3</sup> )	Porosity (cm <sup>3</sup> /cm <sup>3</sup> )
Kalkaska-A	3.9	$1.540 \pm 0.024$	$0.384 \pm 0.013$
SPCF	1.9	$1.405 \pm 0.010$	$0.423 \pm 0.006$
Plume-A sand	ND	$1.650 \pm 0.016$	$0.354 \pm 0.016$

Analyzed at the Plant and Soil Sciences Laboratory in Michigan State University

Sorption isotherms. Three-day sorption isotherms were performed on each soil to determine sorption distribution coefficient  $(K_d)$  for each soil. The protocols for the isotherms have been described in Chapter 3. Independent tests of extraction efficiency of the solvent (i.e., methanol) were also carried out on separate batch samples involving an equilibration period of three days. The method was reliable as  $100 \pm 5$ % of naphthalene could be recovered.

Step increase-decrease column experiments with naphthalene. Column studies were conducted using stainless steel columns (15 cm length and 1.1 cm i.d.) with reducing

unions at both ends fitted with 25-micrometer frits to prevent the loss of fine particles (Figure 5-2). The column fittings included stainless steel tubing 1/16 inches outer diameter (i.d 1.27 mm) and Teflon valves. The columns and fittings were autoclaved for 30 minutes at 120 °C and were oven-dried at 105 °C for 24 hours prior to use. The columns were dry-packed for each experiment and flushed with approximately 4-6 pore volumes of CO<sub>2</sub> to replace the air in soil pores prior to saturation. These columns were then saturated from the bottom by injecting approximately 8-10 pore volumes of CaCl<sub>2</sub>. After saturation, the columns were removed for the system, capped and weighed to determine the saturated water content. Column densities and porosities are summarized in Table 5-1. A pulse of approximately 2 pore volumes of the aqueous phase containing naphthalene was injected and effluent samples were collected over time in 10 mL glass tubes containing scintillation fluid to minimize volatilization losses. The sampling continued until the activity in the collected samples was lower than approximately 200 dpm/mL. The soil columns were then taken off and the soil was pushed out in preweighed vials. These vials were capped after topping up with methanol and were tumbled end-over-end at 6 rpm for 24 hours. Phase separation was achieved by centrifugation at 1076 x g for 15 minutes and the liquid phase was analyzed for naphthalene by liquid scintillation counting (LSC).

To characterize each soil for dispersion, identical soil columns were prepared using the same procedure as outlined in the previous section. Approximately two pore volumes of Tritiated water (<sup>3</sup>H<sub>2</sub>O) with an activity of 28000-31000 dpm/mL was injected and the

effluent was sampled every five minutes. Activity of  ${}^{3}\mathrm{H}_{2}\mathrm{O}$  was determined by LSC.

These tracer tests were performed over a range of pore-water velocities for each soil.

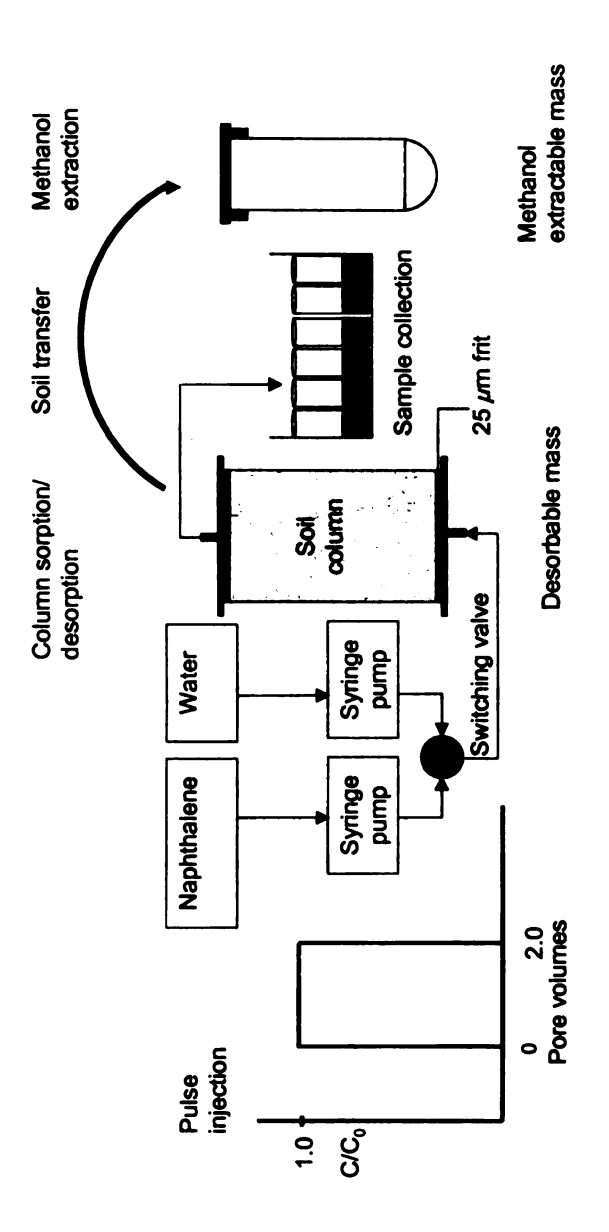


Figure 5-1: Experimental setup for pulse-type experiments with naphthalene and tritiated water

## 5.3 Analysis

Mathematical models. For the flow-through systems, the most widely used model is the two-site model (Van Genuchten and Wagenet, 1989) in which the available sorption sites in a solid matrix are divided into equilibrium sites and nonequilibrium/rate-limited sites. For steady flow in a homogeneous soil, the governing equations for a linearly sorbed solute are:

$$(1 + \frac{f_{eq}\rho K_d}{\theta})\frac{\partial C}{\partial t} = D\frac{\partial^2 C}{\partial r^2} - v\frac{\partial C}{\partial x} - \frac{\alpha\rho}{\theta}[(1 - f_{eq})K_dC - S_{neq}]$$
 (5-1)

$$\frac{\partial S_{neq}}{\partial t} = \alpha [(1 - f_{eq}) K_d C - S_{neq}]$$
 (5-2)

where C is the aqueous concentration ( $\mu g/L$ ), S is the sorbed-phase concentration ( $\mu g/kg$ ), v is the pore-water velocity (cm/hr), D is the hydrodynamic dispersion coefficient (cm<sup>2</sup>/hr), x is the distance along the principal direction of flow (cm) and t is the time (hr),  $\alpha$  is the first order kinetic rate coefficient (hr<sup>-1</sup>) for solute exchange between the aqueous phase and nonequilibrium sites. Employing the dimensionless parameters summarized in Table 5-2, the two-site model reduces to the following dimensionless form:

$$\beta_1 R \frac{\partial C_1}{\partial T} = \frac{1}{P} \frac{\partial^2 C_1}{\partial Z^2} - \frac{\partial C_1}{\partial Z} - \omega_1 (C_1 - C_2)$$
 (5-3)

$$(1 - \beta_1)R \frac{\partial C_2}{\partial T} = \omega_1 (C_1 - C_2)$$
 (5-4)

Subscripts 1 and 2 refer to the equilibrium sites and the rate-limited sites respectively,  $\beta_1$  is the dimensionless partitioning coefficient and  $\omega_1$  is the dimensionless mass transfer coefficient. In the presence of a significant amount of the contaminant

and a model based on the conceptualization of three-domains in a solid matrix may be a more appropriate description of the observed behavior. For the three-site model, the governing equations are:

$$(1 + \frac{f_{eq}\rho K_d}{\theta})\frac{\partial C}{\partial t} = D\frac{\partial^2 C}{\partial r^2} - v\frac{\partial C}{\partial x} - \frac{\alpha_1 \rho}{\theta}[(1 - f_{eq} - f_{nd})K_dC - S_{neq}] - \frac{\alpha_3 \rho}{\theta}f_{nd}K_dC$$
 (5-5)

$$\frac{\partial S_{neq}}{\partial t} = \alpha_1 [(1 - f_{eq} - f_{nd}) K_d C - S_{neq}]$$
 (5-6)

$$\frac{\partial S_{nd}}{\partial t} = \alpha_3 f_{nd} K_d C \tag{5-7}$$

The dimensionless equations for this formulation are:

$$\beta_1 R \frac{\partial C_1}{\partial T} = \frac{1}{P} \frac{\partial^2 C_1}{\partial Z^2} - \frac{\partial C_1}{\partial Z} - \omega_1 (C_1 - C_2) - \omega_3 C_1 \tag{5-8}$$

$$R(1-\beta_1-\beta_2/R)\frac{\partial C_2}{\partial T} = \omega_1(C_1-C_2)$$
(5-9)

$$\beta_2 \frac{\partial C_3}{\partial T} = \omega_3 C_1 \tag{5-10}$$

In this model conceptualization (hereafter referred to as Model 1), the solute flux between the aqueous phase and the nonequilibrium domain is represented by a driving force formulation based on the linear distribution coefficient  $K_d$  and a single rate coefficient  $\alpha_1$  (Figure 5-2). For soils exhibiting a comparatively higher degree of nonequilibrium (i.e., extensive tailing) due to a greater difference between the sorption and the desorption rate, a single rate coefficient to represent the solute flux between the two phases may be inadequate. In that case, it is appropriate to represent both fluxes with two separate rate coefficients and the resulting governing equations for the three-site model (hereafter referred to as Model 2) become:

$$(1 + \frac{f_{eq}\rho K_d}{\theta})\frac{\partial C}{\partial t} = D\frac{\partial^2 C}{\partial x^2} - v\frac{\partial C}{\partial x} - \frac{\alpha_1 \rho}{\theta}(1 - f_{eq} - f_{nd})K_dC +$$
(5-11)

$$\frac{\alpha_2 \rho}{\theta} S_{neq} - \frac{\alpha_3 \rho}{\theta} f_{nd} K_d C$$

$$\frac{\partial S_{neq}}{\partial t} = \alpha_1 (1 - f_{eq} - f_{nd}) K_d C - \alpha_2 S_{neq}$$
 (5-12)

$$\frac{\partial S_{nd}}{\partial t} = \alpha_3 f_{nd} K_d C \tag{5-13}$$

The dimensionless equations for this case become:

$$\beta_1 R \frac{\partial C_1}{\partial T} = \frac{1}{P} \frac{\partial^2 C_1}{\partial Z^2} - \frac{\partial C_1}{\partial Z} - \omega_1 C_1 + \omega_2 C_2 - \omega_3 C_1$$
 (5-14)

$$R(1-\beta_1-\beta_2/R)\frac{\partial C_2}{\partial T} = \omega_1 C_1 - \omega_2 C_2 \tag{5-15}$$

$$\beta_2 \frac{\partial C_3}{\partial T} = \omega_3 C_1 \tag{5-16}$$

One of the limitations of the  $K_d$ -based formulations (i.e., the two-site model, Model 1 and Model 2) is the time scale dependence of  $K_d$ . The time-independence in these formulations can be achieved by replacing  $K_d$  with  $K_{eq}$  (i.e., the distribution coefficient for the equilibrium domain) and utilizing kinetic rate coefficients to describe the solute exchange between the aqueous phase and nonequilibrium/non-desorption domain. In this formulation, sorption/desorption is instantaneous for the equilibrium compartment with equal rates and is rate-limited for the nonequilibrium compartment, as is the case in Model 1 and Model 2, but is kinetically controlled. The governing equations for this case (Model 3) are:

$$(1 + K_{eq} \frac{\rho}{\theta}) \frac{\partial C}{\partial t} = D \frac{\partial^2 C}{\partial r^2} - v \frac{\partial C}{\partial x} + \frac{\alpha_2 \rho}{\theta} S_{neq} - \alpha_1 C - \alpha_3 C$$
 (5.17)

$$\frac{\partial S_{neq}}{\partial t} = \frac{\alpha_1 \theta}{\rho} C - \alpha_2 S_{neq} \tag{5.18}$$

$$\frac{\partial S_{nd}}{\partial t} = \frac{\alpha_3 \theta}{\rho} C \tag{5-19}$$

The dimensionless equations for Model 3 are represented by:

$$R\frac{\partial C_1}{\partial T} = \frac{1}{P}\frac{\partial^2 C_1}{\partial Z^2} - \frac{\partial C_1}{\partial Z} - \omega_1 C_1 + \omega_2 C_2 - \omega_3 C_1 \tag{5-20}$$

$$\frac{\partial C_2}{\partial T} = \omega_1 C_1 - \omega_2 C_2 \tag{5-21}$$

$$\frac{\partial C_3}{\partial T} = \omega_3 C_1 \tag{5-22}$$

Models 1,2 and 3 treat sorption to the nonequilibrium/rate-limited sites and non-desorption sites as simultaneous and are based on the assumption that each solid phase particle is in direct contact with liquid phase. The evidence in certain aging experiments is, however, to the contrary, which reveal a shift of contaminant from the nonequilibrium domain to the non-desorption domain. For such a case, the governing equations become (Model 4):

$$(1 + K_{eq} \frac{\rho}{\theta}) \frac{\partial C}{\partial t} = D \frac{\partial^2 C}{\partial x^2} - v \frac{\partial C}{\partial x} - \alpha_1 C + \frac{\alpha_2 \rho}{\theta} S_{neq}$$
 (5-23)

$$\frac{\partial S_{neq}}{\partial t} = \frac{\alpha_1 \theta}{\rho} C - \alpha_2 S_{neq} - \alpha_3 S_{nd}$$
 (5-24)

$$\frac{\partial S_{nd}}{\partial t} = \frac{\alpha_3 \theta}{\rho} C \tag{5-25}$$

and the dimensionless equations for Model 4 are:

$$R\frac{\partial C_1}{\partial T} = \frac{1}{P}\frac{\partial^2 C_1}{\partial Z^2} - \frac{\partial C_1}{\partial Z} - \omega_1 C_1 + \omega_2 C_2$$
 (5-26)

$$\frac{\partial C_2}{\partial T} = \omega_1 C_1 - \omega_2 C_2 - \omega_3 C_2 \tag{5-27}$$

$$\frac{\partial C_3}{\partial T} = \omega_3 C_2 \tag{5-28}$$

Solution technique and parameter estimation. The dimensionless equations for all model formulations were solved using a high-resolution numerical scheme. The spatial derivatives were approximated using a fourth-order compact scheme with spectral-like resolution (Lele, 1992). A fourth-order Runge-Kutta scheme was used for temporal differencing. Parameters for two-site model were estimated using the non-linear least squares inversion program CXTFIT (Toride et al., 1999). Parameters for all formulations of the three-site model were estimated using sequential quadratic programming (SQP) as implemented in MATLAB. The solution technique and the parameter estimation methods have been described in detail in Chapter 3. The same methods were utilized for parameter estimation in this study.

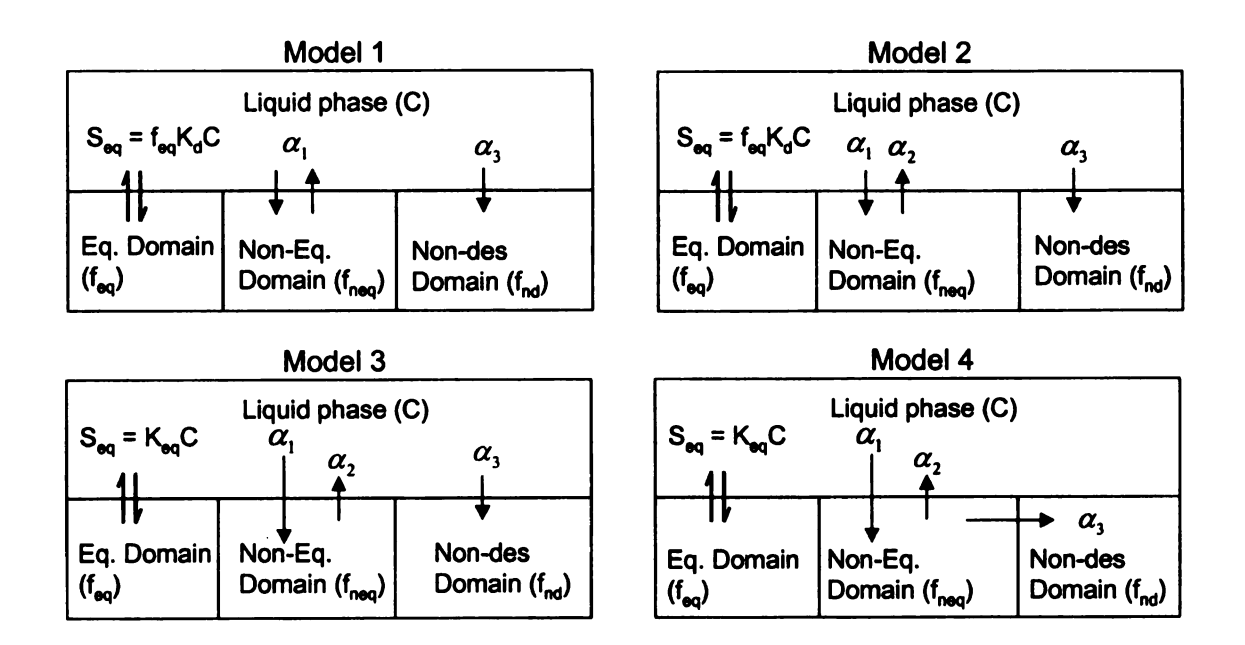


Figure 5-2: Box model representations of four variations of the three-site model

Table 5-2: Dimensionless parameters for the two-site and the three-site models

Para- meter	Two-site model	Three-	site model formulations	S .
	-	Model 1	Model 2	Model 3&4
$C_1$	$\frac{C}{C_0}$	$\frac{C}{C_0}$	$\frac{C}{C_0}$	$\frac{C}{C_0}$
$C_2$	$\frac{S_{neq}}{(1 - f_{eq})K_dC_0}$	$\frac{S_{neq}}{(1 - f_{eq} - f_{nd})K_dC_0}$	$\frac{S_{neq}}{(1 - f_{eq} - f_{nd})K_dC_0}$	$\frac{S_{neq}\rho_b}{\theta C_0}$
$C_3$	Not applicable	$\frac{S_{nd}}{f_{nd}K_dC_0}$	$\frac{S_{nd}}{f_{nd}K_dC_0}$	$\frac{S_{nd} \rho_b}{\theta C_0}$
R	$1 + \frac{\rho_b K_d}{\theta}$	$1 + \frac{\rho_b K_d}{\theta}$	$1 + \frac{\rho_b K_d}{\theta}$	$1 + \frac{\rho_b K_{eq}}{\theta}$
$oldsymbol{eta_{l}}$	$\frac{\theta + f_{eq}\rho_b K_d}{\theta + \rho_b K_d}$	$\frac{\theta + f_{eq} \rho_b K_d}{\theta + \rho_b K_d}$	$\frac{\theta + f_{eq} \rho_b K_d}{\theta + \rho_b K_d}$	Not applicable
$\beta_2$	Not applicable	$\frac{ ho_b f_{nd} K_d}{ heta}$	$rac{ ho_b f_{nd} K_d}{ heta}$	Not applicable
$\omega_{ m l}$	$\frac{\alpha(1-\beta)LR}{\nu}$	$\frac{\alpha_1(1-\beta_1-\beta_2/R)LR}{\nu}$	$\frac{\alpha_1(1-\beta_1-\beta_2/R)LR}{v}$	$\frac{\alpha_1 L}{v}$
$\omega_2$	Not applicable	Not applicable	$\frac{\alpha_2(1-\beta_1-\beta_2/R)LR}{\nu}$	$\frac{\alpha_2 L}{v}$
$\omega_3$	Not applicable	$\frac{\alpha_3 L \beta_2}{v}$	$\frac{\alpha_3 L \beta_2}{\nu}$	$\frac{\alpha_3 L}{v}$
P	$\frac{vL}{D}$	$\frac{vL}{D}$	$\frac{vL}{D}$	$\frac{vL}{D}$
T	$\frac{vt}{L}$	$\frac{vt}{L}$	$\frac{vt}{L}$	$\frac{vt}{L}$
Z	$\frac{x}{L}$	$\frac{x}{L}$	$\frac{x}{L}$	$\frac{x}{L}$

## 5.4 Results and discussion

**Sorption isotherms**. Sorption of naphthalene was linear for all the three soils (Figures 5-3).  $K_d$  values were 9.22 mL/g for Kalkaska-A, 5.82 mL/g for SPCF and 1.46 mL/g for Plume-A sand respectively. The  $K_d$  values in our experiments are consistent with the organic content of the three soils i.e., 1.9 % and 3.9 % and < 0.03% respectively.

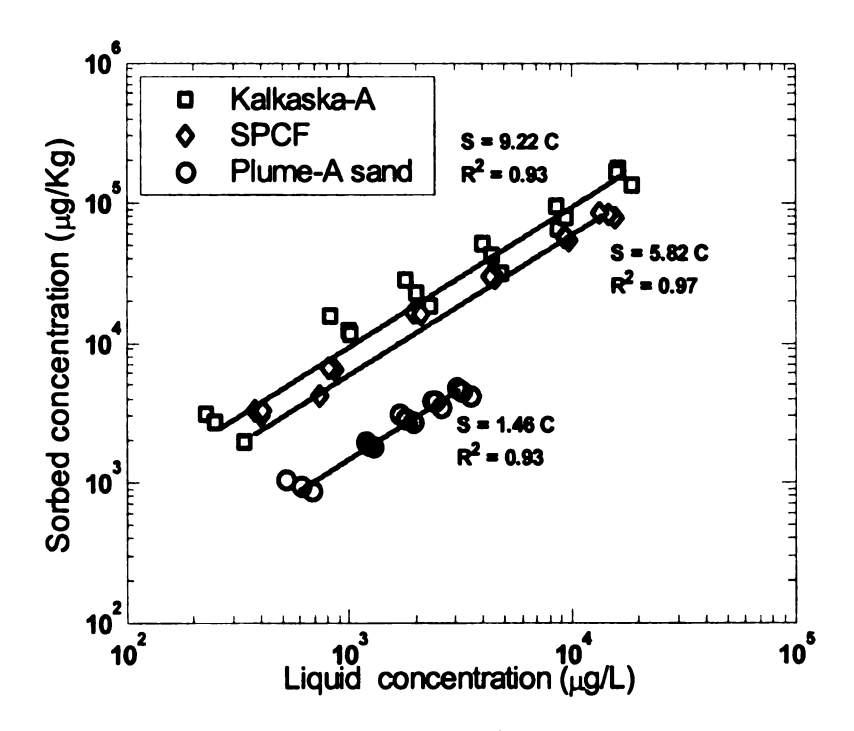


Figure 5-3: Three-day sorption isotherms for naphthalene

Analysis of tritiated water BTCs. The choice of the nonequilibrium model i.e., mobile-immobile model (MIM) or sorption-related nonequilibrium model is normally made based on the results of independent tracer studies that employ a conservative tracer and are conducted under experimental conditions similar to those employed for the solute of interest. Fitting the observed tritiated water breakthrough curves to the equilibrium model

and determining the retardation coefficient is a means to confirm the presence/absence of immobile water. Inappropriate estimation of pore-water velocity is indicated by values of R less than unity, which is based on the assumption that all the pores do not participate in flow (Maraqa et al., 1998). Values of R less than unity for tritiated water have been reported (Nkedikizza et al., 1983) and attributed to the transport-related nonequilibrium created by the presence of immobile water regions. In our experiments, we estimated R using the non-linear least squares inversion program CXTFIT (Toride et al., 1999) by fitting the equilibrium model to the observed tritiated water BTCs (Figure 5-4 to 5-6). In our data, no evidence of immobile water was found, as the estimated values of R for Kalkaska-A and Plume-A sand at four different velocities were found to be not different than unity (Table 5-3). For SPCF, R was significantly greater than unity. Values of R greater than unity for tritiated water have been reported. For example Seyfried and Rao (1987) reported a value of R for tritiated water between 1.10-1.18 for their columns. We also observed a velocity-dependent R for SPCF (i.e., 1.083 to 1.282) for a velocity range of 3.16 – 15.79 cm/hour and we attribute this to the isotopic exchange of tritium with crystallatic hydroxyls of clay particles as proposed by Van Genuchten and Wierenga, (1977). Note that the SPCF contains clay content of 5 %, which is comparatively higher than the other two soils.

Based on our analysis of retardation, the dispersion coefficients for Kalkaska-A and Plume-A sand were estimated using the equilibrium model with a value of R fixed at unity. Due to a significant velocity-dependent R for SPCF, dispersion coefficient for SPCF was estimated by using the values of R estimated in step 1. These estimated dispersion coefficients were used in all the nonequilibrium model applications and were

not estimated by curve fitting. Dispersion coefficients so obtained for the three soils were consistent with their respective mechanical characteristics. For Plume-A sand (97.6% sand), Kalkaska-A (91% sand) and SPCF (78% sand), the dispersion coefficient ranged between 1.494-12.336 cm<sup>2</sup>/hr, 1.493-5.666 cm<sup>2</sup>/hr and 0.423-1.672 cm<sup>2</sup>/hr respectively. Dispersion coefficients also correlated well with the pore-water velocity with R<sup>2</sup> values of 0.974, 0.916 and 0.981 for Plume-A sand, Kalkaska-A and SPCF respectively.

Table 5-3: Retardation factors and the dispersion coefficients with 95% confidence intervals

Soil	Velocity (cm/hr)	Normalized pulse time,	Retardation factor	Dispersion coefficient D	Correlation coefficient
	(0112111)	<i>T</i>	R	(cm <sup>2</sup> /hr)	R <sup>2</sup>
	18.34	2.10	0.9704	5.6664	0.994
			$(\pm 0.10)$	$(\pm 1.1052)$	
	12.84	2.00	0.9896	4.9734	0.996
Kalkaska-A			$(\pm 0.011)$	$(\pm 0.7152)$	
Naikaska-A	9.17	2.01	0.9782	4.014	0.984
			$(\pm 0.022)$	(± 1.098)	
	3.67	2.53	1.006	1.4934	0.992
			$(\pm 0.014)$	$(\pm 0.261)$	
	15.79	2.00	1.083	1.6728	0.998
			$(\pm 0.005)$	(±0.1968)	
	11.06	1.84	1.139	1.0662	0.997
SPCF			$(\pm 0.007)$	(±0.1602)	
SPCF	7.90	2.00	1.182	0.78	0.997
			$\pm 0.005$ )	(±0.090)	
	3.16	1.99	1.282	0.4236	0.958
			$(\pm 0.030)$	(±0.201)	
	17.18	2.00	0.9945	12.336	0.998
			$(\pm 0.009)$	$(\pm 1.032)$	
	12.03	2.00	1.008	7.626	0.995
Plume-A			$(\pm 0.012)$	$(\pm 0.846)$	
sand	8.59	2.00	1.007	6.69	0.994
			$(\pm 0.014)$	$(\pm 0.870)$	
	3.44	1.97	1.021	1.494	0.982
			$(\pm 0.019)$	$(\pm 0.4026)$	

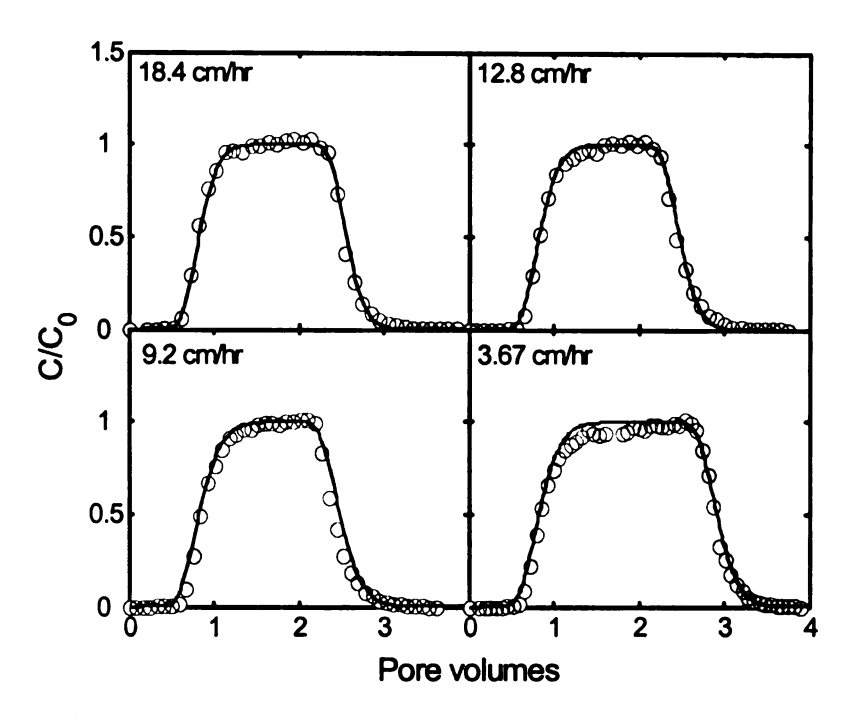


Figure 5-4: Tritiated water BTCs for Kalkaska-A. Circles represent the experimental data and solid lines are simulations using the equilibrium model

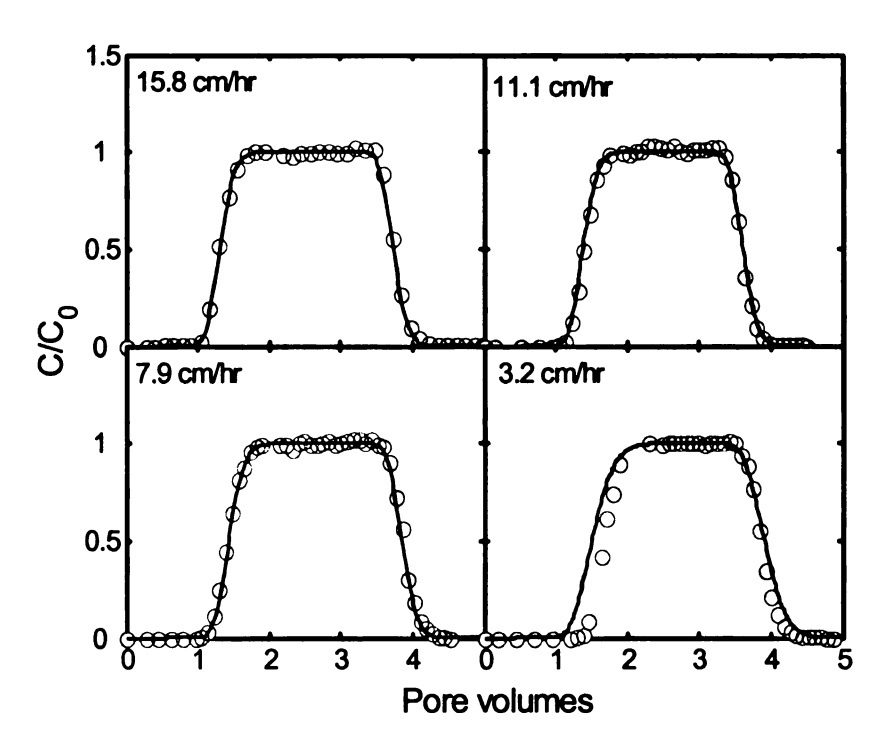


Figure 5-5: Tritiated water BTCs for SPCF. Circles represent the experimental data and solid lines are simulations using the equilibrium model

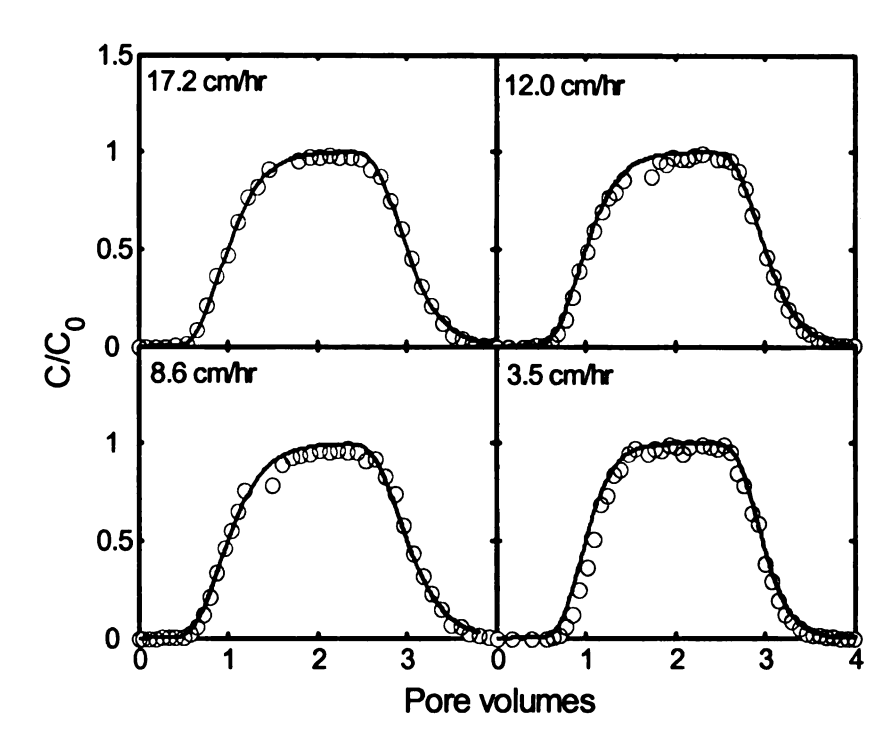


Figure 5-6: Tritiated water BTCs for Plume-A sand. Circles represent the experimental data and solid lines are simulations using the equilibrium model

Analysis of naphthalene BTCs. Mass balance calculations for naphthalene show a recovery range between 73-97% for all the pulse-type experiments with one exception of SPCF at a velocity of 14.9 cm/hr, which appears to be an experimental artifact. For the two surface soils, i.e., Kalkaska-A and SPCF, the non-desorbable naphthalene mass was unaffected by pore-water velocity i.e., 14.80-16.30 % for Kalkaska-A and 3.54-5.83 % for SPCF (Table 5-4). However, an increase in non-desorbable naphthalene for Plume-A sand (i.e., 6.33-18.31%) with a decrease in pore-water velocity (35.9 - 8.7 cm/hr) was evident in our data.

Table 5-4: Column Peclet numbers and mass fractions for the three soils at different velocities

Soil	Velocity (cm/hr)	C <sub>init</sub> (mg/L)	Peclet Number	Desorbable mass (%)	Non- desorbable mass (%)	Recovery (%)
	33.82	13.843	48.3	83.7	16.3	86.26
Kalkaska-A	16.62	14.952	44.0	84.81	15.19	85.74
	7.91	11.49	37.3	85.20	14.80	73.96
<u> </u>	29.39	15.13	149.6	96.46	3.54	96.40
SPCF	14.94	20.00	147.0	95.27	4.73	101.52
	7.55	11.87	141.8	94.17	5.83	78.43
	35.92	14.83	20.4	93.67	6.33	88.39
Plume-A sand	17.01	14.69	21.1	91.54	8.46	81.45
	8.68	8.062	22.4	81.69	18.31	93.80

The observed BTCs of naphthalene were analyzed using nonequilibrium models only (i.e., the two-site model and four variations of the three-site model). Optimized parameters for the two-site model were estimated under two different scenarios (1) parameter  $\beta_1$  and  $\omega_1$  were estimated with a fixed R based on isotherm  $K_d$  (designated as  $R_{isotherm}$ ) and (2) R was also estimated as a fitting parameter (designated as  $R_{fit}$ ) in addition to  $\beta_1$  and  $\omega_1$ . For all applications of the two-site and the three-site model, the dispersion coefficients estimated from the tritiated water BTCs were used. The optimized parameters with 95% confidence intervals and the correlation coefficients are listed in Table 5-5 to Table 5 7.

Table 5-5: Estimated parameters for Kalkaska-A using the two-site and the three-site models

Velocity Model (cm/hr)	/ Model	R	$\beta_{\rm l}$	$\beta_2$	l <sub>Ø</sub>	ω2	<i>®</i> 3	feq	feq fneq $f_{nd}$ $\alpha_1(hr^{-1})$ $\alpha_2(hr^{-1})$ $\alpha_3(hr^{-1})$ $R^2$	$\alpha_1(hr^{-1})$	$\alpha_2 (hr^{-1})$	$\alpha_3 (hr^{-1})$	$\mathbb{R}^2$
	2-site with Risotherm	38.88	0.5136 38.88 (±0.014)		1.665 (±0.14)			0.48	0.52	0.2379			0.89
	2-site with R <sub>ftt</sub>	42.99	0.4853 (±0.107)		1.47 (±0.12)			0.48	0.52	0.2620			0.90
33.82	3-site (Model 1)	33.99	0.479	0.521	3.325		0.209	0.464	0.209 0.464 0.521 0.016	0.4364		0.907	0.97
	3-site (Model 2)	37.57	0.524	0.474	1.861	2.576	0.305	0.511	2.576 0.305 0.511 0.476 0.013	0.241	0.334	1.448	0.97
	3-site (Model 3)	19.6			1.892	0.150 0.306	0.306			4.26	0.3397	0.690	0.97
	3-site (Model 4) 20.328	20.328			2.051	0.118	0.118 0.0202			4.63	0.2661	0.0455	0.97
	2-site with	39.02	0.5938 39.02 (±0.036)		0.7835			0.45 0.55	0.55	0.1196			0.55
	2-site with R <sub>fit</sub>	62.69	0.3463 67.99 (±0.025)		1.342 (±0.081)			0.38	0.62	0.0646			0.90
16.62	3-site (Model 1)	1		2.599	1.384		0.200	0.516	0.200 0.516 0.424 0.061	0.0846		0.085	0.98
	3-site (Model 2)	37.71	0.612	0.341	1.385	1.088	1.088 0.199 0.601		0.390 0.009	0.107	0.084	0.646	0.98
	3-site (Model 3)	22.69			1.438	0.079 0.206	0.206			1.594	0.087	0.228	0.98
	3-site (Model 4) 23.094	23.094			1.5776	0.066 0.057	0.057			1.74	0.073	0.0105	0.98

Table 5-5 (cont'd).

	2-site with		0.6149		2.206							
	Risotherm	36.13	36.13 (±0.0297)		$(\pm 0.377)$	9.0	0.60 0.40	0.0768	<b>∞</b>			0.90
	2-site with		0.5858		1.392							
	$R_{fit}$	42.66 (±0.01	$(\pm 0.0146)$		$(\pm 0.112)$	0.5	0.58 0.42	0.0416	9			96.0
7.91	3-site (Model 1) 39.68 0.636 0.242 1.563	39.68	0.636	0.242	1.563	0.162 0.62	0.162 0.627 0.367 0.006 0.0582	5 0.05	7	0.35	0.352 0.99	66.
	3- site											
	(Model 2)	37.69	0.671	0.371	1.549	Model 2) 37.69 0.671 0.371 1.549 1.315 0.162 0.663 0.3270.013 0.068	53 0.327 0.01	3 0.06		0.058 0.230 0.99	0	66.
	3-site											
	(Model 3) 23.79	23.79			1.804	1.804 0.120 0.1711		0.952	1	0.063 0.090 0.99	0	66.
	3-site							,		0	į	(
	(Model 4) 25.32	25.32			1.707	1.707 0.099 0.0104		0.9004	ı	0.052 0.0055 0.99	<u>ک</u> ا	8

Table 5-6: Estimated parameters for SPCF using the two-site and the three-site models

Velocity (cm/hr)	Model	R	В	$\beta_2$	ď	ans	ø3	feq	fneg	$f_{nd}$	$\alpha_1(\mathrm{hr}^{-1})$	$f_{neq}$ $f_{nd}$ $\alpha_1(hr^{-1})$ $\alpha_2(hr^{-1})$ $\alpha_3(hr^{-1})$ $R^2$	$\alpha_3 (hr^{-1})$	R <sup>2</sup>
	2-site with											ļ		
	Risotherm	20.11												
	2-site with		0.5824		3.211									
	Rfit	23.15	$(\pm 0.021)$		$(\pm 0.43)$			0.56	0.44	1	0.6508			96.0
(	3-site													
29.39	(Model 1) 24.80	24.80	0.543	2.398 3.605	3.605		0.133 0.524		0.375	0.101	0.375 0.101 0.7912		0.109	0.98
	3-site													
	(Model 2)	27.99	0.486	1.803	3.498	4.993	0.132 0.468	- 1	0.466 0.067 0.545	0.067	0.545	0.778	0.144	0.98
	3-site													
	(Model 3)	13.67			3.467	0.395	0.132				6.793	0.773	0.259	0.98
	3-site													
	(Model 4)	13.84			3.441	3.441 0.3673 0.0144	0.0144				6.742	0.7197	0.028	0.98
	2-site with	i	0.4153		8.921									
	Risotherm	20.20	$20.20 (\pm 0.245)$		$(\pm 0.543)$			0.38	0.62	•	0.7526			0.87
	2-site with		0.6615		1.891									
	Rfit	25.57	$(\pm 0.008)$		$(\pm 0.112)$			0.64	0.36	٠	0.2177			0.98
•	3-site													
14.94	(Model 1)	26.64	0.645	1.334	1.888		0.064	0.63	0.32	0.05	0.05 0.2317		0.048	0.99
	3- site													
	(Model 2)	28.58	0.6017	1.22	1.887	2.363	0.064	0.587	0.368 0.044 0.185	0.044	0.185	0.232	0.053	0.99
	3-site													
	(Model 3)	17.224			1.877	1.877 0.2324 0.0639	0.0639				1.87	0.2315	0.064	0.99
	3-site													
	(Model 4) 17.207	17.207			1.943	1.943 0.2245 0.0078	0.0078				1.935	0.2236	0.0078	0.99

Table 5-6 (cont'd).

(±0.018) 0.6598 (±0.018) 0.643 1.012 0.571 1.668	2-site with		0.6622		2.378									
2-site with 0.0 $R_{fit}$ 24.17 ( $\pm 0$ 3-site (Model 2) 28.13 0.3-site (Model 3) 16.130 3-site (Model 3) 16.130 3-site		0.63	$(\pm 0.018)$		$\pm 0.309$ )			0.64	0.36	•	0.1718			96.0
R <sub>fu</sub> 24.17 (±0 3-site (Model 1) 24.28 0. 3-site (Model 2) 28.13 0. 3-site (Model 3) 16.130 3-site			0.6598		2.694		i							
3-site (Model 1) 24.28 0. 3-site (Model 2) 28.13 0. 3-site (Model 3) 16.130 3-site	$R_{fit}$ 2	4.17	$(\pm 0.018)$		$\pm 0.389$			0.65	0.35	1	- 0.1649			0.97
(Model 1) 24.28 0.  3-site (Model 2) 28.13 0.  3-site (Model 3) 16.130  3-site	3-site													
3-site (Model 2) 28.13 0. 3-site (Model 3) 16.130 3-site	(Model 1) 2	4.28	0.643	1.012	3.614		0.122	0.63	0.33	0.043	0.2374		0.061 0.98-	0.98
0	3-site													
	(Model 2) 2	8.13	0.571	1.668	3.005	4.123	0.1158	0.556	0.383	0.061	0.146	0.200	0.035	0.98
	3-site													
	(Model 3) 16	5.130			2.961	0.392	0.116				1.491	1.491 0.1977 0.058 0.98	0.058	0.98
	3-site													
(Model 4) 16.202 2.9656 0.5649 0.0142	(Model 4) 16.202	5.202			2.9656	0.3649	0.0142				1.493	1.493 0.1837 0.0071 0.98	0.0071	0.98

Table 5-7: Estimated parameters for Plume-A sand using the two-site and the three-site models

Velocity (cm/hr)	Velocity Model (cm/hr)	R	В	$\beta_2$	l <sub>w</sub>	w <sub>2</sub>	ø3	feq	fneg	$f_{nd}$	$a_1(hr^{-1})$	feq fneq $f_{nd}$ $\alpha_1(\text{hr}^{-1})$ $\alpha_2(\text{hr}^{-1})$ $\alpha_3(\text{hr}^{-1})$	$a_3 (hr^{-1})$	$\mathbb{R}^2$
	2-site with Risotherm	7.84	0.2453 (±0.004)	•	0.4078 (±0.028)			0.13	0.87		0.1651			0.98
	2-site with R <sub>ft</sub>	4.52	0.4145 (±0.038)	•	0.4366 (±0.027)			0.25	0.75	•	0.3947			0.99
35.92	3-site (Model 1)	4.42	0.439	1.262	0.390		0.117	0.117 0.275 0.356 0.369	0.356	0.369	0.745		0.179	0.99
	3-site (Model 2)	5.38	0.361	0.388	0.375	0.975	0.975 0.09480.215 0.696 0.089	0.215	969.0	0.089	0.295	0.766	0.616	0.99
	3-site (Model 3)	1.942			0.3789	0.3102	0.094				0.907	0.7403	0.225	0.99
	3-site (Model 4)	1.941			0.4738	0.2497	0.2497 0.0626				1.135	0.598	0.150	0.99
	2-site with Risotherm	7.39	0.3072 (±0005)		0.4723 (±0.033)			0.20	0.80		0.1046			0.98
	2-site with R <sub>ftt</sub>	5.51	0.4055 (±0.042)		0.4894 (±0.034)			0.27	0.73	•	0.1694			0.98
17.01	3- site (Model 1)	4.893	0.4734 1.00	1.00	0.4324		0.1362	0.338	0.405	0.257	0.13620.338 0.405 0.257 0.3110		0.1276	0.99
	3-site (Model 2)	5.98	0.387	1.221	0.432	0.673	0.13750.264 0.489	0.264	0.489	0.24	0.2009	0.313	0.1276	0.99
	3-site (Model 3)	2.33			0.4256	0.271	0.136				0.483	0.3070	0.154	0.99
	3-site (Model 4)	2.31			0.5686	0.2090 0.066	0.066			:	0.645	0.237	0.075	0.99

Table 5-7(cont'd).

	2-site with		0.2285		8.299.0								
	Risotherm	7.74	7.74 (±0.005)	)	$(\pm 0.039)$		0.11	0.11 0.89	- 1	- 0.0647			0.98
	2-site with		0.2172		0.6656								
	$R_{fit}$	8.16	$8.16 (\pm 0.031)$		$(\pm 0.039)$	:	0.11	0.11 0.89	ı	0.0603			0.98
(	3-site												İ
8.68	(Model 1) 4.43 0.4023 1.22 0.519	4.43	0.4023	1.22	0.519		0.299 0.228 0.416 0.355 0.2097	0.416	0.355	0.2097		0.142 0.99	0.99
	3-site												1
	(Model 2)	5.82	0.306	1.32	0.518	0.987	Model 2) 5.82 0.306 1.32 0.518 0.987 0.299 0.163 0.564 0.273 0.1104 0.2102 0.1308 0.99	0.564	0.273	0.1104	0.2102	0.1308	0.99
	3-site												
	(Model 3) 1.815	1.815			0.5055 0.344 0.2957	0.344	0.2957			0.293	0.1992 0.171 0.99	0.171	0.99
	3-site												
	(Model 4) 1.786	1.786			0.816 0.231 0.132	0.231	0.132			0.472	0.472 0.133	0.076 0.99	0.99

## **Model comparisons**

Comparison of  $\mathbb{R}^2$  values listed in Tables 5-5 to 5-7 reveals that the two-site model with a retardation factor based on the isotherm  $K_d$  performed poorly in all cases compared to other model formulations. The model failed to converge to a solution in case of SPCF at a velocity of 29.4 cm/hour. The model performance appears to increase with a decrease in SOM as  $\mathbb{R}^2$  values ranged between 0.54 to 0.89 for Kalkaska-A, 0.87 to 0.96 for SPCF and a constant value of 0.98 for plume-A sand respectively. In the second application of the two-site model, in which, we estimated R in addition to  $\beta_1$  and  $\omega_1$ , a significant improvement in the model performance was observed for Kalkaska-A with  $\mathbb{R}^2$  values ranging between 0.90-0.96. For the other two soils, the model fits improved compared to the preceding case, however, the resulting  $K_d$  values (i.e., 10.22-16.24 for Kalkaska-A and 6.75-6.87 for SPCF) are significantly higher than the respective isotherm  $K_d$  which is not expected as the batch environment is more conducive for partitioning to sorbed phase than the columns.

Mathematical formulations based on the three-site model described naphthalene BTCs better than the two-site model in general, as is evident by a comparison of the respective correlation coefficients. An important feature of the model fits using different formulations of the three-site model was identical BTCs by all four formulations (i.e., Model 1,2,3&4) for all nine cases (i.e., three soils and three velocities). The identical fits with Model 1 and Model 2 also support the idea that an increase in number of parameters

other than those necessary to describe the observational regimes does not result in an improved description of the observed behavior.

Different formulations of the three-site model stated earlier are based on two different conceptualizations of mass transfer mechanism between the sorbed phase and the aqueous phase. In Models 1 and 2, the solute flux between the sorbed and aqueous phases is described by a driving force formulation based on linear distribution coefficient. Models 3 and 4, on the other hand, treat sorption and desorption purely based on kinetics and the solute flux between the two phases is mathematically described by the kinetic rate coefficients for each domain. The choice of the appropriate model to describe the naphthalene transport in soil columns requires a little more than merely a comparison of goodness of fit or the correlation coefficients. Due to the fact, that Model 2 with an extra rate coefficient, resulted in BTCs that were identical to Model 1, it was not considered for further analysis.

A comparison of Model 1 and Model 3 was done to explore the appropriateness of the two different classes of models. In Model 1, the parameter  $K_d$  and the fractions of the solid matrix (i.e.,  $f_{eq}$ ,  $f_{neq}$  and  $f_{nd}$ ) are time-dependent. The dependence of  $K_d$  on contact time is well established in our data as well as other sorption studies. In a separate study involving desorption experiments with aged soils, we also found an evidence of the dependence of the domain size on the soil-contaminant contact time. Another limitation in  $K_d$ -based models is the interdependence of the parameters in the dimensionless form of the governing equations that results in a higher parameter uncertainty. Models 3 and 4, which are based on time-independent parameters are free from these limitations. The

retardation factor R in Model 3 is based on  $K_{eq}$  (i.e., the partitioning coefficient for equilibrium compartment) and not  $K_d$ . Furthermore, the domain size in these models is arbitrary and the solute flux between the aqueous phase and each solid phase domain is kinetically controlled. We did an analysis of sensitivity to initial parameter values for Models 1 and 3 and found that the parameter uncertainty in Model 1 was as high as 136% compared to less than 5% in Model 3.

The evidence, in aging experiments (data not reported here) suggests however, that soil-contaminant contact time affects the size of nonequilibrium and non-desorption domains only and the size of equilibrium domain remains more or less unaffected. This in mind, it is fair to assume that nonequilibrium compartment and non-desorption compartments are arranged in series rather than in parallel. Model 4 is a representation of this arrangement of compartments in the solid matrix. Therefore, we contend that Model 4 is a conceptual 3-site model that includes the effects of aging and provides a superior description of pulse-type injection experiments in soil columns.

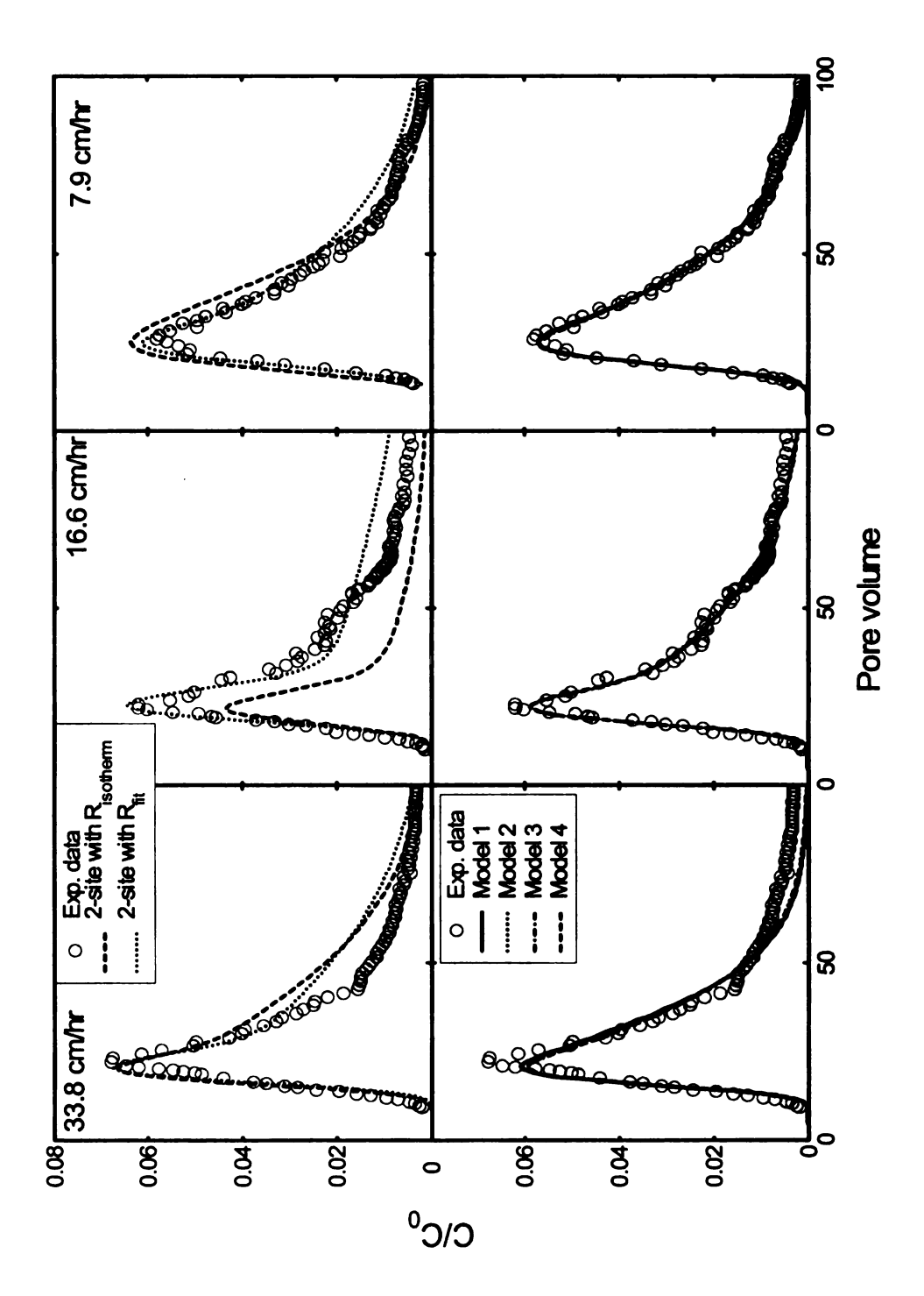


Figure 5-7: Best fits of the two-site and the three-site models to the observed naphthalene breakthrough data for Kalkaska-A

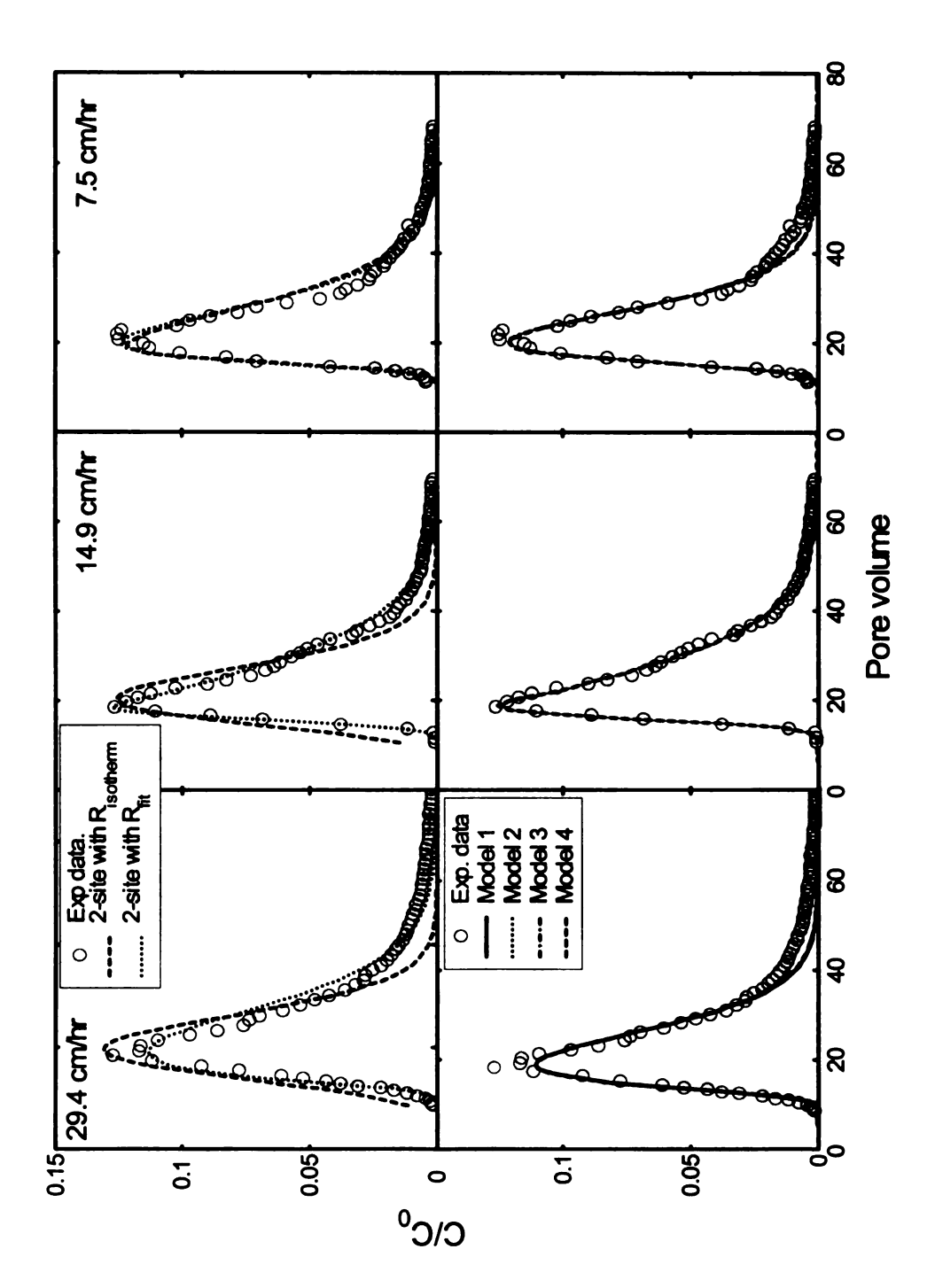


Figure 5-8: Best fits of the two-site and the three-site models to the observed naphthalene breakthrough data for SPCF

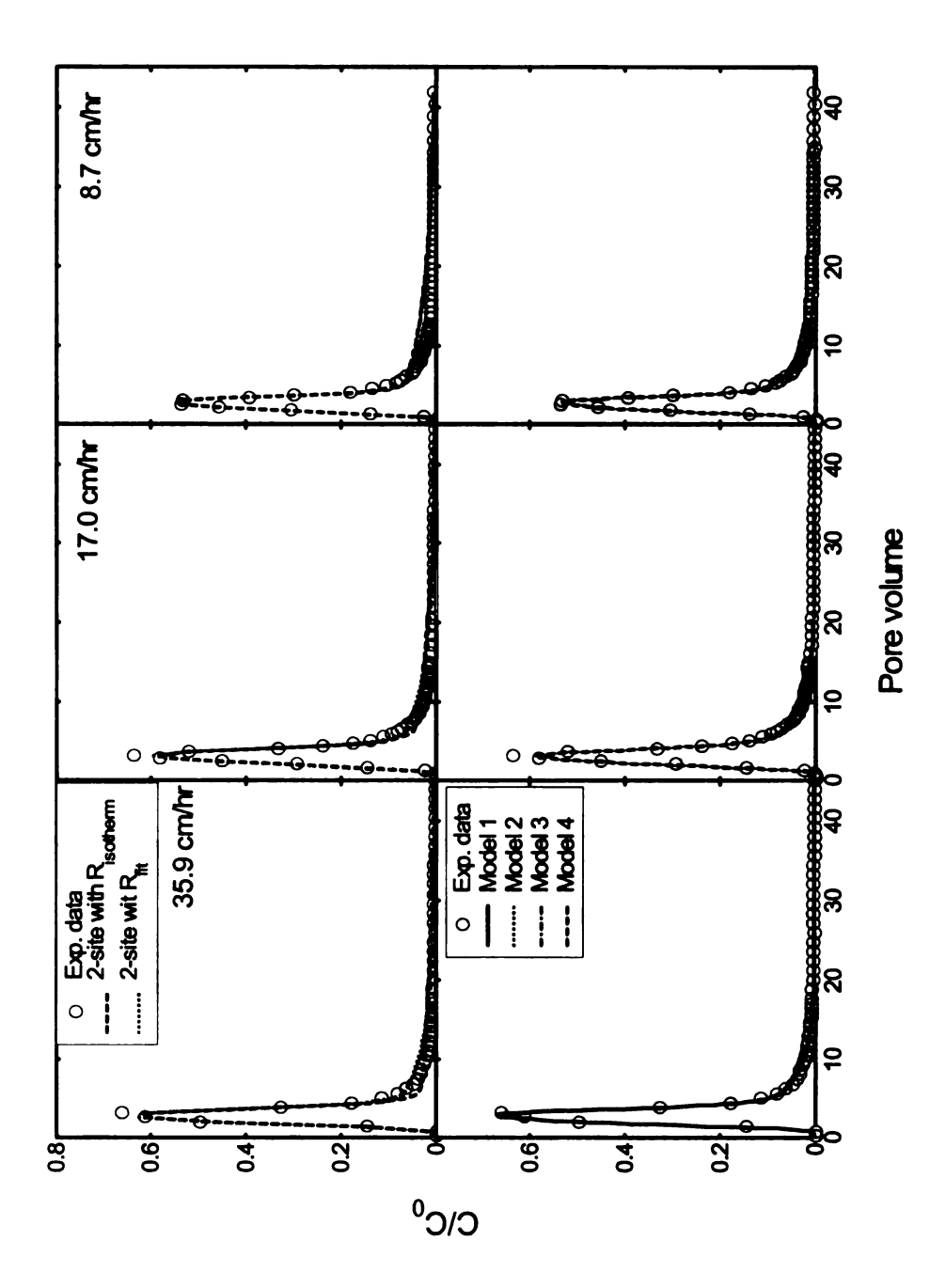


Figure 5-9: Best fits of the two-site and the three-site models to the observed naphthalene breakthrough data for Plume-A sand

## Effect of SOM on sorption nonequilibrium

Figure 5-10 represents the observed BTCs of naphthalene in the three soils at three different flow rates. A shift of the BTC to the right is evident at all flow rates indicating an enhanced retardation with an increase in the SOM. A direct correlation of  $K_d$  with SOM is well established for HOCs. In our experiments also, we observed an increase in  $K_d$  with an increase in SOM (Figure 5-3). The retardation factors calculated on the basis of isotherm  $K_d$  values correlate to SOM with an  $R^2$  of 0.994. If R values are obtained by curve fitting in columns, these should also correlate with SOM as the column properties do not differ significantly in terms of density and porosity (Table 5-1). The average values for R for Kalkaska-A, SPCF and plume-A sand were 36.03, 25.03 and 4.64 respectively using Model 1, which correlates well with SOM ( $R^2 = 0.963$ ). Our findings are also consistent with those of (Maraqa, 1995) who found an increase in R for Benzene and DMP in soils with different SOM.

Nonequilibrium is generally considered to exit if the BTCs exhibit a non-gaussian/asymmetric shape. The asymmetrical nature of BTCs is an evidence of a rate-limited mass transfer in a fraction of the soil matrix. Since  $\beta_l$  is defined as the fraction of retardation caused by instantaneous sorption sites, a higher value of  $\beta_l$  means that either the sorption sites are more readily accessible or it is easier for the compound to access/react with the sorption sites (Maraqa, 1995). No difference was observed in  $\beta_l$  values for Kalkaska-A and SPCF. The  $\beta_l$  values for Kalkaska-A ranged between 0.56-0.65 while for SPCF the range was 0.56-0.61 suggesting no correlation with SOM.

Plume-A sand with the least amount of organic content showed  $\beta_l$  values between 0.40 and 0.45. The variation in the values of  $\beta_l$  in the three soils is not as significant as the differences in SOM. This was also not true for plume-A sand that showed lower  $\beta_l$  values and resultantly lesser number of instantaneous sorption sites. A similar trend was also observed by Maraqa (1995) who reported that the instantaneous sorption sites were not well correlated with SOM, although in the author's case, the three soils employed differed in SOM but were similar in texture and origin (i.e., all soils were aquifer material).

Inspection of Tables 5-5 to 5-7 indicates that for all model applications of the three-site model (except Model 1 which is based on a net mass transfer rate coefficient), values of  $\alpha_1$  and  $\alpha_2$  for Kalkaska-A are lower than those of SPCF for a given flow rate. This suggests a strong correlation between SOM and the degree of nonequilibrium. In general, the sorption and desorption rate coefficients for SPCF are 2.5-4 times higher than Kalkaska-A, with almost double SOM as compared to SPCF. This is consistent with the results from our batch sorption/desorption rate studies and those of Park (2000) but contradicts the findings of Maraqa (1995) who reported no change in desorption rate coefficients of benzene and DMP in soils with different SOM. This may be due to a difference in the origin of soils. In our work, Kalkaska-A and SPCF are surface soils while those used by Maraqa (1995) are all of an aquifer origin. It is also important to note the differences in  $\alpha_3$  values that are higher for Kalkaska-A than SPCF indicating a faster rate of mass transfer to the non-desorption compartment. Mass transfer coefficient values for Plume-A sand fall between the values of SPCF and Kalkaska-A, which although, is difficult to explain based on SOM correlation alone, it is an indication that in aquifer

material, the predominant sorption mechanism may be other than partitioning to SOM.

This aspect however, requires further investigation.

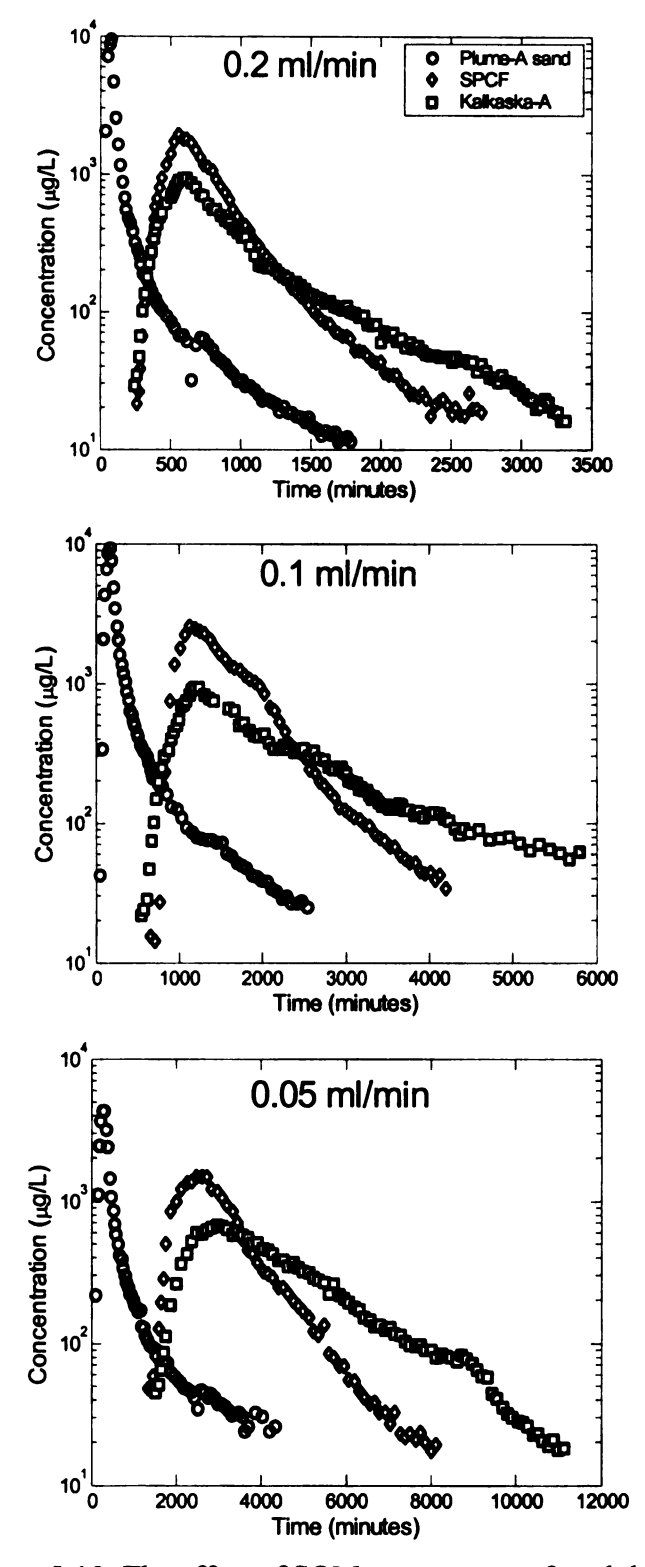


Figure 5-10: The effect of SOM on transport of naphthalene

## Effect of pore-water velocity on nonequilibrium

Observed BTCs of naphthalene at three different pore-water velocities are presented in Figure 5-11. A reduction in the peak concentration was observed for Kalkaska-A and plume-A sand at the lowest flow rate, while for SPCF no significant change in the peak concentrations is apparent. Based on its dimensionless form, the parameter  $\beta_1$  in the twosite and the three-site models is independent of pore-water velocity, therefore, should be velocity invariant. As a result the fraction of equilibrium sites ( $f_{eq}$ ) and rate-limited sites (  $f_{neq}$  ) should also be independent of velocity. Several investigators have reported conflicting results with regard to a correlation of the fraction of the rate-limited sites with velocity. For example, Kookana et al. (1993) suggested a correlation between the ratelimited site fractions and velocity. On the contrary, Brusseau et al. (1991) and Maraqa et al. (1999) found no correlation between both entities in their work. Schawarzenbach and Westall (1981) suggest that the fraction of rate-limited sites is likely to be a function of velocity due to a difference in the sorption reaction time if the nonequilibrium due to a predominant chemical interaction exists. The dependence of  $K_d$  on soil-contaminant contact time, in our data and many other studies, supports the assertion of Schawarzenbach and Westall (1981).  $K_d$  is likely to increase with an increase in the residence time at low pore-water velocities, will affect the magnitude of  $\beta_1$  and hence  $f_{eq}$ . However, in another study involving desorption experiments with differentially aged soils (data not reported here), we found that an increase in soil-naphthalene contact time affects the distribution of naphthalene in nonequilibrium and non-desorption domains and that the fraction of equilibrium sites ( $f_{eq}$ ) remains more or less unaffected.

Inspection of Tables 5-5 to 5-7 reveals that the estimated  $f_{eq}$  values for Kalkaska-A, SPCF and plume-A sand (estimated using Model 1) vary slightly with pore-water velocity but fail to reveal a consistent trend. The fraction of contaminant mass partitioned to rate-limited and non-desorption compartments, however, is likely to be time-dependent and is likely to increase at low velocities as a result of a longer residence time as supported in many studies. For example, Connaughten et al. (1993) argue that an increase in the exposure time would increase the contaminant mass in the rate-limited compartment. Similarly, Lee et al. (2002) reported that the effluent breakthrough curves at low pore-water velocities had a greater degree of nonequilibrium. With evidences from previous studies and our data from desorption experiments involving differentially aged soils, lack of a consistent trend in the fraction of nonequilibrium and non-desorption sites with a change in pore-water velocity, is counter intuitive. A probable cause might be the range of velocities employed resulting in the residence times, that are insignificant compared to the soil contact time needed to cause an observable variation in the distribution of contaminant in different domains.

The presence of a third site fraction (i.e., a non-desorbable fraction) will result in a reduction in  $f_{eq}$ ,  $f_{neq}$  or both and subsequently the lower  $\beta$  values. Some researchers have also found an evidence of a finite-sized desorption-resistant domain. For example, Kan et al. (1997) conducted batch adsorption-desorption experiments on natural and surrogate sediments involving multiple adsorption-desorption steps, and concluded a finite compartment size for the irreversible fraction on natural sediments as well as surrogate solids. The authors also concluded that the amount in irreversibly sorbed compartment increased linearly with the number of adsorption steps until its maximum

capacity is reached, after which, it becomes reversible. If that is true, then the size of irreversible compartment will depend on the contact time, which is function of porewater velocity.

An increase in the degree of nonequilibrium with an increase in the exposure time also suggests that a fraction of the rate-limited compartment turns into a desorptionresistant compartment. This is explained by the presence of residual amounts of naphthalene in the field samples used in some studies even 6-8 months after their removal from the source (Connaughten et al., 1993). There is also evidence that desorption is much slower in aged soils as compared to freshly contaminated soils. For example, Pignatello (1990a) studied the slowly reversible or non-labile fraction of non-polar halogenated hydrocarbons on soils and observed that the non-labile fraction increased non-linearly with incubation time and applied concentration. The functional form of  $\omega_i$  in the two-site and the three-site model suggests its dependence on pore-water velocity, however, the net desorption rate coefficient  $\alpha_1$  is independent of the velocity. The same is also true for  $\alpha_1$ ,  $\alpha_2$  and  $\alpha_3$  in all variations of the three-site model. A strong correlation exists for all rate coefficients in our experiments with the pore-water velocity in all formulations of the three-site model. Although, inconsistent with expectations of a constant rate coefficient being able to explain the BTCs at all velocities, an increase in the rate coefficients with an increase in the pore-water velocity have previously been noted in some studies e.g., (Ball and Roberts, 1991; Brusseau et al., 1991; Maraqa, 1995). This dependence of  $\alpha$  is viewed to be caused by an increase in the  $K_d$  in first two cases, however Maraqa (1995) related this to a time-averaged nature of the mass transfer coefficient. In our case, the dependence of  $K_d$  on the pore-water velocity is not

established i.e., the estimated retardation factor R does not exhibit any consistent increase with a decrease in pore-water velocity.

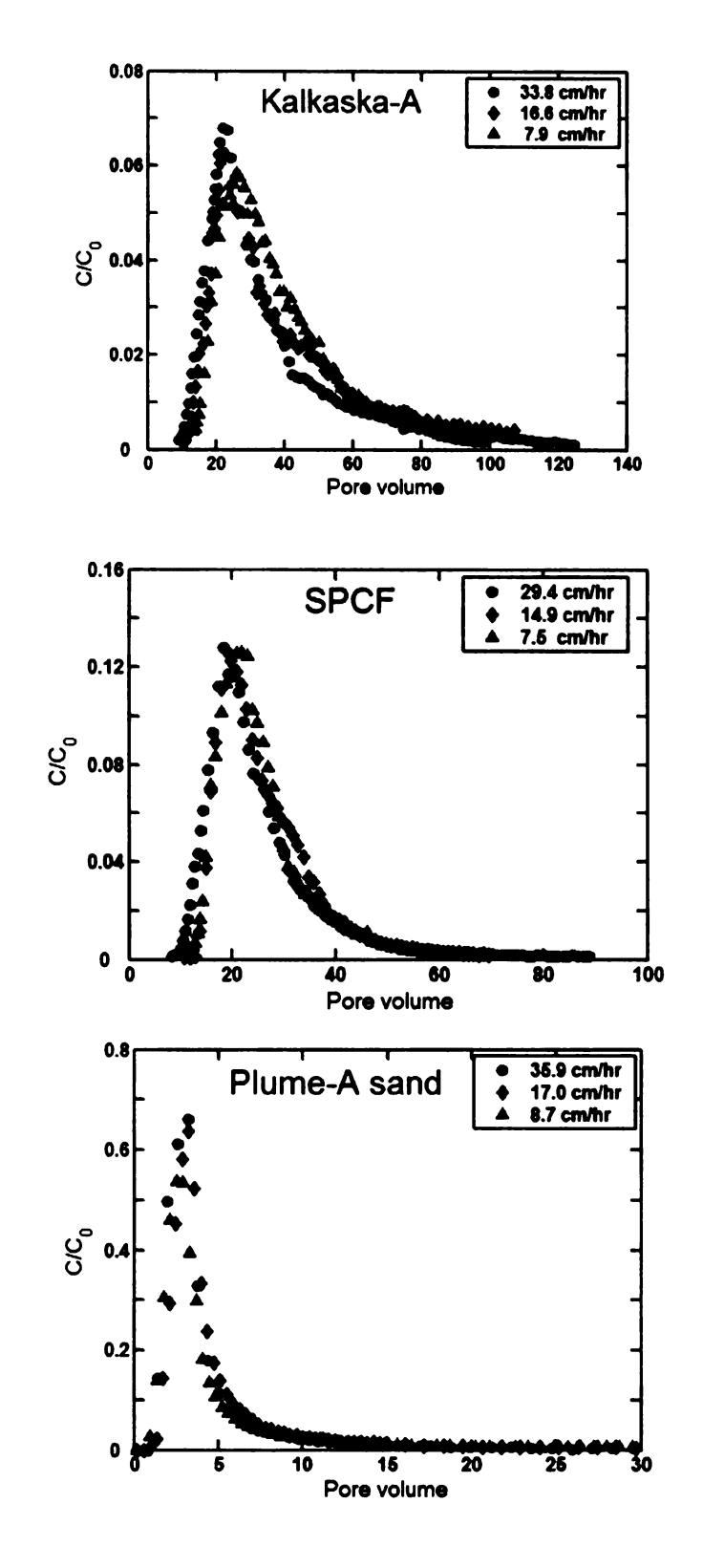


Figure 5-11: The effect of pore-water velocity on transport of naphthalene

### **5.5 Conclusions**

Based on the experimental evidence, we conclude that the extent of irreversible sorption is unaffected by the pore-water velocity. Out of the two surface soils, the soil with a high SOM had a higher percentage of non-desorbable naphthalene mass (i.e., 14.80-16.3% for Kalkaska-A compared to 3.54-5.83% for SPCF). However, the non-desorbable mass in both soils was unaffected by the pore-water velocity. For Plume-A sand, the non-desorbable naphthalene mass appeared to increase with a reduction in pore-water velocity. The variation in pore-water velocity did not affect the different fractions of soil matrix (i.e., equilibrium, rate-limited and non-desorption fraction) and the parameters  $\omega$  for the range of pore-water velocities employed in this study. The same may not, however, be true for extremely low pore-water velocities resulting in residence times that are orders of magnitude higher. SOM, on the other hand, had a more pronounced effect, as the  $\omega$  values for Kalkaska-A (1.168-1.574) were consistently lower than those for SPCF (1.753-2.538) for all BTCs.

Our results also indicate that, the three-site model better describes the breakthrough of naphthalene than the two-site model for all nine cases (i.e., three soils at three different velocities). However, all variants of the three-site model resulted in identical fits to the observed naphthalene BTCs, which indicates, that an increase in the number of model parameters to enhance the description of the observed BTCs is not justified. We also suggest that a mathematical formulation that accounts for a shift of the contaminant from the equilibrium domain to the non-desorption domain and utilizes time-independent

parameters, may be preferred over formulations based on the linear sorption distribution coefficient.

#### 5.6 References

- Ahn, I.S., Lion, L.W. and Shuler, M.L., 1999. Validation of a hybrid "two-site gamma" model for naphthalene desorption kinetics. Environmental Science & Technology, 33(18): 3241-3248.
- Ball, W.P. and Roberts, P.V., 1991. Long-term sorption of halogenated organic chemicals by aquifer material .2. Intra-particle diffusion. Environmental Science & Technology, 25(7): 1237-1249.
- Brusseau, M.L., Larsen, T. and Christensen, T.H., 1991. Rate-limited sorption and nonequilibrium transport of organic chemicals in low organic-carbon aquifer materials. Water Resources Research, 27(6): 1137-1145.
- Connaughten, D.F., Stedinger, J.R., Lion, L.W. and Schuler, M.L., 1993. Description of time-varying desorption kinetics: Release of naphthalene from contaminated soils. Environmental Science & Technology, 27(12): 2397-2403.
- Cornelissen, G., Rigterink, H., Ferdinandy, M.M.A. and Van Noort, P.C.M., 1998a.
  Rapidly desorbing fractions of PAHs in contaminated sediments as a predictor of the extent of bioremediation. Environmental Science & Technology, 32(7): 966-970.
- Cornelissen, G., Van Noort, P.C.M. and Govers, H.A.J., 1998b. Mechanism of slow desorption of organic compounds from sediments: A study using model sorbents. Environmental Science & Technology, 32(20): 3124-3131.
- Cornelissen, G., Van Noort, P.C.M., Parsons, J.R. and Govers, H.A.J., 1997. Temperature dependence of slow adsorption and desorption kinetics of organic compounds in sediments. Environmental Science & Technology, 31(2): 454-460.
- Johnson, M., Keinath, T. and Weber, W.J., 2001. A distributed reactivity model for sorption by soils and sediments. 14. Characterization and modeling of phenanthrene desorption rates. Environmental Science & Technology, 35(8): 2734-2740.
- Kan, A.T., Fu, G., Hunter, M.A. and Tomson, M.B., 1997. Irreversible adsorption of naphthalene and tetrachlorobiphenyl to Lula and surrogate sediments. Environmental Science & Technology, 31(8): 2176-2185.
- Kookana, R.S., Schuller, R.D. and Aylmore, L.A.G., 1993. Simulation of simazine transport through soil columns using time-dependent sorption data measured under flow conditions. Journal of Contaminant Hydrology, 14(2): 93-115.
- Lee, J.H., Hundal, L.S., Horton, R. and Thompson, M.L., 2002. Sorption and transport behavior of naphthalene in an aggregated soil. Journal of Environmental Quality, 31(5): 1716-1721.

- Lele, S.K., 1992. Compact finite difference schemes with spectral-like resolution. Journal of Computational Physics, 103: 16-42.
- Maraqa, M.A., 1995. Transport of dissolved volatile organic compounds in the unsaturated zone. Ph.D. Thesis, Michigan State University, East Lansing, 154 pp.
- Maraqa, M.A., Wallace, R.B. and Voice, T.C., 1999. Effects of residence time and degree of water saturation on sorption nonequilibrium parameters. Journal of Contaminant Hydrology, 36(1-2): 53-72.
- Maraqa, M.A., Zhao, X., Wallace, R.B. and Voice, T.C., 1998. Retardation coefficients of nonionic organic compounds determined by batch and column techniques. Soil Science Society of America Journal, 62(1): 142-152.
- Nkedikizza, P. et al., 1983. Modeling tritium and chloride-36 transport through an aggregated oxisol. Water Resources Research, 19(3): 691-700.
- Park, J.H., 2000. Bioavailability of sorbed organic contaminants. Ph.D. Thesis, Michigan State University, East Lansing, 155 pp.
- Park, J.H., Feng, Y.C., Ji, P.S., Voice, T.C. and Boyd, S.A., 2003. Assessment of bioavailability of soil-sorbed atrazine. Applied and Environmental Microbiology, 69(6): 3288-3298.
- Park, J.H., Zhao, X.D. and Voice, T.C., 2001. Biodegradation of non-desorbable naphthalene in soils. Environmental Science & Technology, 35(13): 2734-2740.
- Park, J.H., Zhao, X.D. and Voice, T.C., 2002. Development of a kinetic basis for bioavailability of sorbed naphthalene in soil slurries. Water Research, 36(6): 1620-1628.
- Pignatello, J.J., 1990a. Slowly reversible sorption of aliphatic halocarbons in soils .2.

  Mechanistic aspects. Environmental Toxicology and Chemistry, 9(9): 1117-1126.
- Pignatello, J.J., 1990b. Slowly reversible sorption of aliphatic halocarbons in soils. 1. Formation of residual fractions. Environmental Toxicology and Chemistry, 9: 1107-1115.
- Prata, F., Lavorenti, A., Jan, V., Burauel, P. and Vereecken, H., 2003. Miscible displacement, sorption and desorption of atrazine in a Brazilian oxisol. Vadose Zone Journal, 2: 728-738.
- Rao, P.S.C., Davidson, J.M., Jessup, R.E. and Selim, H.M., 1979. Evaluation of conceptual models for describing nonequilibrium adsorption-desorption of pesticides during steady flow in soils. Soil Science Society of America Journal, 43(1): 22-28.

- Schawarzenbach, R.P. and Westall, J., 1981. Transport of non-polar organic compounds from surface water to groundwater. Laboratory sorption studies. Environmental Science & Technology, 15(11): 1360-1367.
- Seyfried, M.S. and Rao, P.S.C., 1987. Solute transport in undisturbed columns of an aggregated tropical soil Preferential flow effects. Soil Science Society of America Journal, 51(6): 1434-1444.
- Sharer, M., Park, J.H., Voice, T.C. and Boyd, S.A., 2003a. Aging effects on the sorption-desorption characteristics of anthropogenic organic compounds in soil. Journal of Environmental Quality, 32(4): 1385-1392.
- Sharer, M., Park, J.H., Voice, T.C. and Boyd, S.A., 2003b. Time dependence of chlorobenzene sorption/desorption by soils. Soil Science Society of America Journal, 67(6): 1740-1745.
- Toride, N., Leij, F.J. and Van Genuchten, M.T., 1999. The CXTFIT code for estimating transport parameters from laboratory or field tracer experiments. 137, U.S Salinity Laboratory, Riverside, California.
- Van Genuchten, M.T. and Wagenet, R.J., 1989. Two-site/two-region models for pesticide transport and degradation: Theoretical development and analytical solutions. Soil Science Society of America Journal, 53(5): 1303-1310.
- Van Genuchten, M.T. and Wierenga, P.J., 1977. Mass transfer studies in sorbing porous media .2. Experimental evaluation with tritium (<sup>3</sup>H<sub>2</sub>O). Soil Science Society of America Journal, 41(2): 272-278.
- Xing, B. and Pignatello, J.J., 1996. Time-dependent isotherm shape of organic compounds in soil organic matter: Implications for sorption mechanism. Environmental Toxicology and Chemistry, 15: 1282-1288.

# CHAPTER 6 DISSERTATION SUMMARY AND CONCLUSIONS

## 6.1 Dissertation summary

The objective of this research was to evaluate the importance of desorption resistance in modeling desorption in soil columns which mimic subsurface systems. Understanding the influence of desorption resistance on desorption kinetics and sorption nonequilibrium is important for decision making in remediation. We selected naphthalene as a representative HOC because it is included in EPA's list of 16 priority PAHs, has a high solubility, relatively moderate hydrophobicity and has been used by our research group for bioavailability and phytoremediation studies in the past. Two surface soils with different organic matter content and an aquifer sand with almost no organic content were used as natural sorbents.

The first objective focused at evaluating the differences in desorption kinetics in batch and column systems. Our approach was based on the hypothesis, that if three regimes of desorption behavior are observed in batch for a soil-contaminant combination, the same should be observable in column desorption. We completed the sorption phase (three days) in batch for both types of experiments to ensure identical conditions and period of equilibration. This approach allowed an assessment that is free from those discrepancies which normally exist between batch and column systems due to a non-identical sorption environment. Batch and column desorption experiments were augmented with the three-day sorption isotherms to determine the sorptive capacity of each soil for the same period. In addition, the analysis of tritiated water breakthrough curves with equilibrium model not only allowed an independent assessment of the

dispersive properties of each soil, but also enabled us to establish the conditions of physical equilibrium. As a result, we could conclude that the rate limitations were due to sorptive interaction of naphthalene with the soil matrix and not due to the entrapment of a fraction of water in the dead-end pores.

Based on experimental evidence of solvent extractable naphthalene in batch and columns, we analyzed the naphthalene desorption in columns using the existing two-site model and a proposed three-site model. The three-site model that is based on the conceptualization of the soil matrix comprising three types of sorption sites rather than two, could successfully describe naphthalene desorption from the soil columns. A lack of non-desorption sites in the soil matrix in the two-site model resulted in greater-than-actual mass elution. This makes the traditional approach of assuming the solid matrix comprising of only two types of sorption sites questionable. A comparison of kinetic parameters for batch and columns also provided evidence that longer diffusion path lengths due to packing of aggregate particles in soil columns limit the ability of the contaminant to diffuse to the bulk solution. This results in a greater fraction of soil matrix to behave as rate-limited sites in columns than those in the batch systems.

The second objective was aimed at evaluating the effects of soil-contaminant contact time on the extent of irreversible sorption and desorption kinetics. Contact time is known to have a considerable influence on the sorptive capacity of the sorbents, distribution of contaminant in equilibrium, non-equilibrium and non-desorption compartments and desorption rates in batch studies. The same, however, has not been systematically addressed in column studies. We followed an approach, in which, the column desorption experiments conducted under identical conditions (except the period

of equilibration in sorption phase) revealed the influence of contact time on the extent of non-desorption and desorption kinetics. Results of these experiments were substantiated by 2-month and 5-month sorption isotherms and serial dilution desorption experiments involving differential equilibration period (i.e., between 10 minutes to 12 days).

Sorption isotherms revealed an increase in the distribution of naphthalene to the sorbed phase for the two organic soils. Maximum increase in sorptive capacity was, however, noted for the aquifer sand that showed a 100% increase from 3 days to 2 months and no increase thereafter. Another notable finding was a considerable increase in solvent extractable naphthalene over time, with a corresponding decrease in the desorbable naphthalene, for all three soils.

Based on our results we conclude that partitioning of HOCs to solid phase is a time-dependent process and is likely to increase with soil contact times as we witness an increase in the sorbed-phase concentration for all soils with an increase in contact time. We also conclude, based on the comparison of the two-site and the three-site models, that for contaminants exhibiting significant non-desorption, a three-site model results in a better description and the data are difficult to reconcile with the dual domain approach. We also suggest that our aging conceptual model that accounts for a shift of contaminant from nonequilibrium domain to non-desorption domain is consistent with our observations and explains the resistance to desorption exhibited by contaminants over long-term contact times.

The third objective was aimed at exploring the impact of pore-water velocity on the extent of non-desorption and sorption nonequilibrium. Pore-water velocity in column experiments is a variable that is inversely related to column residence time, which in turn is analogous to soil-contaminant contact time or "aging". We approached this objective by conducting pulse-type column experiments in the three soils at different pore-water velocities ranging between 7-35 cm/hour. Tracer tests with tritiated water allowed an independent characterization of each soil for dispersion that resulted in a reduction in the number of fitting parameters.

Theoretically, an increased soil-naphthalene contact time as a result of low porewater velocity should increase the distribution of contaminant to the non-desorption domain, which we verified by solvent extractions in batch and column desorption studies. The same was however, not apparent in our pulse-type experiments, as the naphthalene mass extracted at the end of the column experiments failed to show a variation with the pore-water velocity for the two organic soils. Furthermore, only a slight variation for Plume-A sand was observed. The velocity range employed provided a column residence time ranging between 7-68 hours for Kalkaska-A, 10-41 hours for SPCF and from 3-14 hours for the plume-A sand. Due to our inability to achieve longer residence times by further reducing the velocity, we refrain from drawing conclusions about the invariance of non-desorbable naphthalene with a change in pore-water velocity and hence the residence time, as it is not supported by other experiments in batch involving a similar range of equilibration times.

The observed time-concentration data for naphthalene was analyzed using a twosite model and four variations of the three-site model. Two of these were based on the driving force formulation using the linear distribution coefficient while the other two utilized kinetic rate coefficients. Our results indicate that, the three-site model better describes the breakthrough of naphthalene than the two-site model for all nine cases (i.e., three soils at three different velocities). However, all formulations based on the three-site model resulted in identical fits to the observed naphthalene BTCs, which indicates that increase in the number of model parameters to enhance the description of the observed BTCs is not justified. We also suggest that a formulation that accounts for the shift of contaminant from equilibrium domain to non-desorption domain and utilizes time-independent parameters may be preferred over the  $K_d$  based formulations.

## 6.2 Recommendations

Our recommendations for future research based on the present study are as follows:

- No conclusive evidence so far exists for a correlation between the non-desorption
  fraction of soil matrix and the chemical characteristics of the contaminant or
  mechanical and compositional properties of the soil. In order to be able to develop
  such correlations, systematic studies are required to build a comprehensive database
  for the non-desorption of PAHs.
- An evidence of change in the domain size with an increase in the contact time and instantaneous mass distribution to the non-desorption domain in addition to equilibrium domain, has been found in many studies. Current experimental methods employed in sorption rate studies donot allow a differentiation in mass distribution to each of these compartments. A first order mass transfer does not adequately describe the exact nature of non-linear increase in the size of the non-desorption domain.
  Carefully planned batch experiments that allow realistic comparisons of the differences in mass transfer in batch and column environments are needed to separate these effects.

Employing a volatile compound like naphthalene involves mass balance problems
and data is sometimes difficult to reconcile inspite of strong expectations.
 Development of online detection methods, in which, the concentration of the eluting
solute could be monitored would solve the mass balance problems. Current online
detection methods, which normally rely on fluorescence measurements, are not
appropriate for the soils that are high in organic content due to the possibility of
interferences.

Table A-1: Details of the independently measured and estimated parameters for the two-site and the three-site models in column desorption experiments

Parameter	Two-site model	Three-site model
Batch sorption distribution coefficient $K_d$ (isotherm)	Measured by conducting indep soils	endent isotherm on the three
Column distribution coefficient $K_d$ (column)	$K_d(column)$ calculated by usi $K_d = \frac{M_e - P_v C_o}{m_{soil} C_0}$	ng the relation
Retardation factor (R)	Calculated using the relation $R = 1 + \frac{\rho K_d}{\theta} \text{ with } K_d$ (isotherm) and $K_d$ (column)	Calculated using the relation $R = 1 + \frac{\rho K_d}{\theta} \text{ with } K_d$ (column)
Peclet number $(P_e)$	Calculated using the relation $P_{e}$ The dispersion coefficient $D$ w by fitting the equilibrium mode water breakthrough.	as independently estimated
$\beta$ or $\beta_{\parallel}$ $\omega$ or $\omega_{\parallel}$	Estimated by fitting the two- site model (Equation 3-10 & 3-11) to observed naphthalene desorption using CXTFIT code	Estimated by fitting the three-site model (Equation 3-20 & 3-21) to observed naphthalene desorption using sequential quadratic
$\beta_2$	Not applicable programming (SQP)	
Fraction of equilibrium sites $(f_{eq})$	Calculated using the relation $\beta$	$P \text{ or } \beta_{1} = \frac{\theta + f_{eq} \rho K_{d}}{\theta + \rho K_{d}}$
Fraction of non- desorption sites $(f_{nd})$	Not applicable	Calculated using the relation $\beta_2 = \frac{\rho f_{nd} K_d}{\theta}$
Fraction of nonequilibrium sites $(f_{neq})$	Calculated using the relation $f_{eq} + f_{neq} = 1$	Calculated using the relation $f_{eq} + f_{neq} + f_{nd} = 1$
Desorption rate coefficients ( $\alpha$ or $\alpha_1$ )	Calculated using the relation $\omega = \frac{\alpha(1 - \beta_1)LR}{\nu}$	Calculated using the relation $\omega = \frac{\alpha_1 LR}{v} (1 - \beta_1 - \frac{\beta_2}{R})$